

5-2020

Modulation Of Pi3K-Akt Pathway In Colorectal Cancer

Maliha Nusrat

Follow this and additional works at: https://digitalcommons.library.tmc.edu/utgsbs_dissertations



Part of the [Oncology Commons](#)

Recommended Citation

Nusrat, Maliha, "Modulation Of Pi3K-Akt Pathway In Colorectal Cancer" (2020). *Dissertations and Theses (Open Access)*. 1003.

https://digitalcommons.library.tmc.edu/utgsbs_dissertations/1003

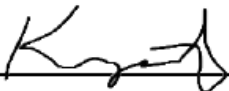
This Thesis (MS) is brought to you for free and open access by the MD Anderson UTHealth Houston Graduate School at DigitalCommons@TMC. It has been accepted for inclusion in Dissertations and Theses (Open Access) by an authorized administrator of DigitalCommons@TMC. For more information, please contact digcommons@library.tmc.edu.

MODULATION OF PI3K-AKT PATHWAY IN COLORECTAL CANCER

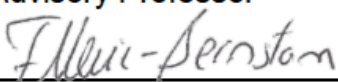
by

Maliha Nusrat, MBBS

APPROVED:



Scott Kopetz, M.D., Ph.D.
Advisory Professor



Funda-Meric Bernstam, M.D.



Lawrence N. Kwong, Ph.D.

Imad Shureiqi

Imad Shureiqi, M.D., M.S.



Jennifer A Wargo, M.D., M.M.Sc.

APPROVED:

Dean, The University of Texas
MD Anderson Cancer Center UTHealth Graduate School of Biomedical
Sciences

MODULATION OF PI3K-AKT PATHWAY IN COLORECTAL CANCER

A

THESIS

Presented to the Faculty of

The University of Texas

MD Anderson Cancer Center UTHealth

Graduate School of Biomedical Sciences

in Partial Fulfillment

of the Requirements

for the Degree of

MASTER OF SCIENCE

by

Maliha Nusrat, MBBS

Houston, TX

May, 2020

Dedication

To my dad who left the world too early for lack of better cancer therapies and would have rejoiced in this accomplishment.

To my loving mother who inspired me to pursue medicine and supported me at every step of my life.

Acknowledgments

I would like to express my sincere appreciation and gratitude to the following:

- Dr. Scott Kopetz for his tremendous guidance, time, patience and support of my translational research aspirations.
- Dr. Funda Meric-Bernstam, Dr. Imad Shureiqi, Dr. Jennifer Wargo and Dr. Lawrence Kwong for their guidance and time as members of my advisory committee.
- Dr. Robert Bast and Dr. Patrick Hwu for inspiration and encouragement to pursue a career in translational research.
- Dr. Robert Wolff, program director of Hematology-Oncology fellowship, for supporting and sponsoring my participation in the GSBS MS program during fellowship.
- Dr. Sarina A Piha-Paul, program director of Investigational Cancer Therapeutics fellowship, for the opportunity to complete the GSBS MS coursework during fellowship.
- Colorectal cancer patients who provided tumor samples for this research to advance scientific knowledge and improve therapeutic options for future patients.
- Members of Dr. Kopetz's laboratory - namely Dr. David Menter, Dr. Ji Wu, Muddassir A. Syed, Dr. Jennifer S. Davis, Preeti K Marie, Lea A Bitner and Dr. Alexey Sorokin - for helping me learn laboratory research techniques and data interpretation.
- Dr. Jisu Oh for the development and treatment of patient derived xenografts.

- Ms. Shanequa Manuel for her assistance with patient sample collection.
- The Reverse Phase Protein Array core facility at MD Anderson, and The Cancer Center Support Grant that partially funds these shared resources.
- Dr. Jorge Blando, Dr. Pam Sharma and Dr James Allison (members of The MD Anderson Immunotherapy Platform) for quantitative immunohistochemistry (IHC) data.
- Dr. Riham Katkhuda and Dr Dipen Maru, for PTEN IHC staining and pathology support.
- Dr. Ganiraju Manyam and Dr. Jason Roszik for their contributions to gene expression data.
- Dr. Timothy Yap for his mentorship on the clinical trial protocol of combined PI3K and checkpoint inhibition.
- Dr. Michael Overman, Dr Filip Janku and Dr Gregory Lizee for their guidance and resources for my research.
- National Cancer Institute Cancer Therapy Evaluation Program for their sponsorship of the phase II clinical trial with MK2206, and our new protocol of combined PI3K and checkpoint inhibition in advanced cancers.
- The American Society of Clinical Oncology (ASCO) for merit awards to present parts of my thesis research at ASCO annual meetings in 2018 and 2019.
- The ASCO, the Tomasello Family and Women Who Conquer Cancer Foundation for sponsoring 2018 ASCO Young Investigator Award to test further hypothesis derived from this thesis work.

- Dr. Sharon Giordano, Department of Health Services at MD Anderson, for additional funds to test further hypothesis derived from this thesis work.
- The GSBS course directors, faculty members, and administrative staff, including Ms. Jene Reinartz.
- My fellow graduate students and co-fellows for mutual learning and moral support.

MODULATION OF PI3K-AKT PATHWAY IN COLORECTAL CANCER

Maliha Nusrat, MBBS.

Advisory Professor: Scott Kopetz, M.D., Ph.D.

The phosphatidylinositol-3-kinase (PI3K) signaling pathway is activated in 20-40% colorectal cancers (CRC) through PTEN loss (PTEN^{loss}) and *PIK3CA* mutations (*PIK3CA*^{mut}). Allosteric AKT inhibition with MK2206 monotherapy has been ineffective in CRC patients. We investigated the impact of MK2206 on pharmacodynamic (PD) markers and signaling pathways using reverse phase protein array (RPPA) on (1) paired tumor biopsies from a clinical trial of MK2206 in PI3K-altered metastatic CRC, (2) PTEN^{loss} CRC patient derived xenografts (PDX) treated with MK2206 or carrier, and (3) MK2206-treated cell lines. PD inhibition was deep in cell lines, less but significant in PDX, and only modest in patients. Expression of several receptor tyrosine kinases (RTKs) increased after AKT inhibition; insulin like growth factor 1 receptor (IGF1R) was significantly upregulated in patients, PDX and cell lines ($P < 0.05$). IGF1R levels increased after 24 hours of exposure to MK2206 in cell lines ($P < 0.01$), and correlated inversely with pFoxO3a levels in patients' tumors ($r = -0.65$, $P = 0.01$). Levels of pFoxO3a also inversely correlated with AKT pS473, suggesting partial AKT re-phosphorylation.

The PI3K pathway also modulates tumor immune microenvironment and may influence response to emerging immunotherapies. Using quantitative immunohistochemistry, we found increased densities of effector T cells and increased expression of several checkpoints (including PD-L1) at the center of PI3K-

altered early-stage MSS CRC. Subgroup analysis showed increased CD8+ cells among *PIK3CA*^{mut} but not *PTEN*^{loss} cases. Using Agilent microarrays, we found higher PD-L1 and TIGIT mRNA levels in PI3K-altered MSS CRC ($P < 0.05$). On hierarchical clustering analysis, the immune signature of PI3K-altered MSS CRC clustered with that of inflamed CMS1 and CMS4 tumors. Among MSS CRC patients enrolled in immunotherapy trials, *PIK3CA*^{mut} MSS CRC patients derived clinical benefit more frequently than *PIK3CA* wild-type patients (50% vs 8.6%, $P = 0.015$). We further showed synergism of combined PI3K and PD-1 inhibition in CT26 CRC mouse model.

We conclude that AKT inhibition in metastatic CRC induces FOXO-mediated adaptive upregulation of RTKs, namely IGF1R, possibly reactivating the pathway. PI3K-altered MSS CRC is an immunologically distinct subgroup with increased immune engagement, but also checkpoint upregulation, resulting in overall immunosuppression. Our results highlight potential targeted therapy and immunology combinations for PI3K-altered CRC patients.

Table of Contents

Approval Sheet.....	i
Title Page	ii
Dedication.....	iii
Acknowledgments	iv
Abstract.....	vii
Table of Contents	ix
List of Illustrations	xi
List of Tables	xiv
Chapter I: Introduction	1
Chapter II: Methods	12
Chapter III: Results	24
Aim 1: Demonstrate pharmacodynamics inhibition of AKT pathway in tumor and surrogate tissue from a clinical trial of MK2206 in CRC	24
Aim 2: Determine the mechanisms of adaptive resistance to AKT inhibition in PI3K activated colorectal cancer patients, patient derived xenografts and cell lines.	34
Aim 3: Evaluate the impact of PI3K activating alterations on immune landscape of colorectal cancer, and design a therapeutic intervention to improve the immune microenvironment.	52
Chapter IV: Discussion	71
Aim 1: Demonstrate pharmacodynamics inhibition of AKT pathway in tumor and surrogate tissue from a clinical trial of MK2206 in CRC	71

Aim 2: Determine the mechanisms of adaptive resistance to AKT inhibition in PI3K activated colorectal cancer patients, patient derived xenografts and cell lines. 75

Aim 3: Evaluate the impact of PI3K activating alterations on immune landscape of colorectal cancer, and design a therapeutic intervention to improve the immune microenvironment. 79

Conclusions 84

Bibliography..... 85

Vita 107

List of Illustrations

Figure 1: A schematic of PI3K-AKT signaling pathway and its interaction with parallel oncogenic signaling pathways.....	4
Figure 2: Feedback inhibition loops in PI3K-AKT signaling pathway and potential loss of inhibition after treatment with allosteric AKT inhibitor (MK2206).	8
Figure 3: Phase 2 clinical trial of MK2206 in previously treated metastatic colorectal cancer patients with PTEN ^{loss} or PIK3CA ^{mut}	13
Figure 4: PTEN ^{loss} Patient derived xenograft trial with MK2206 vs 30% Captisol control.	16
Figure 5: Change in protein expression of pharmacodynamic markers after AKT inhibition with MK2206 among patient tumors, patient-derived xenografts and cell lines.	25
Figure 6: Change in protein expression of pharmacodynamic markers of AKT inhibition in three cell lines (KM12L4, SW480, MDA468) at different time-points during treatment with MK2206	27
Figure 7: Change in protein expression of pharmacodynamic markers of AKT inhibition in patients' tumors using paired biopsies at baseline and C1D15 of treatment with MK2206.....	28
Figure 8: Correlation matrix of change in protein levels after AKT inhibition in CRC patients shows distinct clusters.	30
Figure 9: Correlation matrix of change in levels of PI3K signaling proteins and receptor tyrosine kinases after AKT inhibition in CRC patients	32
Figure 11: Increased membranous staining of IGF1Rb beta in MK2206-treated PDX as compared to control PDX.....	36
Figure 12: IGF1R upregulation begins 8-24 hours after treatment with MK2206 in cell lines.	41

Figure 13: Increased nuclear staining and decreased cytoplasmic staining of FOXO in MK2206-treated PDXs as compared to control PDXs.....	43
Figure 14: As phosphorylation of FoxO3a decreases, levels of receptors tyrosine kinases start to rise.....	45
Figure 15: As phosphorylation of FoxO3a decreases, total AKT levels rise (A), and PI3K signaling also increases as shown by increase in AKT pS473 (B).	46
Figure 16: Protein levels of AKT directly correlate with protein levels of receptor tyrosine kinases (RTKs) namely IGF1R, IR-b and PDGFRb.....	47
Figure 17: Inverse correlation between expression levels of IGF1R and IGF1R pY1135/1136.	48
Figure 18: Increased peritumoral lymphocytes in PI3K-altered CRC	54
Figure 20: Density of immune infiltrates in microsatellite stable primary CRC by PI3K pathway alteration status.....	57
Figure 21: PI3K alterations are more frequent among microsatellite stable colorectal cancer with high immune density score of 3 or 4.	58
Figure 22: Quantitative IHC for immunomodulatory proteins shown increased checkpoint expression among MSS CRC with PI3K pathway alterations..	60
Figure 23: Increased T cell engagement is seen in <i>PIK3CA</i> ^{mut} , but not in PTEN ^{oss} MSS primary CRC.....	62
Figure 24: IHC expression of immunomodulatory proteins among <i>PIK3CA</i> ^{mut} (A) and PTEN ^{oss} (B) MSS primary CRC.....	63
Figure 25: Analysis of mRNA data showed higher expression of immune checkpoints among PI3K altered primary CRC.	64

Figure 26: Hierarchical clustering analysis of top 20 differentially expressed genes in MSS
CRC with and without PI3K alterations65

Figure 27: Outcomes on immunotherapy clinical trials among MSS CRC patients67

Figure 28: Outcomes with immunotherapy among MSS adenocarcinoma patients68

Figure 29: Synergism between anti-PD1 and PI3K inhibitor in CT26 mouse model of CRC
(N=40).69

List of Tables

Table 1: Clinical trials using single agent PI3K/AKT signaling pathway inhibitors in colorectal cancer patients.	6
Table 2: Correlation between changes in levels of AKT pS473 and downstream PI3K signaling proteins in patients after treatment with MK2206.	31
Table 3: Changes in protein expression of receptor tyrosine kinases, phosphorylated FoxO3a and IRS1 after MK2206 treatment in colorectal cancer patients within the assigned treatment cohort.	37
Table 4: Molecular characteristics of patients in assigned treatment cohorts.	39
Table 5: Change in receptor tyrosine kinases and pharmacodynamic markers of AKT inhibition in PDX tumors and the corresponding patient's tumor.	40
Table 6: Correlation between FoxO3a pS318/321 and change in receptor tyrosine kinases after AKT inhibition in metastatic colorectal cancer patients.	44
Table 7: Correlation between AKT levels and change in levels of receptor tyrosine kinases after treatment with MK2206.	47
Table 8: Heatmap of feedback loops in PI3K signaling in individual patients' tumors shows loss of feedback inhibition of only one of the two feedback loops in most patients. .	50
Table 9: Correlation between changes in IRS1 levels and other protein levels in patients' tumors after treatment with MK2206.	50
Table 10: Baseline characteristics of patients in early stage CRC cohort (N=94)	53

Chapter I: Introduction

Colorectal cancer in the United States:

Colorectal cancer (CRC) is the second leading cause of cancer-related death in the United States, with an estimated 53,200 deaths in both genders combined in 2020.¹ In the past three decades, the incidence of both colon and rectal cancers has been increasing annually in adults younger than 55 years of age in the United States.² The trend appears to be global spanning Australia, South America, Asia, Europe and Canada.³ Most of these young onset CRC are sporadic and associated with synchronous metastases.^{4,5} This has resulted in a decrease in recommended age for CRC screening to 45 years for average risk adults by American Cancer Society in 2018.⁶ The five-year survival rate of metastatic CRC remains below 15%.⁷ While curative surgical resection of oligometastases improves survival, better systemic therapies for unresectable metastatic disease are urgently needed. Chemotherapeutic agents 5-fluorouracil, oxaliplatin and irinotecan have been the backbone of systemic treatment for metastatic CRC for decades. Anti-vascular endothelial growth factor antibodies modestly improve survival when added to the chemotherapy backbone.^{8,9} The newer agents for refractory CRC, regorafenib and TAS-102, similarly have had limited success.^{10,11}

Subgroups of CRC are increasingly being recognized using genomic sequencing and gene expression analysis to have distinct biology and treatment implications.¹²⁻¹⁴ Constitutive activation of mitogen-activated protein kinase (MAPK) signaling through molecular aberrations in pathway genes confers resistance to

upstream epidermal growth factor receptor (EGFR) inhibition. Absence of alterations in the RAS genes (*KRAS* and *NRAS*) in about half of CRC patients is routinely used as a predictive biomarker for treatment with anti-EGFR monoclonal antibodies.¹⁵ Activating *BRAF* mutations downstream of RAS have also shown to predict resistance to anti-EGFR therapy. Combined EGFR and BRAF inhibition has been successful in randomized clinical trials for *BRAF* V600E mutant CRC, while trials are ongoing in non-*BRAF* V600E patients.¹⁶ *BRAF* mutations also signify a CRC subgroup with poor prognosis, for which aggressive upfront cytotoxic chemotherapy is warranted.¹⁷ About 2-4% of metastatic CRC have HER2 amplifications, and are candidates for dual HER2 targeted therapy with trastuzumab and pertuzumab.¹⁸ After years of efforts at targeting mutant *KRAS*, new *KRAS* G12C inhibitors are now in clinical development and hold promise for about 3% of metastatic CRC patients whose tumors are *KRAS* G12C mutated (NCT03600883). Immunotherapy has resulted in durable responses and is indicated in microsatellite instability high (MSI) metastatic CRC, which comprises 3-4% of patients.^{19, 20} The more common microsatellite stable (MSS) CRC do not respond to immunotherapy, and new combination strategies are under investigation. Targetable gene fusions (e.g., *RET*, *NTRK1*, *FGFR2/3*, *ALK*, *ROS1*) have also been identified in rare cases of CRC.^{21, 22} Despite these successes of precision oncology, the vast majority of CRC patients lack the relevant biomarkers to qualify for these therapies.

The PI3K-AKT signaling pathway:

The phosphoinositide 3-kinase (PI3K) signaling pathway alterations are common, and implicated in cancer growth, proliferation and angiogenesis in many

cancer types. Class I PI3K comprise a p110 catalytic domain which has four isoforms (α , β , δ and γ which are coded by *PIK3CA*, *PIK3CB*, *PIK3CD* and *PIK3CG* genes respectively) and a regulatory domain. PI3K may be activated by ligand-bound membrane receptor tyrosine kinases, G-protein-coupled receptors, receptor amplification or alterations resulting in constitutive activation of pathway proteins. Activated Ras from MAPK signaling pathway may also bind to and activate p110.²³ Activated PI3K phosphorylates phosphatidylinositol 4,5-bisphosphate to form phosphatidylinositol-3,4,5-trisphosphate (PIP3), which subsequently brings pleckstrin homology (PH) domain-containing proteins in proximity to the plasma membrane, including phosphoinositide-dependent kinase 1 (PDK1) and protein kinase B (AKT).²⁴ AKT is a serine/threonine kinase that requires phosphorylation at T308 by PDK1 and at S473 by TORC2 for full activation. Activated AKT then phosphorylates several downstream targets implicated in cell growth and protein synthesis, cell survival, cell proliferation and angiogenesis.²³⁻²⁵

PI3K signaling is regulated in several ways.^{25, 26} The PI3K regulatory domain inactivates the kinase activity of the catalytic domain in the basal state. Pathway activation is terminated by the phosphatase PTEN which dephosphorylates PIP3. Hence, loss of PTEN (PTEN^{loss}) either through epigenetic silencing, inactivating mutations or biallelic copy number loss, results in PIP3 accumulation at the membrane and pathway activation. PI3K-AKT pathway activation also results in feedback suppression of RTK signaling via mTORC1/S6K dependent degradation of insulin receptor substrates (IRS), stabilization of growth factor receptor bound protein 10 (GRB10), and inhibition of HER and IGF1R/IR tyrosine kinases. PI3K-

AKT pathway activation also decreases RTK transcription via phosphorylation and cytosolic sequestration of FOXO family members.²⁵⁻²⁷

The pathologic role of class II and class III PI3K in cancer is not clear and is not discussed here. The schematic of PI3K-AKT signaling pathway is shown in Figure 1.

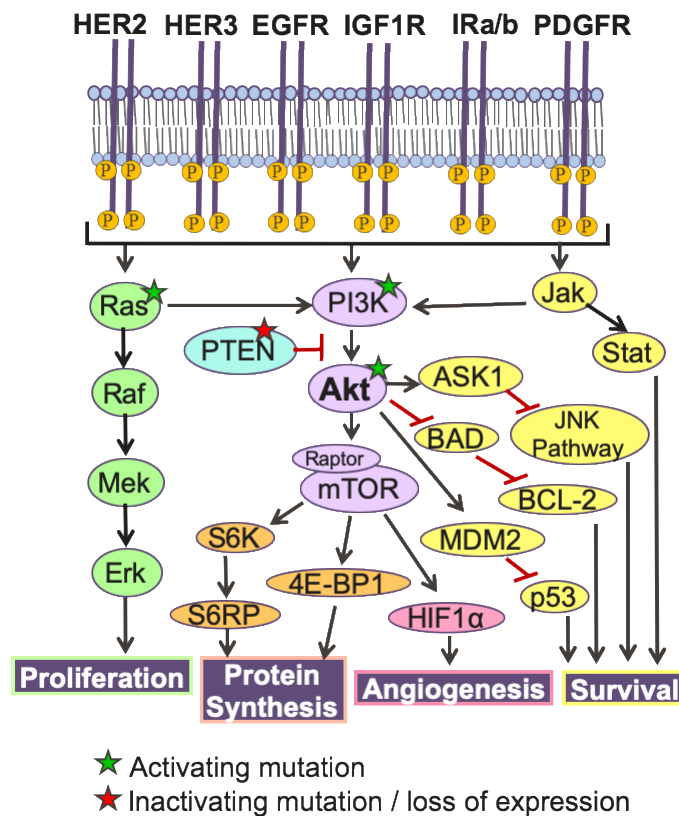


Figure 1: A schematic of PI3K-AKT signaling pathway and its interaction with parallel oncogenic signaling pathways.

PI3K pathway alterations in colorectal cancer:

In CRC, the PI3K pathway may be activated by PTEN^{loss} in 20-40% of patients, activating *PIK3CA* mutations (*PIK3CA*^{mut}) in ~15% of patients, or upstream activation of receptor tyrosine kinases such as HER2 amplifications in 2-4% of patients.²⁸⁻³¹ PI3K pathway activation is an adverse prognostic factor for CRC.³² Higher PI3K expression is seen in metastatic CRC as compared to primary tumors.³³ PI3K pathway alterations may also have treatment implications for CRC patients. PI3K signaling activation can increase proliferation of LGR5+ CRC stem cells and contribute to chemotherapy resistance.³⁴ *PIK3CA* mutations may confer intrinsic resistance to treatment with anti-EGFR monoclonal antibodies.³⁵ Emergence of *PIK3CA* mutations has been reported to confer acquired resistance to anti-EGFR therapy.³⁶ A subgroup analysis of the My Pathway trial of dual HER2-targeted therapy (trastuzumab and pertuzumab) for HER2 positive CRC patients showed less response rate in *PIK3CA*^{mut} patients as compared to *PIK3CA* wild-type (*PIK3CA*^{wild}) patients (13% vs 43%).¹⁸ In Nurses' Health Study and Health Professionals Follow Up study which mostly comprised early stage CRC patients, regular use of aspirin was found to be associated with longer CRC-specific survival and overall survival among *PIK3CA*^{mut} as compared to *PIK3CA*^{wild} cases, suggesting a role for aspirin in secondary prevention of *PIK3CA*^{mut} CRC.³⁷

PI3K pathway inhibition in colorectal cancer:

Several drugs have been developed for targeted inhibition of one or more components of the PI3K-AKT pathway. Evaluation of targeted inhibition of the PI3K

pathway in CRC is underway, but monotherapy has been inactive.^{29-31, 38-40} Table 1 summarizes clinical trials using single agent PI3K-AKT pathway inhibitors in CRC patients.

Trial Number	Trial Name	Results
NCT01802320	Phase 2 study of MK-2206 in previously treated metastatic CRC patients enriched for PTEN loss and <i>PIK3CA</i> mutation	ORR = 0, PFS = 6.8 (5.83 to 7.77), OS = 1.87 (1.83 to 1.90)
NCT01186705	Phase 2 clinical and translational study of MK-2206 in patients with metastatic <i>KRAS</i> wild-type, <i>PIK3CA</i> -mutated CRC	Closed due to lack of accrual
NCT00419159	Phase 2 study of Everolimus in patients with metastatic CRC refractory to an anti-EGFR antibody (if appropriate), Bevacizumab, Fluoropyrimidine, Oxaliplatin, and Irinotecan-based regimens	No meaningful clinical activity
NCT00390364	Phase 2 study of single agent RAD001 (Everolimus) in patients with CRC and activating mutations in the <i>PIK3CA</i> gene	Closed due to low accrual
NCT00337545	Phase II trial of RAD001 in patients with refractory CRC	Results not published
NCT00827684	Phase 2 study of Temsirolimus alone or with Irinotecan in chemotherapy refractory patients with <i>KRAS</i> mutated metastatic CRC (TIRASMUS)	In monotherapy arm, ORR = 0; SD 38%; median PFS 45 days.

Table 1: Clinical trials using single agent PI3K/AKT signaling pathway inhibitors in colorectal cancer patients.

Several factors have been implicated in limiting the successful development to PI3K-AKT pathway inhibitors. These include weak oncogenic activity of PI3K alterations or presence of co-occurring oncogenic driver alterations, suboptimal patient selection in clinical trials without PI3K pathway dependence and failure to exclude patients with other driver alterations, inadequate pharmacodynamic (PD) inhibition or dose limiting toxicities, loss of inhibitory feedback loops resulting in pathway reactivation, emergence of gene alterations conferring acquired resistance, and increase in insulin secretion on PI3K α inhibition.^{26, 41, 42}

A phase 2 study of MK-2206 in previously treated metastatic CRC patients with PTEN^{loss} and *PIK3CA*^{mut} was conducted at MD Anderson (NCT01802320) and achieved an objective response rate of 0%. The mechanisms behind this clinical inactivity of MK2206 in biomarker selected CRC are unknown, yet vital to development of more effective therapies. These include assessment of PD inhibition as well as of adaptive changes in cell signaling in response to AKT inhibition such as through loss of suppression of feedback pathways as shown in Figure 2.^{26, 43}

Hypothesis 1: “AKT inhibition is ineffective in colorectal cancer despite adequate pharmacodynamic inhibition due to activation of alternate signaling pathways.”

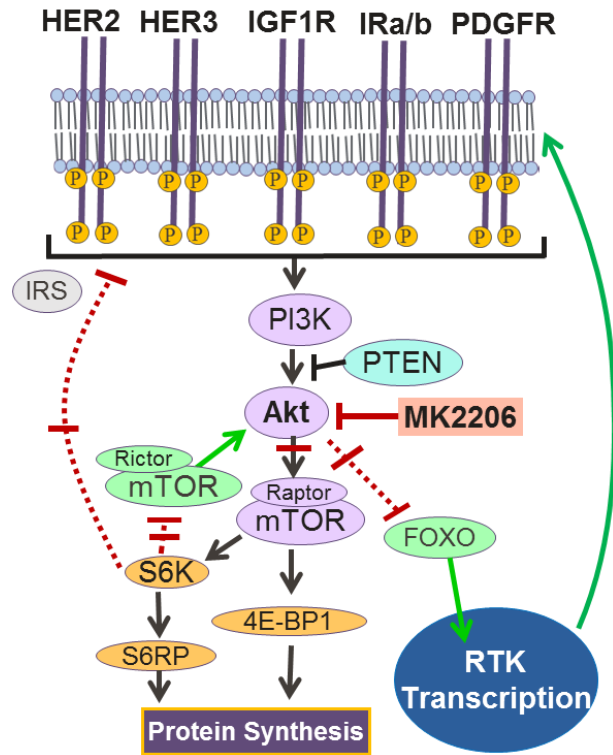


Figure 2: Feedback inhibition loops in PI3K-AKT signaling pathway and potential loss of inhibition after treatment with allosteric AKT inhibitor (MK2206).

Immune microenvironment of colorectal cancer:

Anti-tumor immune microenvironment influences the prognosis of CRC patients.⁴⁴⁻⁴⁸ Higher CD8⁺ T cell infiltrate is associated with improved disease free survival and less advanced CRC.^{44, 46, 49} CRC with high memory T cell infiltration have decreased dissemination and less lymphovascular invasion.⁵⁰ Furthermore, high expression of genes associated with TH1 immunity correlates with cytotoxic T cell mediated immune response and is associated with less tumor recurrence.⁴⁶ Immunoscores have been developed integrating the densities of cytotoxic and memory T cells at the center of tumor as well as at the invasive margin, and have shown to predict disease free survival of CRC patients beyond TNM stage and microsatellite stability status.^{46, 47, 51, 52}

The immune microenvironment of CRC is not uniform across all subtypes. While tumors with MSI have a fairly uniform gene expression signature, MSS CRC is a heterogeneous group with differential expression of immune related genes in various subsets.⁵² The durability of responses seen with single agent immunotherapy in MSI CRC is a testament to the power of an effective anti-tumor immune response in controlling a lethal disease.¹⁹ High tumor-associated cytotoxic T cell infiltrate before treatment has been shown to be predictive of response to immunotherapy.⁵³ Notably, a handful of patients with MSS CRC have responded to immunotherapy combinations, and this may be expanded through a rational mechanistic combination approach.⁵⁴⁻⁵⁶ It is of great importance to improve our understanding of the genomic modulators of immune microenvironment of MSS CRC, in order to develop therapeutic interventions aimed at improving anti-tumor

immune repertoire while decreasing the immunosuppressive mediators, and also to identify subsets of MSS CRC that would benefit from immune targeted treatments.^{57,}

58

PI3K pathway and tumor immune microenvironment:

The PI3K signaling pathway is a known modulator of anti-tumor immune response.⁵⁹⁻⁶³ PI3K activation due to PTEN^{loss} suppresses tumor immune microenvironment by decreasing tumor infiltrating T cells and upregulating immune inhibitory cytokines and checkpoints in other cancers.^{61, 62} Higher PD-L1 protein expression has been noted in PTEN^{loss} CRC cell lines.⁶³ PD-1/PD-L1 interactions negatively regulate the CD8+ cells in the tumor.⁶⁴ Non-response to immunotherapy is associated with PTEN^{loss} and lower pre-treatment intratumoral cytotoxic T cells.^{53, 57, 58} PI3K inhibition improves intratumoral cytotoxic T cell infiltration and function in murine models of melanoma.⁶² Isoform-selective inhibition of PI3K α and PI3K β yields a higher immune response as PI3K δ and PI3K γ inhibition has been associated with immunologic impairment.^{61, 65} Increasing intratumoral CD8+ cell infiltration with PI3K pathway inhibition and increasing T cell activation through checkpoint blockade is a rational combination strategy that has shown promise in mouse models of different cancers.^{62, 66, 67} The immune repertoire of PI3K pathway altered CRC patients is yet to be determined, and is important to investigate given the potential for therapeutic immunomodulation.

Hypothesis 2: “PI3K activating alterations suppress the tumor immune microenvironment of colorectal cancer patients.”

Specific Aims:

Specific Aim 1: Demonstrate pharmacodynamics inhibition of AKT pathway in tumor and surrogate tissue from a clinical trial of MK2206 in colorectal cancer

Specific Aim 2: Determine the mechanisms of adaptive resistance to AKT inhibition in PI3K activated colorectal cancer patients, patient derived xenografts and cell lines.

Specific Aim 3: Evaluate the impact of PI3K activating alterations on immune landscape of colorectal cancer, and design a therapeutic intervention to improve the immune microenvironment.

Chapter II: Methods

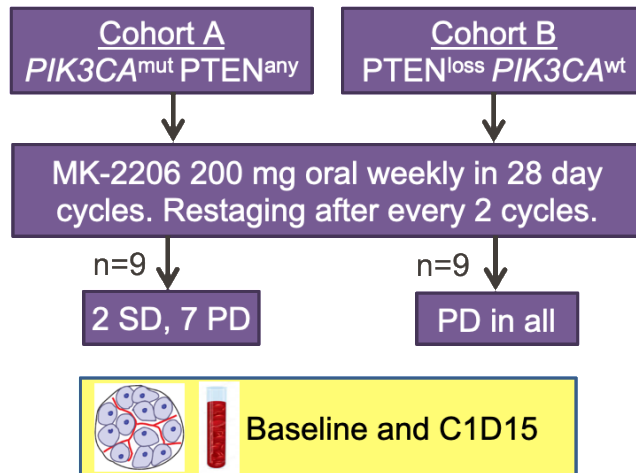
We employed three model systems in our project:

1. Patient samples from clinical trial with MK2206 collected at baseline and day 15 of cycle 1 (C1D15), 20 to 28 hours after dose.
2. Patient-derived xenograft (PDX) model of PTEN^{loss} metastatic CRC
3. Three cell lines treated with MK2206: KM12L4, SW480 and MDA468

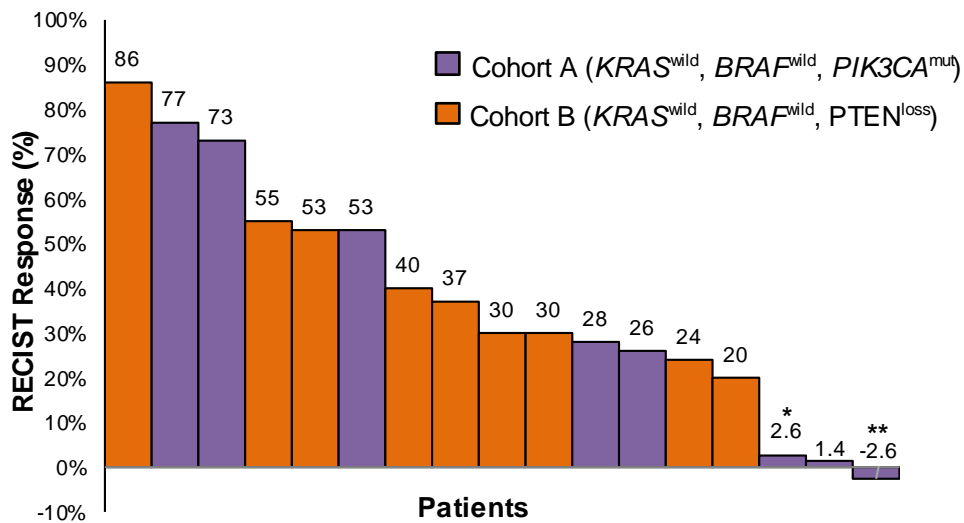
Clinical Trial of AKT inhibitor:

An NCI CTEP sponsored phase II clinical trial with MK2206 (an allosteric AKT inhibitor) in previously treated CRC patients was conducted at MD Anderson Cancer Center (NCT01802320, PI: Dr E. Scott Kopetz) between March 2013 to July 2015. The trial enrolled previously treated metastatic CRC patients with either PTEN^{loss} or *PIK3CA*^{mut}. Patients with *KRAS* and *BRAF* mutations were excluded due to oncogenic MAPK signaling activation which is parallel to the AKT pathway. MK2206 was administered orally at 200 mg per week until unacceptable toxicity or progression. Response was assessed with repeat imaging every 2 months using Response Evaluation Criteria in Solid Tumors (RECIST) version 1.1. Out of 18 patients treated on the trial, 16 progressed and 2 had stable disease. Paired tumor biopsies and blood samples were collected at baseline and C1D15 for translational studies.⁶⁸

(A)



(B)



*Progressive non-target peritoneal carcinomatosis

**Stable disease for 7 months, then passed

1 patient communicated progression after 1 cycle, but did not return for restaging scans

Figure 3: Phase 2 clinical trial of MK2206 in previously treated metastatic colorectal cancer

patients with $PTEN^{loss}$ or $PIK3CA^{mut}$. (A) Study schema. (B) Waterfall plot.

Patient sample collection:

Tumor and blood samples were collected pre-treatment, 20 to 28 hours after MK-2206 dosing on Cycle 1 day 15, and optionally at the time of disease progression. Tumor samples were collected via an imaging-guided biopsy of a metastatic site. In most cases, biopsy was taken from liver metastases. At least 4 fine needle aspirations (FNAs) and 3 core biopsies were obtained. Three FNAs were immediately frozen in liquid nitrogen and then stored in -80°C for use in proteomic analysis using reverse phase protein array (RPPA). One FNA was placed in RNA-later and then stored in -80°C for transcriptional profiling. Two core biopsies were immediately placed in formalin, and one core biopsy was immediately frozen in optimal cutting temperature (OCT) compound. Blood samples were collected by venipuncture, separated into peripheral blood mononuclear cells (PBMC) and platelet-rich plasma, and stored in -80°C in the presence of phosphatase and protease inhibitors.

Patient derived xenograft model development and treatment:

A $\text{PTEN}^{\text{loss}}$ PDX model was generated from liver metastases biopsy of one of the patients in the MK2206 clinical trial, implanted subcutaneously into SCID mice. When the tumors reached 1.5 cm^3 , passage 2 tumor-grafts (F2) were established using 3 mm^3 pieces implanted subcutaneously. The PDXs were treated by oral gavage with either MK2206 (n=12) or 30% Captisol carrier (n=12) thrice a week for 3 weeks. MK2206 treatment was started at 120mg/kg, and dose reduced to 80 mg/kg with dose 5 due to weight loss. Treated PDXs showed slower tumor growth as

compared to controls, and a transient response best seen around day 8. All PDXs eventually progressed. On day 24, the mice were euthanized in CO2 chamber. Tumor tissues and blood were harvested. A portion of the tumor was immediately frozen in liquid nitrogen and then stored in -80°C for use in proteomic analysis using reverse phase protein array. A portion of the tumor was placed in formalin and later embedded in paraffin for immunohistochemistry. PDX development and mouse treatments were performed by a former post-doctoral fellow, Dr Jisu Oh, in Kopetz lab. All mouse work was performed in compliance with institutional guidelines and American Association for Accreditation of Laboratory Animal Care, U.S.

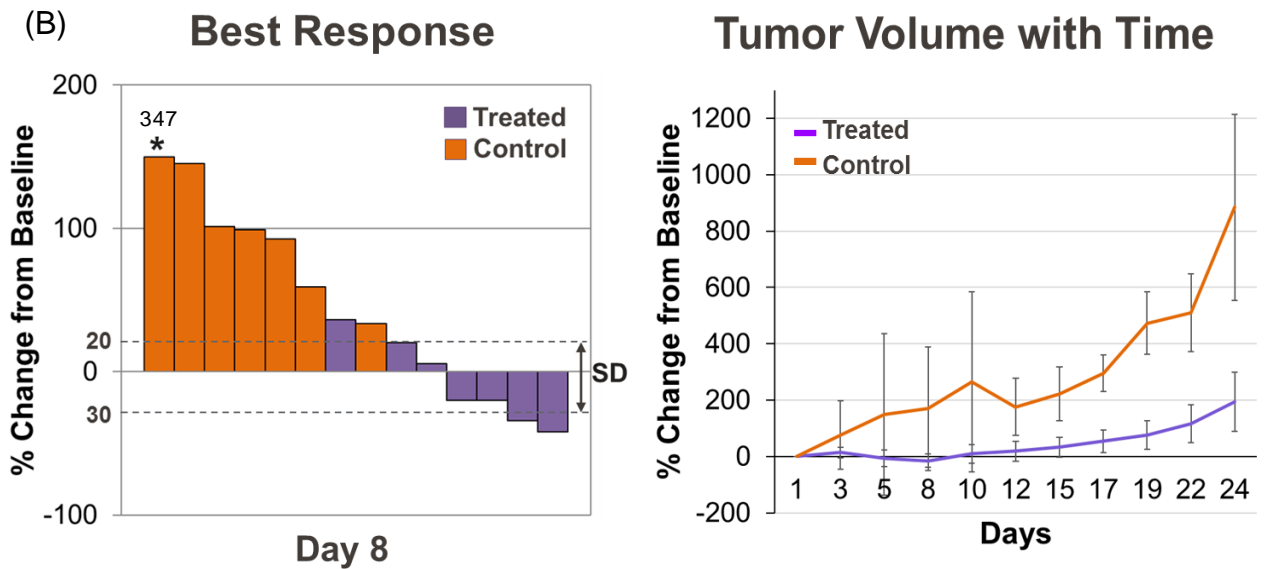
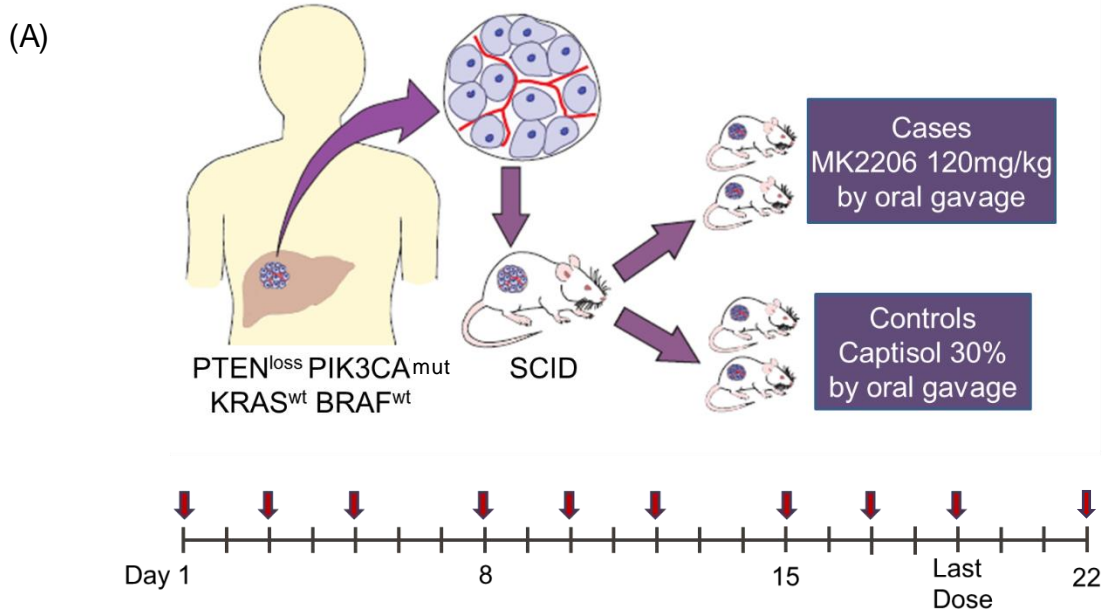


Figure 4: PTEN^{loss} Patient derived xenograft trial with MK2206 vs 30% Captisol control (12 mice in each arm). Treated PDXs showed slower tumor growth as compared to controls, and a transient response best seen around day 8. All PDXs eventually progressed. (A) Study schema. (B) Response assessment. Error bars represent standard error of mean (SEM).

Cell line treatment:

Three 3 cell lines were treated with MK2206: KM12L4, SW480 and MDA468. KM12L4 is a colon carcinoma cell line with MSI and PTEN^{loss}.⁶⁹ SW480 is an MSS *KRAS* mutant colon adenocarcinoma cell line with intact PTEN.⁶⁹ MDA468 is metastatic breast cancer cell line with absent PTEN protein expression.⁷⁰ Cell lines were cultured in growth medium at 37°C with 5% CO₂, passaged at 70% confluence with phosphate-buffered saline rinse and trypsinization. 5000 cells were suspended in 50 µL media with 0.1% DMSO, and co-cultured with 50 µL MK2206 in 96 well plate. Control was plated with 50 µL cell suspension and 50 µL media with 0.1% DMSO. Blank was plated with 100 µL media with 0.1% DMSO. Cell samples were collected at different time points for proteomic analysis.

Reverse phase protein array (RPPA):

Proteomic profiling was performed using RPPA through our functional proteomics core facility as previously described.⁷¹ RPPA used unique primary antibodies to assess expression levels of 290-305 proteins and phospho-proteins in each sample. Briefly, lysis buffer was used to lyse frozen tumor tissue, PBMCs and cells. Lysates' protein concentrations were measured using bicinchoninic acid assay (BCA) and adjusted to 1 µg/µL concentration using lysis buffer. Lysates were then boiled with 1% SDS. Five 2-fold serial dilutions of lysates were prepared (undiluted to 1:16). Lysates were arrayed on nitrocellulose-coated slides, probed with antibodies by tyramide-based signal amplification approach, and visualized by DAB colorimetric reaction. Each antibody stained slide underwent quality control (QC)

tests, and a QC Score above 0.8 was considered good antibody staining. The slides were scanned, and staining was quantified on Array-Pro Analyzer. Relative protein levels for each sample was determined by interpolation of each dilution curve from the "standard curve" (supercurve) of the antibody-stained slide. Standard curve was constructed using SuperCurve R package, and values generated were defined as Supercurve Log2 (Raw) values. All the data points were normalized for protein loading and transformed to linear value, designated as "Normalized Linear". "Normalized Linear" values were transformed to Log2 values, and then median-centered for analysis.

Mouse Immunohistochemistry (IHC) for IGF1R:

Mouse IHC was performed at Science Park Research Histology, Pathology and Imaging Core laboratory. Briefly, formalin fixed paraffin embedded mouse tumor tissue sections were deparaffinized and hydrated in xylene followed by graded alcohols (100%, 95% ETOH) to water. Endogenous peroxidase activity was blocked with 3% H₂O₂ in water for 10 minutes, then washed. Antigen was retrieved with 1.0mM EDTA pH 8.0 in a microwave oven for 10 minutes under standardized conditions, cooled down for 20 minutes, then water washed. Non-specific antibody binding was blocked by incubating slides with Biocare Blocking Reagent # BS966M (Casein in buffer) for 10 minutes. Slides were drained and incubated with primary IGF-1R beta rabbit polyclonal antibody (Cell Signaling #3027) at a 1:200 dilution overnight at 4°C, and then buffer washed for five minutes, changing once. Slides were then incubated with Envision plus labeled polymer, anti-rabbit-HRP (Dako) for

30 minutes at room temperature, then buffer wash five minutes, changing once. Slides were incubated with Dako DAB monitoring staining development. Slides were then washed, counterstained, dehydrated, and made ready for viewing under the microscope.

PTEN IHC:

PTEN^{loss} is defined as complete loss of staining with preservation of expression of stromal components in whole mount slides. IHC for PTEN^{loss} was performed on 4µm FFPE tissue sections using a United States Clinical Laboratory Improvement Act (CLIA) assay at MD Anderson clinical IHC laboratory as previously described.⁷² Briefly, tissue sections were deparaffinized and rehydrated. Antigen retrieval was performed at 100 °C for 20 minutes with Tris-EDTA buffer, pH 6.0. Endogenous peroxidase was blocked with 3% peroxide for 5 minutes. Primary anti-human PTEN antibody (Dako, clone 6H2.1, isotype IgG2a kappa) was applied at 1:100 dilution and detected using a commercial polymer system (Bond Polymer Refine Detection, Leica). Staining development was achieved by incubation with DAB and DAB Enhancer (Leica).⁷²

IHC for immune markers:

Immune infiltrates and checkpoints were evaluated using quantitative IHC for both center of tumor (CT) and invasive margin (IM) on primary CRC specimens at MD Anderson Cancer Centers' Immunotherapy Platform. IHC staining was performed using primary antibodies to detect CD3 (all T cells), CD4 (helper T cells), CD8 (cytotoxic T cells), CD45RO (memory T cells), FOXP3 (regulatory T cells),

Granzyme B (activated T cells), CD20 (B cells), CD57 (NK cells), CD68 (macrophages), immune checkpoints (ICOS, OX40, PD-1, PD-L1 epithelial cells, PD-L1 immune cells, VISTA, LAG3), and human leukocyte antigens (HLA immune cell, HLA epithelial cell). Slides were scanned using the scanscope system (Scanscope XT, Aperio/Leica), and analyzed using image analysis software (ImageScope-Aperio/Leica). Five random areas (at least 1 mm² each) were selected, and scores for each marker were averaged over the areas analyzed. Percent of positive cells was calculated using a customized algorithm specific for each marker. Density of immune infiltrates was defined as the number of positive cells per mm³. H-score (0 to 300) was defined as the percentage of cells positive for membrane staining (0 to 100) multiplied by the staining intensity (0 to 3+).

Gene expression analysis:

Gene expression data was obtained for immuno-regulatory messenger RNAs (mRNA) using Agilent microarrays (Agilent Technologies, Santa Clara, CA, USA) at Clinical Laboratory Improvement Amendments accredited Agendia's laboratories. Briefly, RNAs were isolated from tumor containing areas in frozen tissue sections. After quality assessment, RNA was amplified, labelled and hybridized to the microarray. The following immune markers were assessed: angiogenesis markers VEGF, VEGFA, VEGFB and VEGFC; immune checkpoints ARG1, BTLA, C10orf54 (VISTA), CTLA-4, PDCD1 (PD-1), CD274 (PD-L1), PDCD1LG2 (PD-L2), HAVCR2 (TIM-3), TIGIT, IDO1 and IDO2; co-stimulatory molecules CD80 and ICOS; cytotoxic T cells CD8A, GZMA, GZMB and PRF1; NK cells CD244 (precursor) and CD160 (peripheral blood); dendritic cells CD209 and CD207; macrophages CD14 and

CD68; human leukocyte antigens (HLAs) HLA-A, HLA-B, HLA-C, HLA-DMA, HLA-DMB, HLA-DOA, HLA-DOB, HLA-DPA1, HLA_DRA, HLA_DRB1, HLA-DRB5, HLA-E, HLA-F, HLA-G; and others B2M, CD1A. Data are shown as z-scores.

Mutation profiling:

DNA analysis for *PIK3CA*, *BRAF*, *KRAS* and other mutations was performed at MD Anderson Cancer Center using Sanger sequencing, mass spectroscopy-based multiplex assay for hotspot regions in 11 genes (Sequenom), or Ion Ampliseq-based next-generation sequencing for hotspot regions in 46 genes (Life Technologies).

Patient Characteristics:

Electronic medical charts of patients were reviewed to obtain gender, age at the diagnosis, tumor side, recurrence and other clinical parameters. Pathology reports were reviewed in electronic medical charts to obtain information on tumor grade, mucinous differentiation, lymphovascular invasion, perineural invasion and pathologic stage. For patients whose primary tumor was resected outside of MD Anderson, pathology review was obtained at MD Anderson.

CT26 study:

BALB/C-e mice were obtained from Charles River. One million CT26 cells were implanted on right flank. Treatment was started 48 hours after implantation and continued for 21 days. Copanlisib (SelleckChem, S2802) was administered via tail vein at 10 mg/kg twice a week. Anti-PD-1 (Biolegend, GolnVivo purified anti-mouse

CD279, Clone: 29F.1A12) was administered at 200 µg intraperitoneally twice a week. Controls were treated with IgG2a k isotype (Biolegend, Ultra-LEAF Purified Rat IgG2a k isotype, Clone: RTK2758) intraperitoneal and with copanlisib vehicle (PEG400 20% v/ 80% acidified water, pH 3.5, 0.1N). Mice were weighed and tumors measured at baseline, then weekly. On day 20, mice were euthanized in CO₂ chamber. Blood was collected via heart puncture and plasma was separated for freezing in -80 °C. Tumor tissue was harvested. A portion of the tumor was placed in formalin and later sent for paraffin embedding and multiplex IHC for immune markers. A portion of the tumor was placed in RNA later for RNA analysis, and a portion was immediately frozen in liquid nitrogen for proteomic profiling.

Statistical Analysis:

Aims 1 and 2: Protein levels from treated and untreated samples were compared by paired or student's t-test, or ANOVA as applicable. Strength of relationship between change in levels of different PI3K-AKT signaling pathway proteins was assessed using Pearson correlation. A 2-sided test $P < 0.05$ was considered to be statistically significant. Data was analyzed in SPSS v. 23 and visualized using Tableau v. 9.2. Cross-correlation matrix was created using R studio.

Aim 3: The demographic and clinical characteristics of patients are presented using descriptive statistics. Clinicopathologic data was examined for potential associations with PI3K pathway alterations. Patients were grouped by presence or absence of either $PTEN^{loss}$ or $PIK3CA^{mut}$. $PTEN^{loss}$ and $PIK3CA^{mut}$ are not mutually exclusive and were collectively termed PI3K pathway alterations. MSI and MSS

tumors were analyzed separately. In the light of known differences in immune microenvironment of MSI and MSS tumors, analysis was focused on MSS CRC. Groups were compared using independent sample t test, Mann-Whitney U test, Wilcoxon signed rank test, Chi-square or Fisher's exact test as appropriate. A 2-sided test $P < 0.05$ was considered to be statistically significant. Data was analyzed in SPSS v. 23. Comparisons between groups were visualized using Tableau v. 9.2. Hierarchical clustering was performed on gene expression data in Cluster v. 3.0. Multivariate logistic regression analysis was performed for immune infiltrates, MSS status and PI3K pathway status.

Chapter III: Results

Aim 1: Demonstrate pharmacodynamics inhibition of AKT pathway in tumor and surrogate tissue from a clinical trial of MK2206 in CRC

Using RPPA, we investigated protein expression of PD markers of AKT inhibition in patients' tumors, PDXs and cell lines. Analyzed samples included 15 paired tumor biopsies from patients collected at baseline and at C1D15 of treatment with MK2206; 9 treated PDXs and 10 control PDXs; and 3 cell lines at 13 time-points during treatment with MK2206 (0 hours, 0.5 hours, 1 hour, 2 hour, 4 hour, 8 hour, days 1-7).

As compared to cell lines, PD markers were inhibited to a lesser extent in PDXs and patients. Figure 5.

Treated PDX mice had significant reduction in levels of AKT pS473, AKT pT308, FoxO3a pS318/S321 and p70-S6K pT389 as compared to controls ($p < 0.02$ for all). Other PD markers showed a non-significant decreasing trend. These include S6 pS235/S236, GSK3a/b pS21/9, 4E-BP1 pS65 and PRAS40 pT246.

In patients' tumors, there was a non-significant trend towards decrease in some of the PD markers after treatment, including AKT pS473, S6 pS235 S236, FoxO3a pS318 S321.

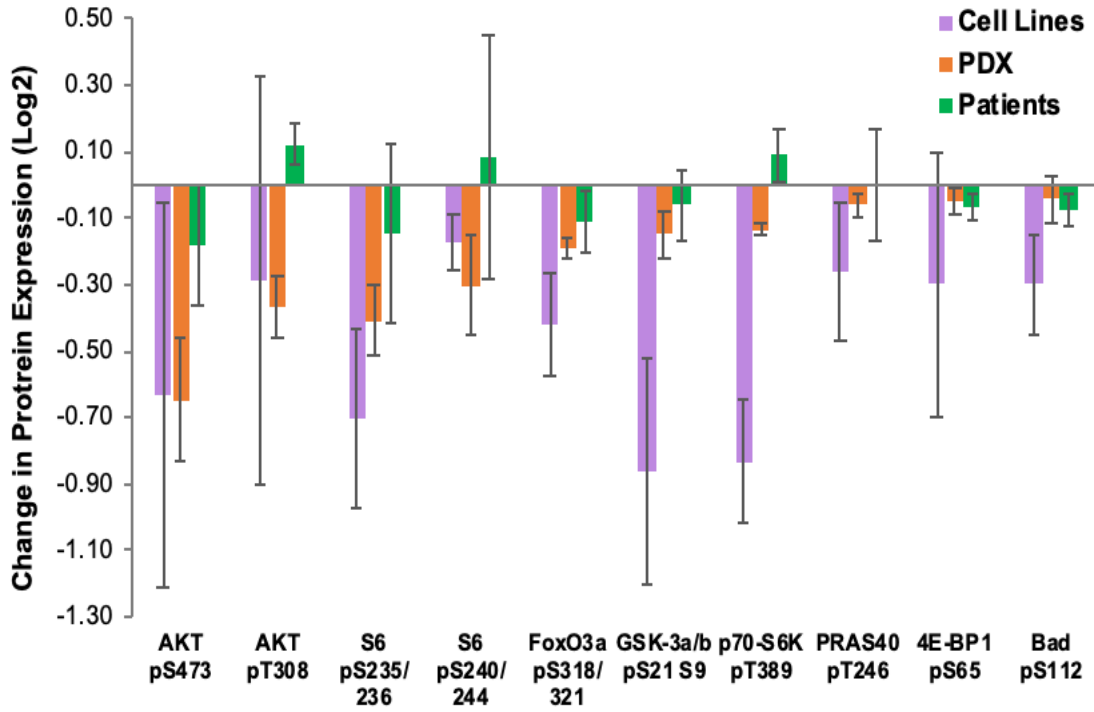


Figure 5: Change in protein expression of pharmacodynamic markers after AKT inhibition with MK2206 among patient tumors, patient-derived xenografts and cell lines. Cell line data is shown at 8 hours of treatment. Error bars represent standard error of mean.

In cell lines, a decrease in AKT pT308 and pS473 was observed within 30 minutes of treatment, which was then sustained throughout treatment. PD inhibition of downstream markers of PI3K signaling S6 pS235/236 and S6 pS240/244 continued to deepen significantly with treatment over time approaching 70% inhibition by day 7 (ANOVA $p < 0.01$ for both). Figure 6.

In 15 paired tumor biopsies of patients, the ratio of AKT pS473 to total AKT decreased to a median of 37.92% (IQ range -26% to -46%, maximum -64.6%). Four out of 15 patients (26.7%) had at least 50% inhibition of AKT pS473. Phosphorylation of AKT at site T308 was decreased to a lesser degree (median -5%, IQ range -40% to +6%). Only 1 patient had >50% decrease in phosphorylation at both sites relative to total AKT levels. Change in PD markers in patients' tumors is shown in Figure 7.

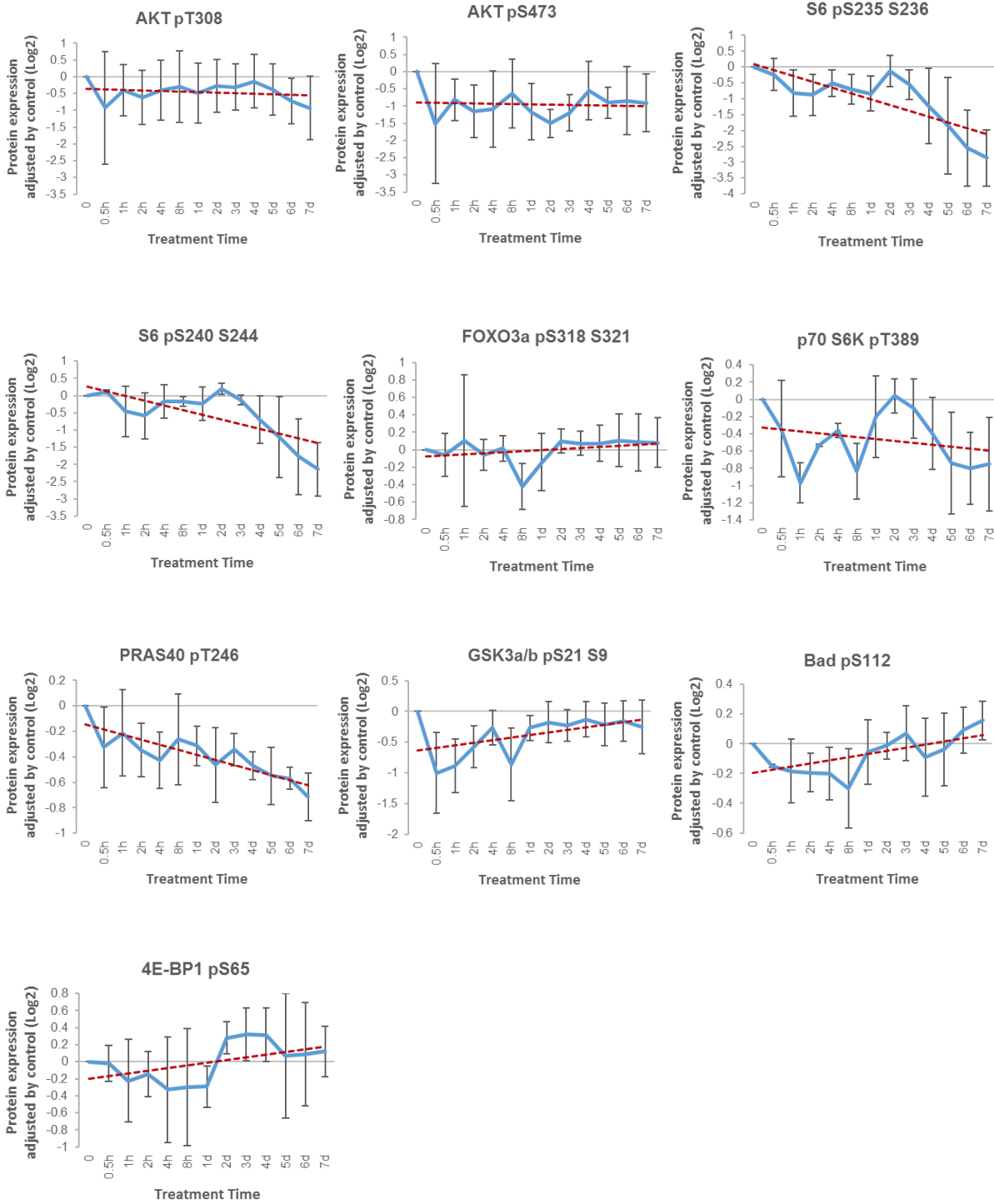


Figure 6: Change in protein expression of pharmacodynamic markers of AKT inhibition in three cell lines (KM12L4, SW480, MDA468) at different time-points during treatment with MK2206. Error bars represent standard error of mean.

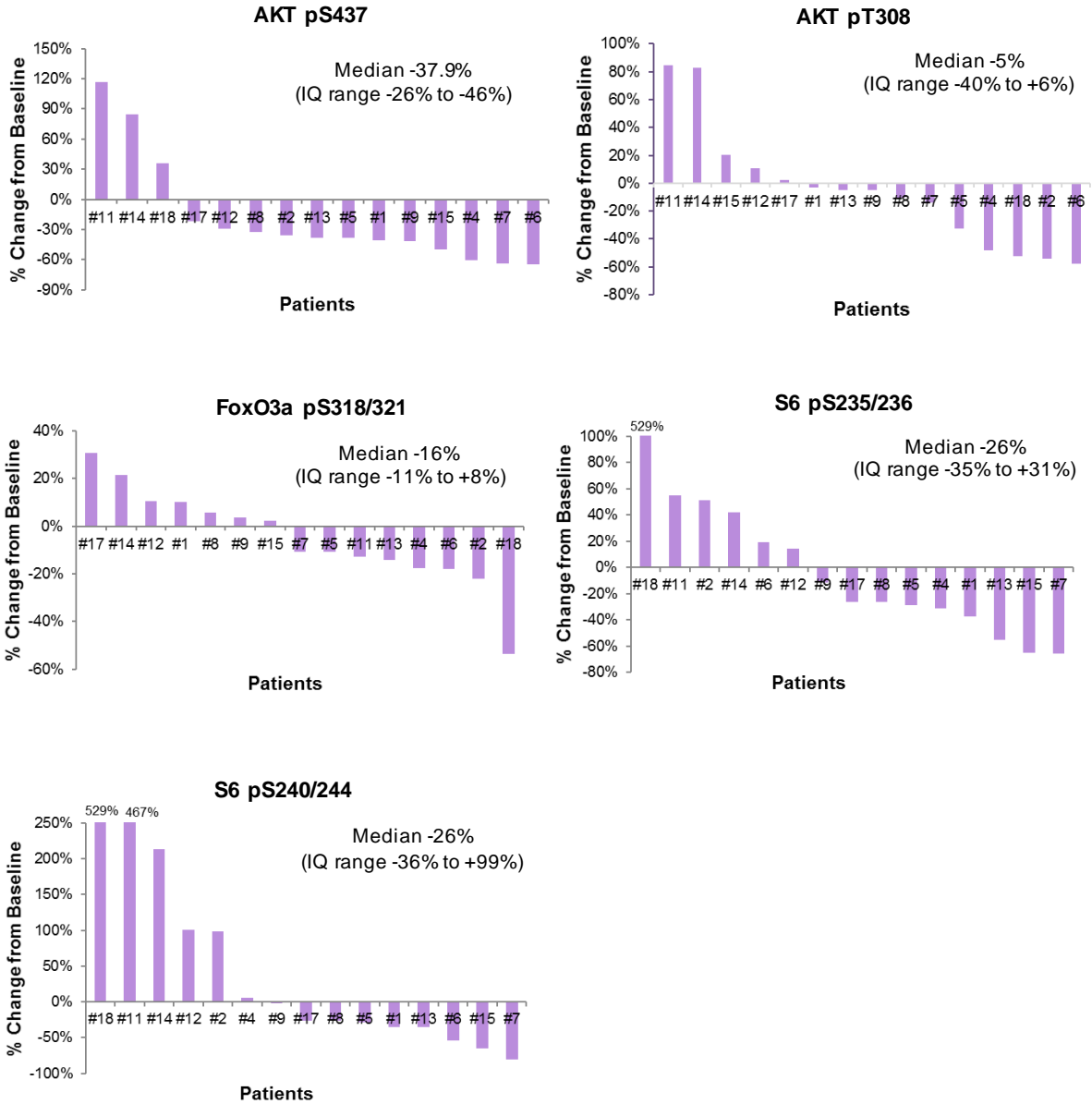


Figure 7: Change in protein expression of pharmacodynamic markers of AKT inhibition in patients' tumors using paired biopsies at baseline and C1D15 of treatment with MK2206.

Each column represents a patient.

Correlation analysis of RPPA data from paired patient tumor biopsies showed several clusters (Figure 8). I examined the correlation between AKT pS473 levels and remote PD markers, such as p70-S6K1 in individual patients to look for sustained changes in the PI3K signaling (Table 2) As expected, there was a direct correlation between change in AKT pS473 levels and changes in downstream phosphorylated p70 and pS6 proteins levels. Furthermore, AKT pS473 levels also correlated inversely with IRS levels and the levels of phosphorylated receptor tyrosine kinases, namely pIGF1R and pHER2, consistent with the loss of feedback inhibition as has been described by other labs (Figure 9). AKT pT308 levels did not correlate with AKT pS473 levels or with the downstream PD markers, suggesting that it is not a reliable PD marker for MK2206.

Interestingly, AKT pS473 had a significant inverse correlation with one PD marker, FoxO3a pS318/321. This suggests that adaptive changes induced by decrease in FoxO3a pS318/321 may be re-phosphorylating AKT S473. This is discussed in detail in Aim 2.

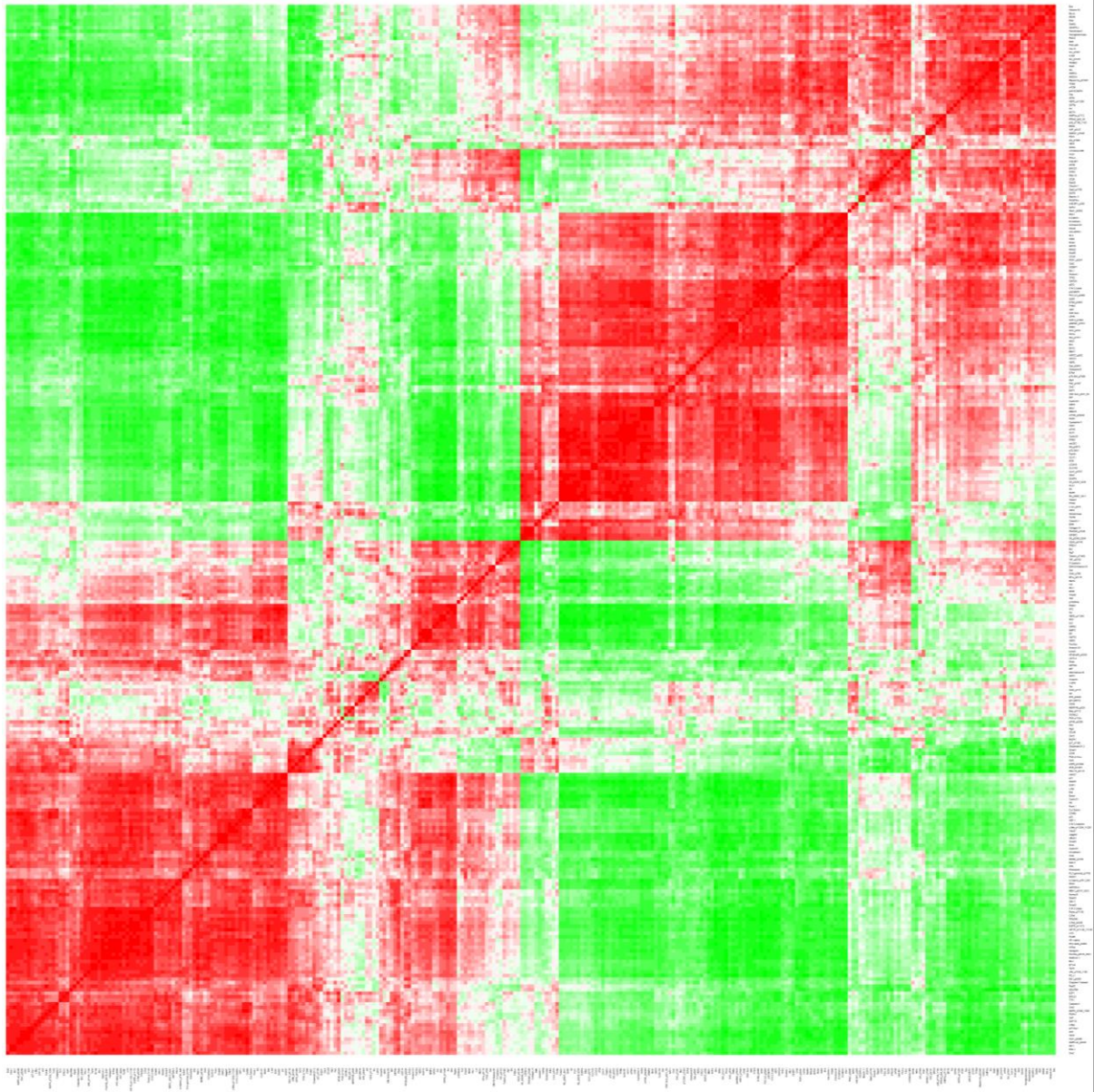


Figure 8: Correlation matrix of change in protein levels after AKT inhibition in CRC patients shows distinct clusters.

PI3K pathway proteins	Pearson Correlation Coefficient 'r'	P value
AKT pT308	0.15	0.589
S6 pS235/236	0.95	<0.001
S6 pS240/244	0.80	<0.001
p70 S6K1	0.89	<0.001
p70 S6K pT389	0.68	0.006
IRS1	-0.79	<0.001
IGF1R pY1135/1136	-0.66	0.008
HER2 pY1248	-0.73	0.002
FoxO3a pS318/321	-0.71	0.003

Table 2: Correlation between changes in levels of AKT pS473 and downstream PI3K signaling proteins in patients after treatment with MK2206.

	PDGFRb	EGFR	AKT pT308	VEGFR2	HER3 pY1289	AKT	IGF1R	IRb	HER2	AKT pS473	p70-S6K pT389	p70 S6K1	S6 pS235/236	S6 pS240/244	IRS	HER2 pY1248	HER3	pIGF1R	FoxO3a pS318/321	FoxO3a
PDGFRb	1	0.36	-0.29	0.44	0.28	0.52*	0.39	0.32	-0.13	-0.28	-0.37	-0.21	-0.3	-0.54*	0.09	0.35	0.38	-0.05	-0.21	-0.16
EGFR	0.36	1	0.33	0.48	0.38	0.32	0.55*	0.17	0.14	-0.2	-0.09	-0.21	-0.42	-0.45	0.09	0.03	0.07	-0.29	-0.33	-0.03
AKT pT308	-0.29	0.33	1	0.31	0.41	0.15	0.43	-0.06	0.15	0.15	0.42	0.13	0.05	-0.05	-0.13	-0.41	0.04	-0.24	-0.11	0.09
VEGFR2	0.44	0.48	0.31	1	0.56*	0.68**	0.67**	0.52*	0.4	0.13	0.21	0.17	-0.01	-0.24	-0.24	-0.05	-0.03	-0.53*	-0.45	-0.2
HER3 pY1289	0.28	0.38	0.41	0.56*	1	0.81**	0.56*	0.43	0.4	0.21	0.27	0.11	0.19	-0.15	-0.19	-0.35	-0.18	-0.49	-0.42	-0.51
AKT	0.52*	0.32	0.15	0.68**	0.81**	1	0.58*	0.67**	0.3	0.32	0.11	0.21	0.27	-0.16	-0.26	-0.26	-0.16	-0.58*	-0.68**	-0.39
IGF1R	0.39	0.55*	0.43	0.67**	0.56*	0.58*	1	0.67**	0.54*	0.32	0.47	0.42	0.19	-0.03	-0.48	-0.2	-0.26	-0.73**	-0.65**	-0.48
IRb	0.32	0.17	-0.06	0.52*	0.43	0.67**	0.67**	1	0.5	0.64*	0.33	0.66**	0.57*	0.34	-0.75**	-0.42	-0.56*	-0.8**	-0.79**	-0.68**
HER2	-0.13	0.14	0.15	0.4	0.4	0.3	0.54*	0.5	1	0.52*	0.72**	0.65**	0.45	0.43	-0.47	-0.3	-0.68**	-0.68**	-0.54*	-0.62*
AKT pS473	-0.28	-0.2	0.15	0.13	0.21	0.32	0.32	0.64*	0.52*	1	0.68**	0.89**	0.95**	0.8**	-0.79**	-0.73**	-0.76**	-0.66**	-0.71**	-0.5
p70-S6K pT389	-0.37	-0.09	0.42	0.21	0.27	0.11	0.47	0.33	0.72**	0.68**	1	0.7**	0.69**	0.69**	-0.69**	-0.52*	-0.73**	-0.71**	-0.5	-0.48
p70 S6K1	-0.21	-0.21	0.13	0.17	0.11	0.21	0.42	0.66**	0.65**	0.89**	0.7**	1	0.83**	0.78**	-0.8**	-0.63*	-0.72**	-0.63*	-0.61*	-0.63*
S6 pS235/236	-0.3	-0.42	0.05	-0.01	0.19	0.27	0.19	0.57*	0.45	0.95**	0.69**	0.83**	1	0.86**	-0.78**	-0.67**	-0.77**	-0.58*	-0.59*	-0.54*
S6 pS240/244	-0.54*	-0.45	-0.05	-0.24	-0.15	-0.16	-0.03	0.34	0.43	0.8**	0.69**	0.78**	0.86**	1	-0.76**	-0.62*	-0.83**	-0.43	-0.35	-0.5
IRS	0.09	0.09	-0.13	-0.24	-0.19	-0.26	-0.48	-0.75**	-0.47	-0.79**	-0.69**	-0.8**	-0.78**	-0.76**	1	0.71**	0.73**	0.78**	0.67**	0.68**
HER2 pY1248	0.35	0.03	-0.41	-0.05	-0.35	-0.26	-0.2	-0.42	-0.3	-0.73**	-0.52*	-0.63*	-0.67**	-0.62*	0.71**	1	0.54*	0.54*	0.54*	0.48
HER3	0.38	0.07	0.04	-0.03	-0.18	-0.16	-0.26	-0.56*	-0.68**	-0.76**	-0.73**	-0.72**	-0.77**	-0.83**	0.73**	0.54*	1	0.73**	0.6*	0.65**
pIGF1R	-0.05	-0.29	-0.24	-0.53*	-0.49	-0.58*	-0.73**	-0.8**	-0.68**	-0.66**	-0.71**	-0.63*	-0.58*	-0.43	0.78**	0.54*	0.73**	1	0.88**	0.59*
FoxO3a pS318/321	-0.21	-0.33	-0.11	-0.45	-0.42	-0.68**	-0.65**	-0.79**	-0.54*	-0.71**	-0.5	-0.61*	-0.59*	-0.35	0.67**	0.54*	0.6*	0.88**	1	0.48
FoxO3a	-0.16	-0.03	0.09	-0.2	-0.51	-0.39	-0.48	-0.68**	-0.62*	-0.5	-0.48	-0.63*	-0.54*	-0.5	0.68**	0.48	0.65**	0.59*	0.48	1

Pearson correlation P values (two-tailed): *<0.05, **<0.01

Figure 9: Correlation matrix of change in levels of PI3K signaling proteins and receptor tyrosine kinases after AKT inhibition in CRC patients

PD inhibition was also assessed in patient PBMCs as surrogate tissue using RPPA. RPPA was performed on 12 paired PBMC samples collected at baseline and either C1D15 or end of treatment with MK2206. Seven paired samples were available with collection at baseline and C1D15, and 9 paired samples were available with collection at baseline and end of treatment. Analysis of the cohort as whole, and separate analyses for patients with on-treatment paired samples, and end of treatment paired samples showed no change in protein expression of any of the PD markers. This may be due to degradation of phospho-proteins between time of collection and time of analysis, despite storage of PBMCs with phosphatase and protease inhibitors.

Conclusion:

MK2206 resulted in significant inhibition of PD markers in preclinical models but not in patients' tumors, with a median decrease in AKT pS473 of 37.9% in patients. The inverse correlation between AKT pS473 and downstream FoxO3a pS318/321 maybe reflective of partial AKT re-phosphorylation due to FoxO3a-mediated adaptive changes. AKT pT308 did not correlate reliably with any other PD marker. No change in PD proteins was seen in patients' surrogate tissue (PBMCs) likely due to degradation of phosphoproteins during sample storage.

Aim 2: Determine the mechanisms of adaptive resistance to AKT inhibition in PI3K activated colorectal cancer patients, patient derived xenografts and cell lines.

RPPA analysis of changes in protein expression levels after treatment with MK2206 in patients, PDXs and cell lines revealed many similarities (Figure 10). Apart from decrease in several PD markers as described in results of Aim 1, there was upregulation of several receptor tyrosine kinases with MK2206. Treated PDXs had increased IGF1R, IR-b and HER3 levels ($P < 0.001$ for all) with a nonsignificant rise in PDGFRb. In patients' biopsies, IGF1R and PDGFRb expression increased significantly after two weeks of MK2206 treatment ($P < 0.05$). In cell lines, IGF1R, IR-b and HER3 levels were significantly upregulated with MK2206 treatment ($P < 0.05$ for all). Protein expression of IGF1R was significantly increased in all three model systems. Treatment with MK2206 did not result in significant change in expression of proteins in the parallel MAPK or JAK-STAT signaling pathways. These data were presented at 2018 ASCO Annual Meeting.⁷³

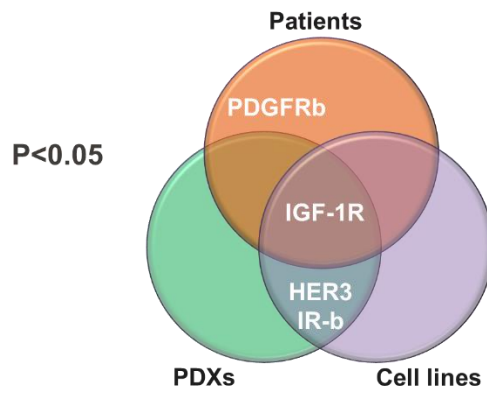
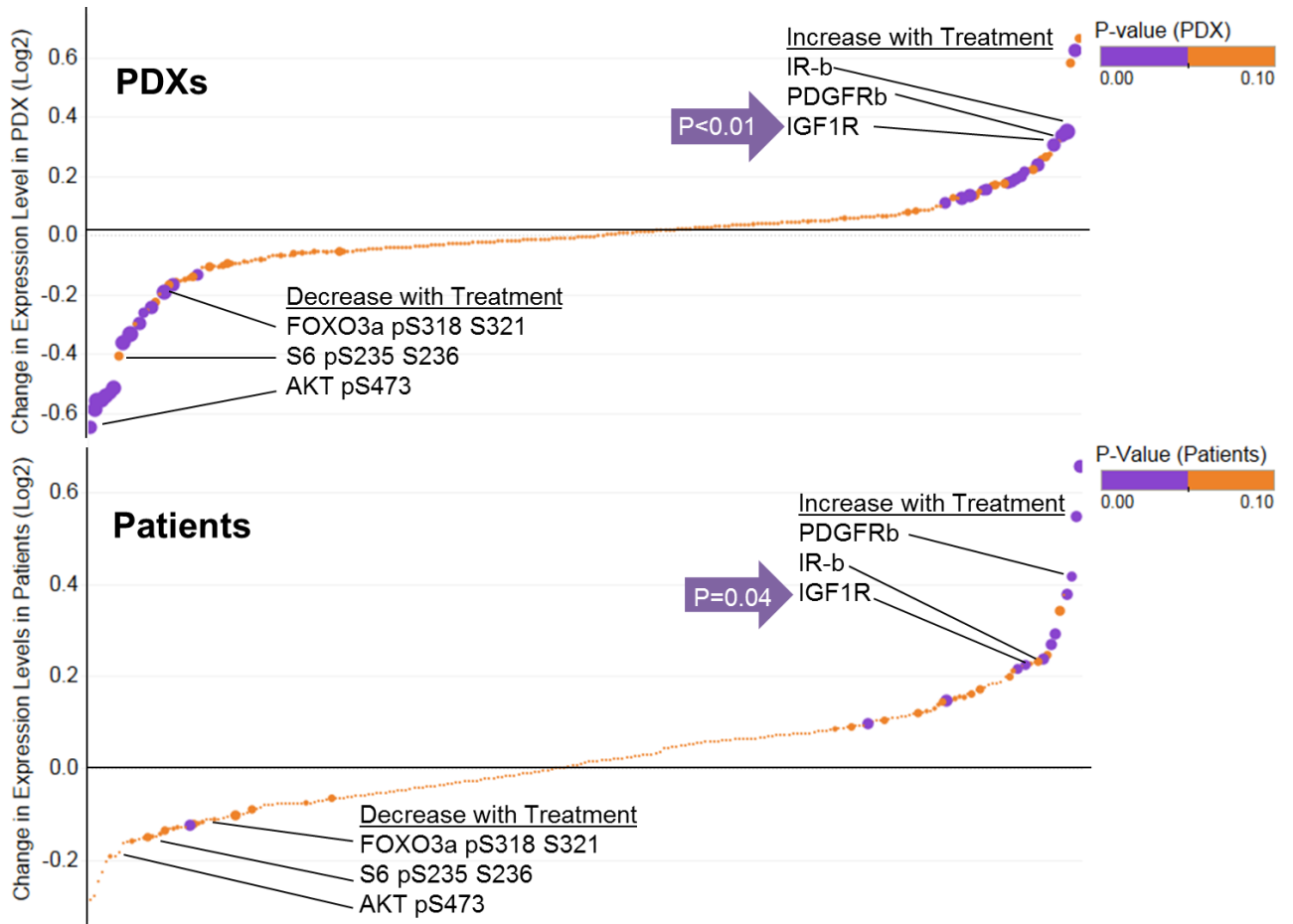


Figure 10: RPPA analysis showed increase in protein expression of several receptor tyrosine kinases after AKT inhibition in patients, PDXs and cell lines.

RPPA results revealed statistically significant increase in protein expression of IGF1R after treatment with AKT inhibitor in patients, PDXs as well as cell lines. To validate these results, we performed immunohistochemical staining for IGF1R on tumors from PDX experiment. Increase in membranous staining for IGF1R was seen in PDXs treated with MK2206 as compared to control PDXs. Figure 11.

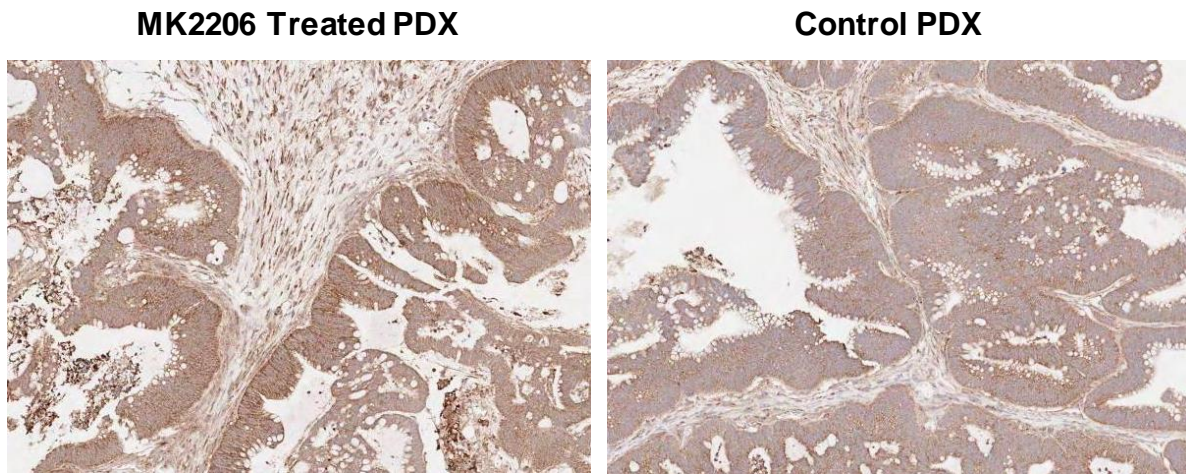


Figure 11: Increased membranous staining of IGF1Rb beta in MK2206-treated PDX as compared to control PDX

When RPPA data from paired tumor biopsies of patients was analyzed within the assigned treatment cohort, the protein expression of IGF1R and HER2 was increased significantly in cohort A (*PIK3CA*^{mut}, *PTEN*^{any}), and a trend towards increase was seen in cohort B (*PTEN*^{loss}, *PIK3CA*^{wild}). A non-significant trend towards decrease in FoxO3a pS318 S321 levels was seen in both cohorts. Table 3. This analysis is limited by small number of patients included in each cohort, and some overlap of molecular characteristics across the two cohorts, which will be discussed next.

Proteins	Cohort A		Cohort B	
	Change from baseline	P value	Change from baseline	P value
IGF1R	↑	0.03	↑	0.30
IR-b	↑	0.51	↑	0.48
PDGFRb	↑	0.23	↑	0.14
HER2	↑	0.04	-	0.80
HER3	↓	0.52	-	0.83
EGFR	↑	0.05	-	0.62
VEGFR2	↑	0.17	↓	0.66
AR	↑	0.02	-	0.96
AKT	↑	0.09	↑	0.31
FoxO3a pS318 S321	↓	0.10	↓	0.60
IRS1	-	0.58	-	0.60
IGF1R pY1135 Y1136	-	0.77	-	0.89
HER2 pY1248	-	0.88	-	0.71
HER3 pY1289	↑	0.14	-	0.86

↑ Increase by >5%; ↓ Decrease by >5%; - No change
 Cohort A: *PIK3CA*^{mut}, *PTEN*^{any}; Cohort B: *PTEN*^{loss}, *PIK3CA*^{wild}

Table 3: Changes in protein expression of receptor tyrosine kinases, phosphorylated FoxO3a and IRS1 after MK2206 treatment in colorectal cancer patients within the assigned treatment cohort.

Next, I looked at the molecular characteristics of patients in the two treatment cohorts (Table 4). In cohort A that enrolled patients with *PIK3CA*^{mut} regardless of PTEN status, PTEN^{loss} by IHC was present in two patients. In cohort B that enrolled patients with PTEN^{loss} and *PIK3CA*^{wild}, more comprehensive molecular analysis performed later (using 11 gene, 46 gene, 50 gene, or 409 gene next generation sequencing) revealed *PIK3CA*^{mut} in 2 patients (exon 2 and exon 10). Four patients had mutations in MAPK signaling pathway including *BRAF*^{non-V600E} mutations and *NRAS* mutations. The pathologic significance of these *NRAS* and *BRAF*^{non-V600E} mutations was not known at the time of clinical trial enrollment and these patients were not excluded. Additionally, one patient was found to have two *KRAS* mutations, in the setting of tumor sequencing after treatment with EGFR inhibitor.

Next, I analyzed the RPPA results of the two patients with stable disease (ID #13, #17) and one patient with stable disease in target lesions but development of new metastases on treatment (ID #18) in comparison with three patients on the other end of the waterfall plot with >70% progression by RECIST 1.1 (ID #12, #6, #9). No discernible patterns or differences were seen. Patient #6 had greater than 50% inhibition of both AKT pS473 and pT308 relative to total AKT. All of these six patients had PTEN^{loss}. Two patients in the worst response group also had *PIK3CA*^{mut}, the rest had *PIK3CA*^{wild}. All patients had received at last 2 prior lines of treatment.

ID	Cohort	PTEN	PIK3CA	Others	CIMP	MSI Status
#2	A	Intact	T1025S (exon 20)	None	0/5	MSS
#4	A	Intact	E545K (exon 10)	<i>BRAF</i> G466V	0/5	MSS
#5	A	Loss	R88Q (exon 2)	<i>TP53</i> R273C	1/6	MSS
#7	A	Intact	E545K (exon 10)	<i>NRAS</i> G12C	2/6	Unk
#8	A	Intact	E542K (exon 10)	None	1/5	Unk
#11	A	Intact	E545K (exon 10)	<i>MET</i> N375S, <i>TP53</i> R213*	Unk	MSS
#12	A	Loss	H1047R (exon 20)	<i>APC</i> , <i>PTEN</i> fs, <i>PTEN</i> E7*, <i>Rb1</i> E137*	Unk	MSS
#1	B	Loss	Q546R (exon 10)	<i>NRAS</i> G12V, <i>TP53</i> L194H, <i>APC</i> G1419*	Unk	MSS
#6	B	Loss	Wild	<i>BRAF</i> D594G	0/5	MSS
#9	B	Loss	K111E (exon 2)	<i>APC</i> , <i>TP53</i> fs	0/6	MSS
#13	B	Loss	Wild	None	Unk	Unk
#14	B	Loss	Wild	None	Unk	MSS
#15	B	Loss	Wild	<i>KRAS</i> G13D, <i>KRAS</i> Q61H, <i>TP53</i> R248W, <i>APC</i> , <i>STK11</i>	2/6	MSS
#17	B	Loss	Wild	<i>APC</i> , <i>SMAD4</i>	Unk	MSS
#18	B	Loss	Wild	<i>TP53</i> R248Q	Unk	MSI

Abbreviations: CIMP = CpG island methylator phenotype; MSI = Microsatellite instability high; MSS = Microsatellite stable; Unk = Unknown.

Table 4: Molecular characteristics of patients in assigned treatment cohorts.

Next, I compared the RPPA analysis of PDX tumors and the corresponding patient's tumor that was used to develop the PDX, and noted several similarities as shown in Table 5.

PI3K pathway proteins	Change from baseline	
	Pt #1	PDXs
IGF1R	↑	↑
IR-b	↓	↑
PDGFRb	↑	↑
HER2	↑	NA
HER3	↑	↑
EGFR	-	-
VEGFR2	↓	-
AKT	↑	-
EGFR pY1173	↑	-
IGF1R pY1135/1136	↑	-
HER2 pY1248	↑	↑
HER3 pY1289	↑	↑
AKT pS473	↓	↓
AKT pT308	-	↓
FoxO3a pS318/321	↑	↓
S6 pS235/236	↓	↓
S6 pS240/244	↓	↓
IRS1	↑	-

↑ Increase by >5%; ↓ Decrease by >5%; - No change
 NA = Not available

Table 5: Change in receptor tyrosine kinases and pharmacodynamic markers of AKT inhibition in PDX tumors and the corresponding patient's tumor.

IGF1R is transcriptionally upregulated after AKT inhibition:

A time-based analysis of cell lines showed that IGF1R upregulation began between 8-24 hours after treatment and continued to increase for up to 7 days (ANOVA, $P < 0.01$). Figure 12. The rise in IGF1R levels after 8-24 hours is suggestive of transcriptional upregulation of IGF1R.

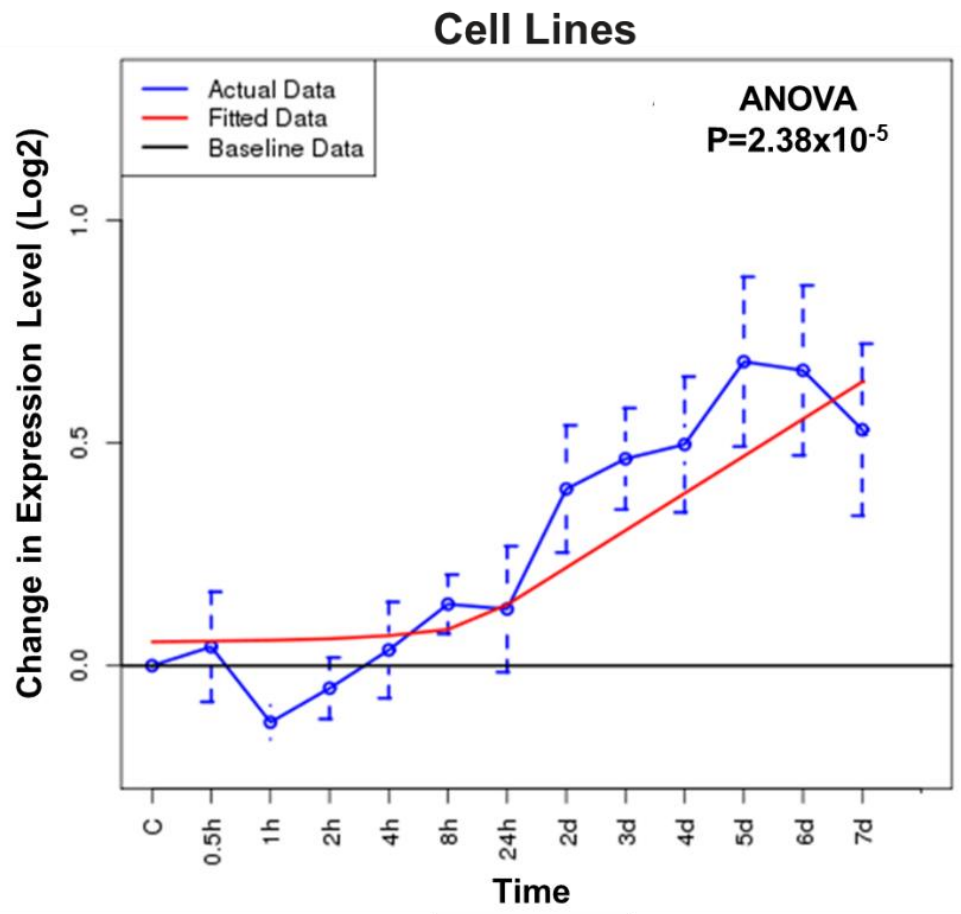
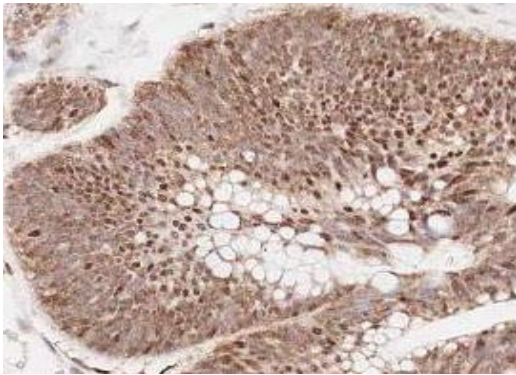


Figure 12: IGF1R upregulation begins 8-24 hours after treatment with MK2206 in cell lines.

FOXO is a transcription factor for many genes involved in varied cellular processes. Phosphorylation of FOXO locks it in the cytosolic compartment and inhibits transcription of its target genes. Decrease in phosphorylation of FOXO after AKT inhibition allows its translocation to the nucleus where it activates transcription.^{27, 74}

To demonstrate this phenomenon, we performed immunohistochemistry for FOXO on tumors harvested from PDXs. Tumors from control PDXs exhibited cytoplasmic staining of FOXO, whereas those treated with MK2206 showed localization of FOXO staining to the nucleus. Figure 13.

Control PDXs



MK2206-Treated PDXs

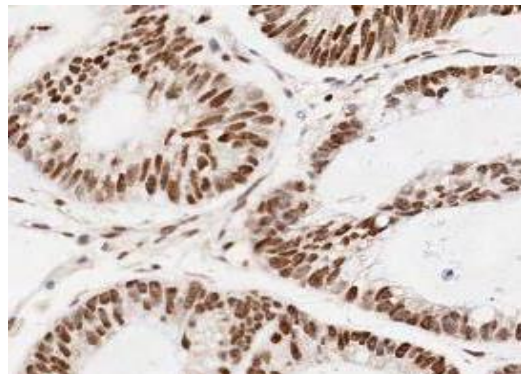
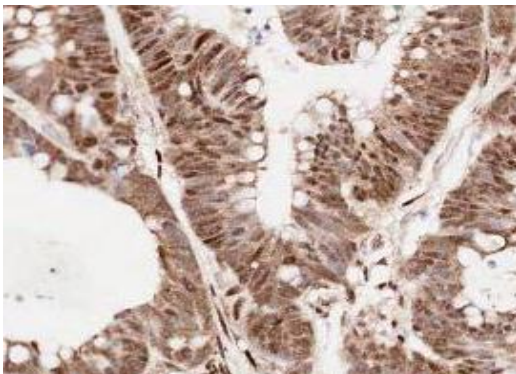
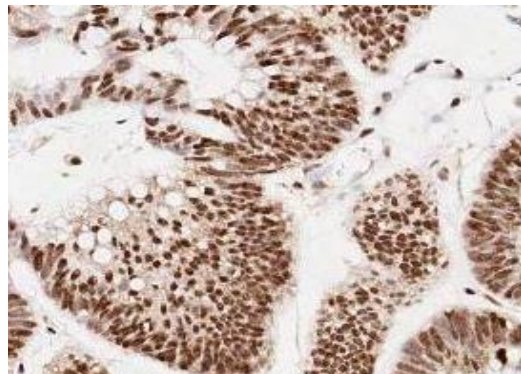
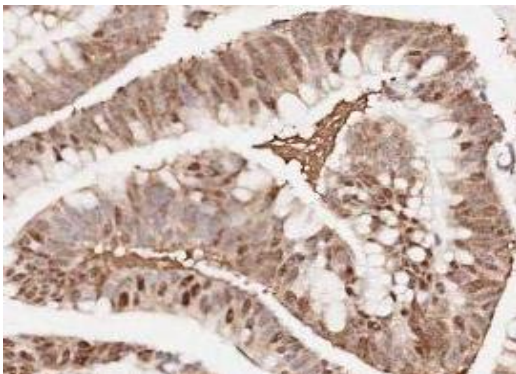
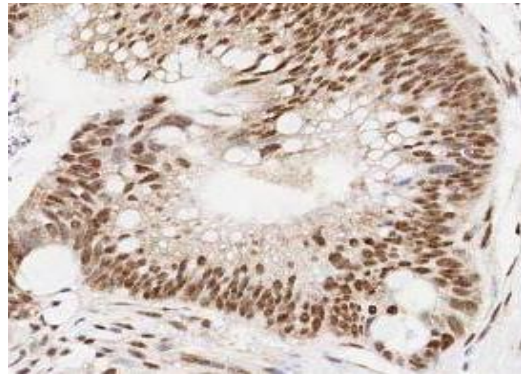


Figure 13: Increased nuclear staining and decreased cytoplasmic staining of FOXO in MK2206-treated PDXs as compared to control PDXs

Next, I hypothesized that nuclear localization of dephosphorylated FOXO results in transcriptional upregulation of RTKs. To test this hypothesis, I analyzed correlation between FoxO3a pS318/321 levels and levels of RTKs using RPPA data from paired patient biopsies. FoxO3a pS318/321 levels showed significant inverse correlation with IGF1R, IR-b and HER2 levels (Table 6, Figure 14).

There was also an inverse correlation between decrease in phosphorylation of FoxO3a and increase in total AKT levels ($r = -0.68$, $P = 0.01$), reflecting adaptive increase in AKT transcription to bypass the allosteric inhibition of pre-existing AKT with MK2206 (Figure 15). Subsequent phosphorylation of the newly formed AKT may have masked the overall PD inhibition of pAKT in patients. Hence, the decrease in phosphorylated FoxO3a levels correlated not only with increase in total AKT levels, but also with increase in AKT pS473 levels ($r = -0.71$, $P = 0.003$).

Receptor Tyrosine Kinase	Pearson Correlation Co-efficient 'r'	P value
IGF1R	-0.65	0.009
IR-b	-0.79	<0.001
PDGFRb	-0.21	0.459
HER2	-0.542	0.037
HER3	0.605	0.017
EGFR	0.328	0.233
VEGFR2	-0.45	0.095

Table 6: Correlation between FoxO3a pS318/321 and change in receptor tyrosine kinases after AKT inhibition in metastatic colorectal cancer patients

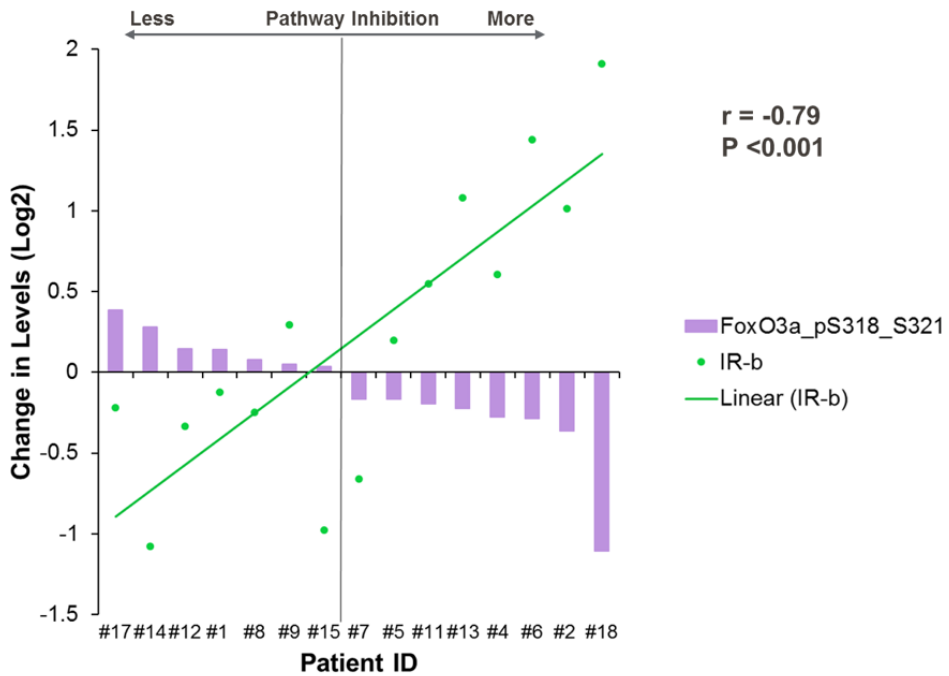
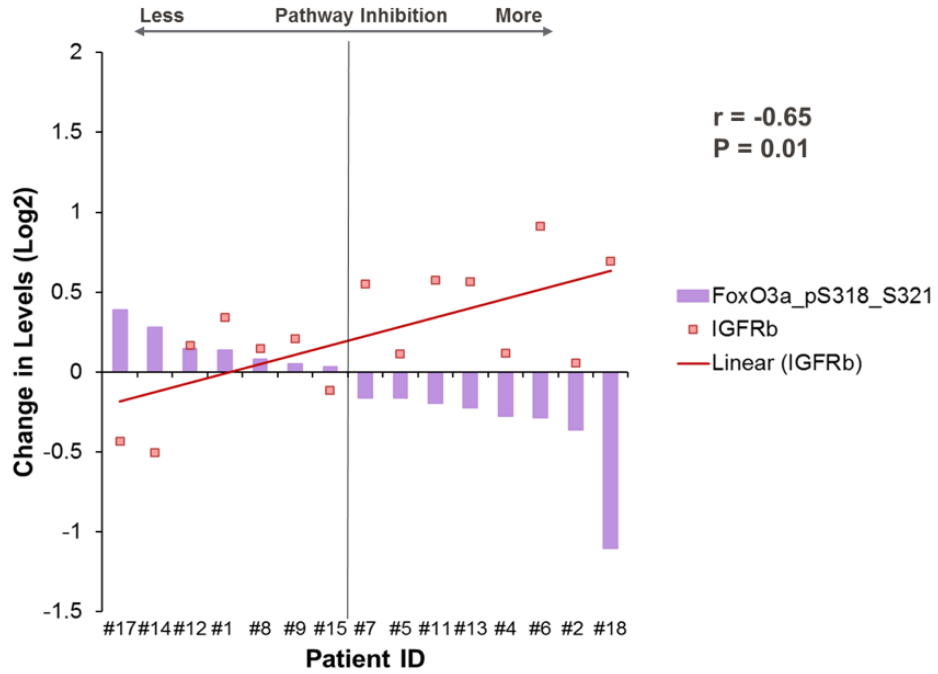


Figure 14: As phosphorylation of FoxO3a decreases, levels of receptors tyrosine kinases start to rise. A significant inverse correlation was seen between levels of FoxO3a pS318/321 and IGF1R levels (A), and IR-b levels (B). Pearson correlation values are shown.

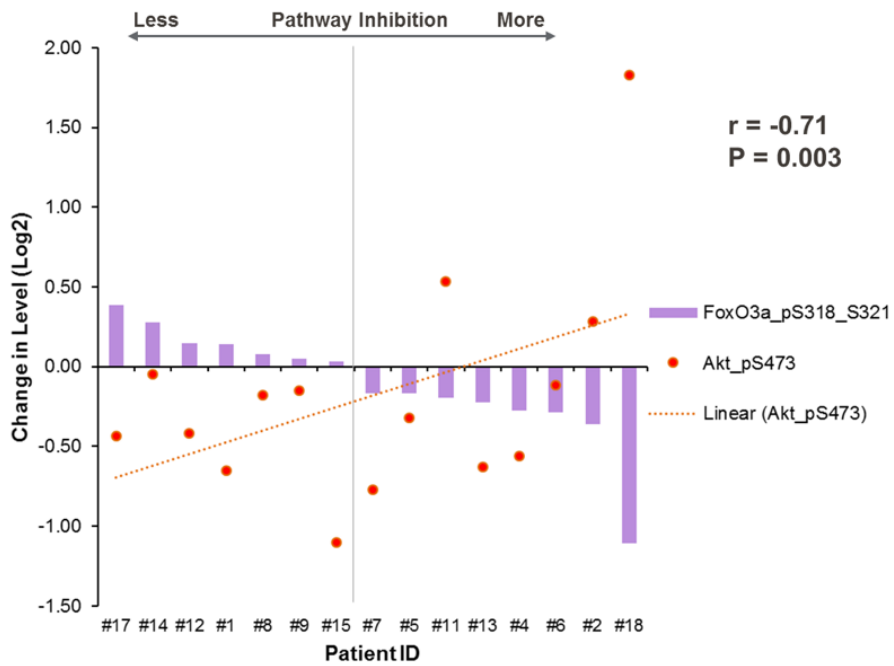
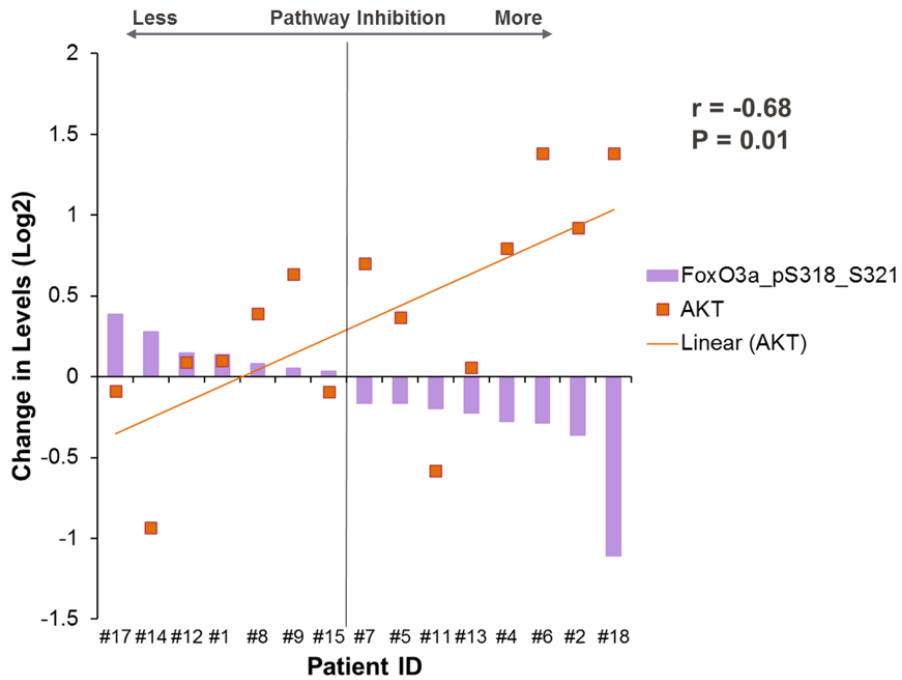


Figure 15: As phosphorylation of FoxO3a decreases, total AKT levels rise (A), and PI3K signaling also increases as shown by increase in AKT pS473 (B).

Pearson correlation values are shown.

The change in total AKT levels directly correlated with the change in RTK levels, namely IGF1R, IRb and PDGFRb. Table 7, Figure 16.

Receptor Tyrosine Kinase	Pearson Correlation Co-efficient 'r'	P value
IGF1R	0.58	0.024
IR-b	0.67	0.006
PDGFRb	0.52	0.049
HER2	0.3	0.279
HER3	-0.16	0.58
EGFR	0.32	0.249
VEGFR2	0.69	0.005

Table 7: Correlation between AKT levels and change in levels of receptor tyrosine kinases after treatment with MK2206.

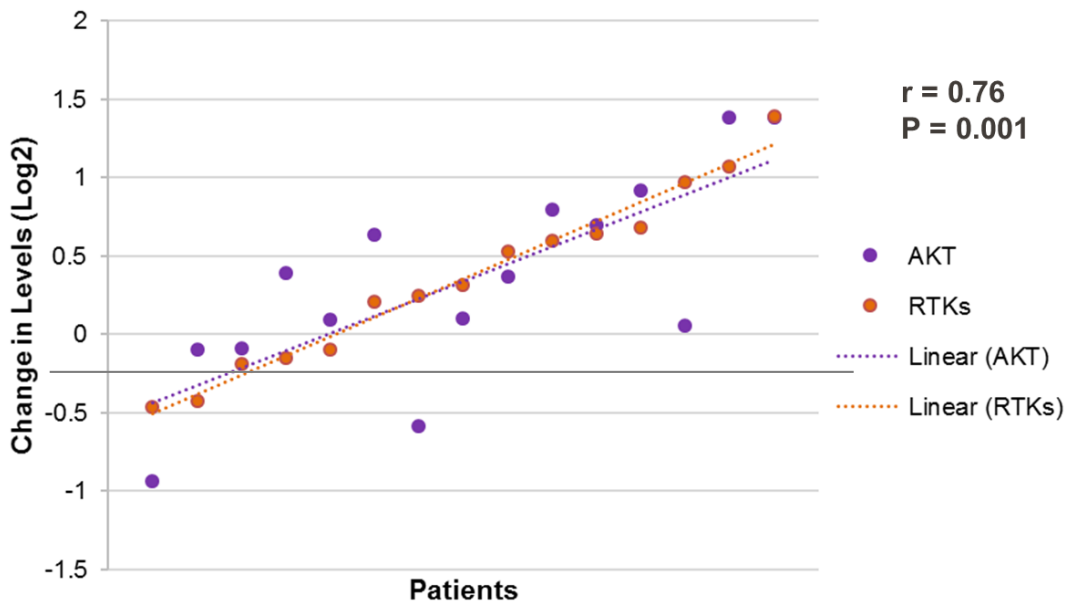


Figure 16: Protein levels of AKT directly correlate with protein levels of receptor tyrosine kinases (RTKs) namely IGF1R, IR-b and PDGFRb. Pearson correlation values are shown.

Next, I investigated if RTK induction was accompanied by RTK phosphorylation in patient samples. Change in IGFR1 expression levels after treatment with MK2206 had a significant negative correlation with change in phosphorylation of IGF1R ($r = -0.73$, $P < 0.01$). Figure 17. I also evaluated change in IGF1R phosphorylation relative to total IGF1R levels in patients. Again, a strong negative correlation was seen between change in relative IGF1R phosphorylation and IGF1R expression levels. Change in IGF1R levels also did not correlate with AKT pS473 levels, or levels of downstream signaling proteins. An antibody against phospho-IR was not included in the RPPA panel. However, IR levels showed a direct correlation with AKT pS473 ($r = 0.64$, $p < 0.01$), p70 S6K1 ($r = 0.66$, $P < 0.01$) and S6 pS235/236 ($r = 0.57$, $P < 0.05$). No correlation was seen between HER3 and phospho-HER3 levels ($r = -0.3$), as shown in Figure 9.

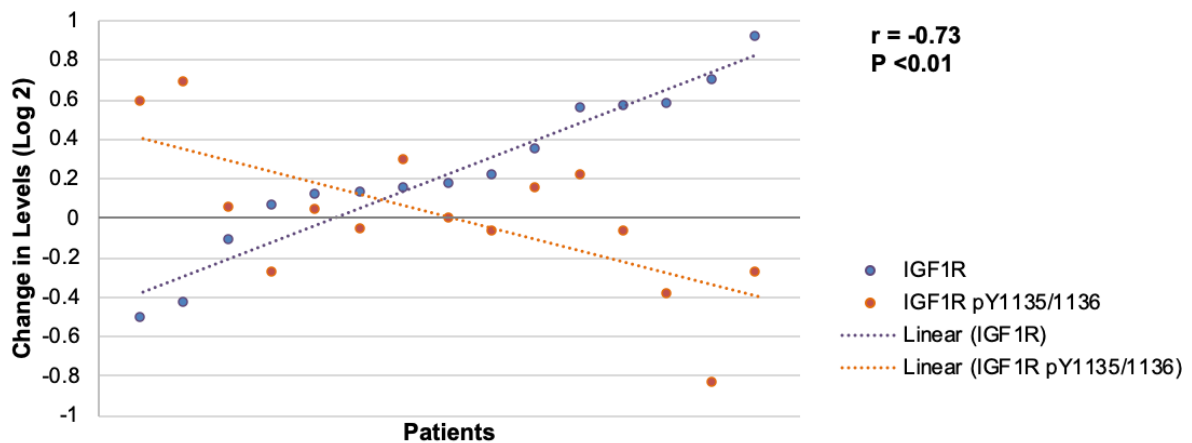


Figure 17: Inverse correlation between expression levels of IGF1R and IGF1R pY1135/1136.

So far, I have shown that decrease in FoxO3a pS318/321 levels correlate significantly with increase in several RTKs, increase in total AKT, and increase in AKT pS473 levels. If AKT phosphorylation and signaling had increased secondary to FOXO mediated induction of RTK and AKT, then we would expect a decrease in IRS levels and RTK phosphorylation through the S6K feedback loop. That is to say, that a decrease in FoxO3a pS318/321 levels would be accompanied by a decrease in IRS levels. Indeed, we observed this in our RPPA data from paired tumors of patients. There was a direct correlation between pFOXO and IRS-1 ($r=0.672$, $p=0.006$). Hence, this suggests that loss of inhibition of one feedback loop activates the other feedback loop. In other words, AKT inhibition with MK2206, would result in loss of inhibition of one of the two feedback mechanisms, but not both. Close examination of the two feedback loops in paired tumors of individual patients showed increase in either IRS1 or RTKs (IGF1R, IR-b) in most patients, consistent with this hypothesis (Table 8).

Also, the feedback inhibition of IRS1 by phosphorylated S6K was demonstrated in our dataset as expected. The phosphorylation of receptor tyrosine kinases such as IGF1R and HER2 also had a direct correlation with IRS1 and correlated inversely with phosphorylated S6K (Table 9).

Patient	FoxO3a			
	IRS1	pS318/321	IGF1R	IR-b
#18	69.1%	46.4%	161.6%	375.7%
#11	76.2%	87.2%	148.9%	146.2%
#2	98.5%	77.8%	103.8%	201.6%
#6	95.1%	82.0%	188.3%	271.2%
#4	100.8%	82.5%	108.6%	152.2%
#13	97.2%	85.6%	147.7%	211.2%
#9	92.7%	103.6%	115.6%	122.5%
#5	105.1%	89.2%	108.1%	114.6%
#7	131.1%	89.2%	146.4%	63.2%
#1	126.7%	110.1%	126.7%	91.7%
#8	135.0%	105.7%	110.8%	84.2%
#15	138.5%	102.3%	92.2%	50.9%
#17	125.7%	130.7%	73.9%	86.1%
#14	108.4%	121.3%	70.4%	47.3%
#12	96.5%	110.5%	112.3%	79.3%

Table 8: Heatmap of feedback loops in PI3K signaling in individual patients' tumors shows loss of feedback inhibition of only one of the two feedback loops in most patients.

PI3K Pathway Protein	Pearson Correlation Co-efficient 'r'	P value
S6 pS235/236	-0.78	0.001
S6 pS240/244	-0.76	0.001
p70 S6K1	-0.80	<0.001
p70 S6K pT389	-0.69	0.004
IGF1R pY1135/1136	0.78	0.001
HER2 pY1248	0.71	0.003

Table 9: Correlation between changes in IRS1 levels and other protein levels in patients' tumors after treatment with MK2206.

Conclusions

Allosteric AKT inhibition with MK2206 in metastatic CRC induces FoxO3a mediated adaptive upregulation of receptor tyrosine kinases, namely IGF1R but also HER3 and IR, which possibly reactivates AKT signaling. Only IR levels correlate significantly with phosphorylation of PI3K signaling proteins. In patients, loss of feedback suppression of one feedback loop seems to activate the other feedback loop. A three model systems (cell lines, PDXs and patient samples) approach allows in-depth investigation of adaptive resistance mechanisms and highlights rational combination therapies for future clinical trials.

Aim 3: Evaluate the impact of PI3K activating alterations on immune landscape of colorectal cancer, and design a therapeutic intervention to improve the immune microenvironment.

For Aim 3, we evaluated primary tumor resection specimens from 94 early stage CRC patients. Out of these 94 patients, PI3K pathway alterations were present in 27 (28.7%) patients. Out of these 27 patients, 16 patients had *PIK3CA*^{mut}, 12 patients had *PTEN*^{loss} and 1 patient had both. Since *PIK3CA*^{mut} and *PTEN*^{loss} were not mutually exclusive, these were grouped as PI3K pathway-altered CRC for initial analysis. IHC data was available for 59 patients, and mRNA data was available for 73 patients.

The baseline characteristics of patients included in early stage CRC cohort are shown in Table 10. MSS CRC patients with PI3K pathway alterations (18 out of 73, 24.7% of MSS patients) were more frequently associated with CMS1 subtype (31.3% vs 3.9%, $P < 0.001$) and right colon (72.2% vs 32.7%, $P = 0.003$).

Characteristics	PI3K Pathway Alteration				P value
	Present		Absent		
	N	%	N	%	
N	27	28.7	67	71.3	
Age Median (range)	70	37-84	64	38-94	0.61
Male Gender	12	44.4	26	38.8	0.61
Right Colon	21	77.8	29	43.3	0.002
MSI Status					
Stable	18	66.7	55	82.1	0.17
High	9	33.3	12	17.9	
CMS					<0.001
1	12	50	13	20.6	
2	2	8.3	32	50.8	
3	5	20.8	5	7.9	
4	5	20.8	13	20.6	
Stage					
2	11	40.7	38	56.7	0.18
3	16	59.3	29	43.3	
KRAS					
Mutant	9	42.9	21	39.6	1.0
Wild	12	57.1	32	60.4	
BRAF					
Mutant	7	33.3	12	23.1	0.39
Wild	14	66.7	40	76.9	

Table 10: Baseline characteristics of patients in early stage CRC cohort (N=94)

Early stage CRC with PI3K pathway alterations also had increased frequency of peritumoral lymphocytes on manual pathology assessment as compared to tumors without PI3K alterations (P=0.04, Figure 18). While peritumoral lymphocytes were increased in early stage MSS CRC with PI3K pathway alterations (P=0.031), this association was not seen in PI3K-altered MSI tumors. On multivariate logistic regression analysis, PI3K pathway alterations significantly increased peritumoral lymphocytes independently of microsatellite status (OR 3.6, 95% CI 1.06-12.24, P=0.04).

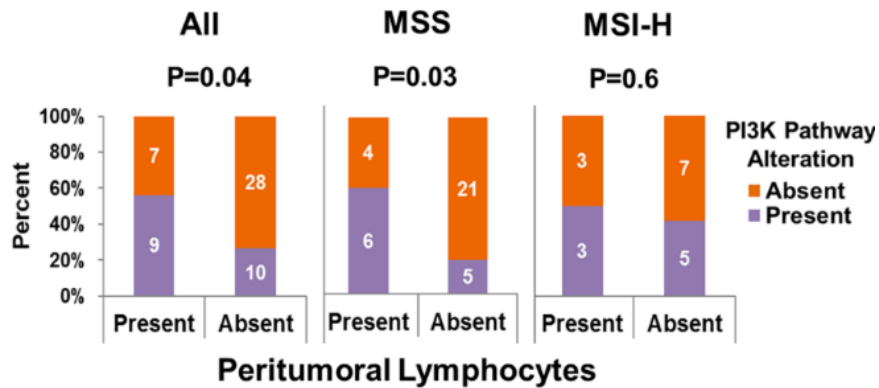


Figure 18: Increased peritumoral lymphocytes in PI3K-altered CRC

Quantitative immunohistochemical analysis

The IHC cohort of 59 pts (40 MSS, 19 MSI) included 23 (39%) pts with PI3K pathway alterations.

Increased immune engagement in PI3K-altered MSS CRC: We observed greater median densities of all immune infiltrates at the invasive margin of primary CRC as compared to the center of the tumor ($P < 0.01$ for all, Figure 19). MSS tumors showed a trend towards decreased density of CD8⁺ cells at CT and CD8⁺ cells at IM as compared to MSI CRC. Further analysis of MSS CRC showed that as compared to tumors without PI3K pathway alterations, center of PI3K-altered MSS CRC had significantly increased median densities of CD3⁺, CD8⁺, CD45RO⁺, and CD57⁺ cells ($P < 0.05$ for all, Figure 20). PI3K altered MSS CRC patients also had increased CD45RO⁺ cells at the IM ($P = 0.04$). We did not observe an association among PI3K pathway alterations and the densities of CD4⁺, CD20⁺, FOXP3⁺, and CD68⁺ cells at CT or IM; or of CD8⁺ and CD57⁺ cells at IM. These data are shown in Figure 20.

No differences were seen in density of immune infiltrates among MSI primary CRC in presence or absence of PI3K pathway alterations (data not shown).

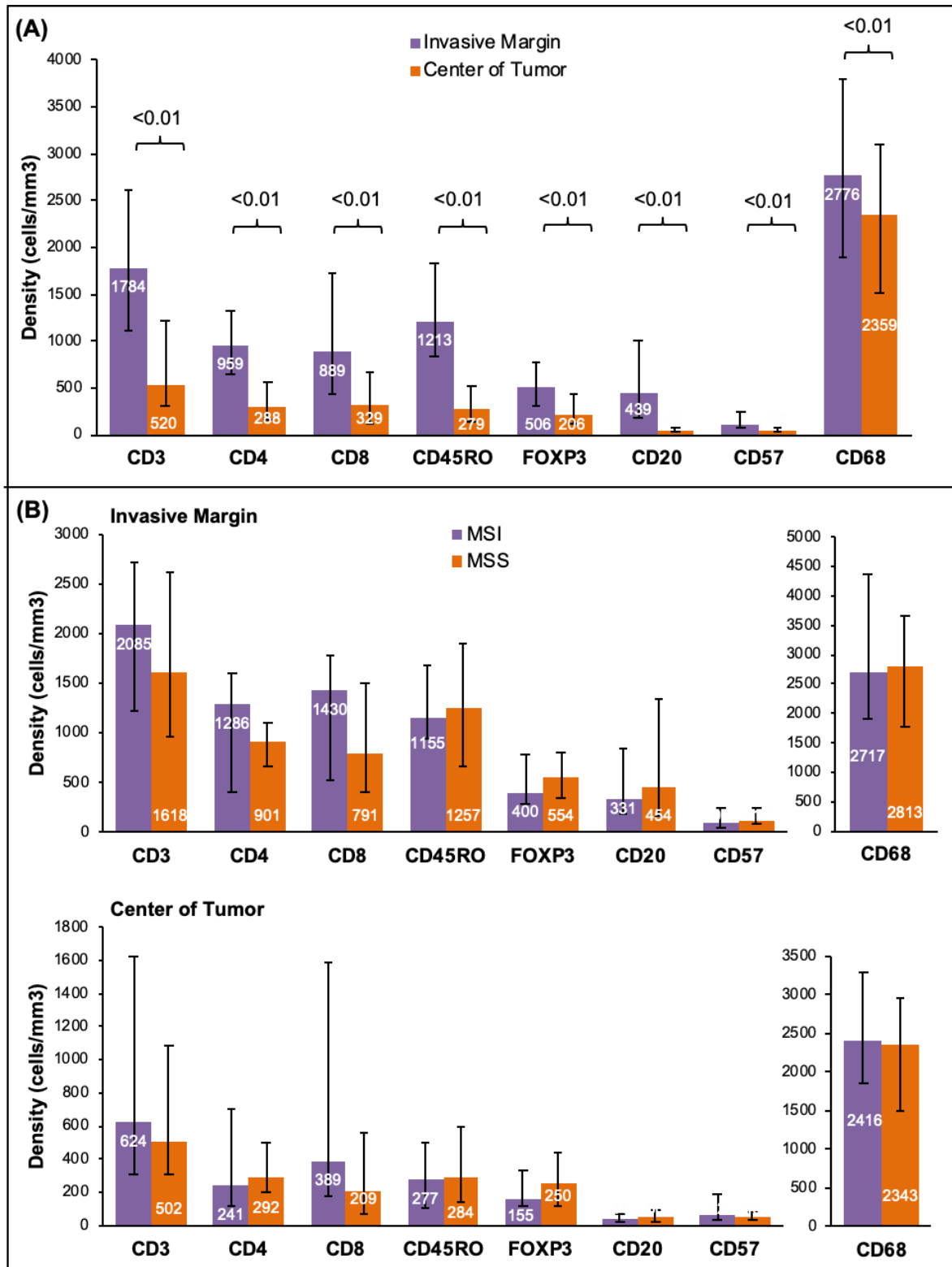


Figure 19: Density of immune infiltrates in primary CRC. (A) All cases. Wilcoxon signed-rank test P values are shown at 5% level of significance (B) Analysis by microsatellite stability status. Mann Whitney U test P values are shown at 5% level of significance. MSI, Microsatellite instability high. MSS, Microsatellite stable.

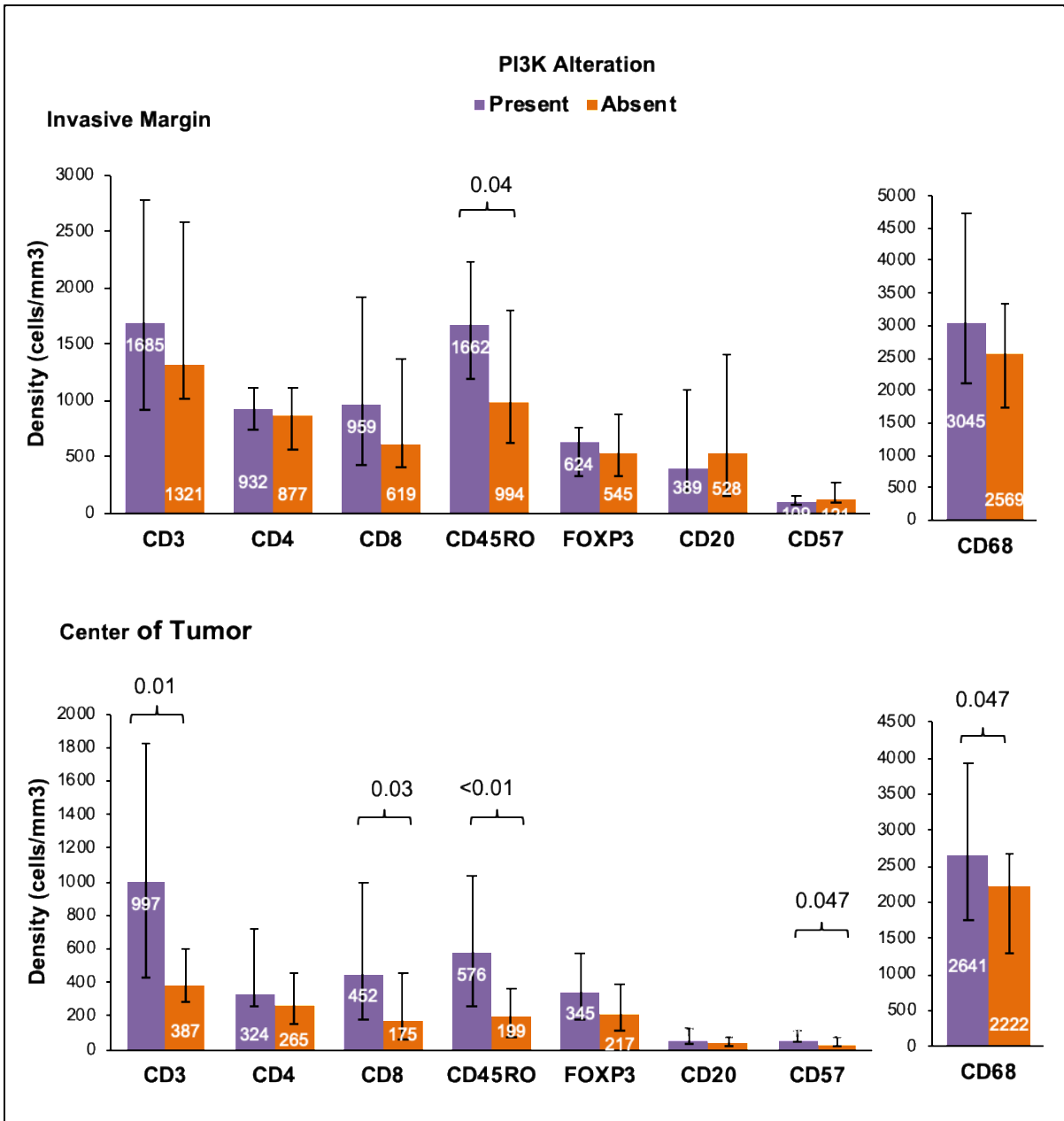


Figure 20: Density of immune infiltrates in microsatellite stable primary CRC by PI3K pathway alteration status. Mann-Whitney U test P-values at 5% level of significance are shown.

Next we grouped the densities of any two of CD3⁺, CD8⁺ and CD45RO⁺ cells at center of tumor (CT) and any two of the above-mentioned immune infiltrates at invasive margin (IM) into an immune density score ranging from 0-4. A score of 0 implied no high-density immune cells at CT and IM, and a score of 4 implied two high density immune infiltrates at CT and two high density immune infiltrates at IM. Median densities were used as the cut off for high or low. A T cell density higher than median density was categorized as high. The scoring methodology was derived from previously described immunoscore by Galon et al.⁷⁵ However, as our immunohistochemical staining and quantification methodology is different, our immune density score is not comparable to the previously reported immunoscore. Most early stage MSS CRC with PI3K pathway alterations (11/14, 78.6%) had an immune density score of 3 or 4 as compared to 9/26 (34.6%) *PIK3CA*^{wild} *PTEN*^{intact} CRC (P=0.019, Figure 21). There was no association between immune density score of MSI tumors and PI3K pathway alterations.

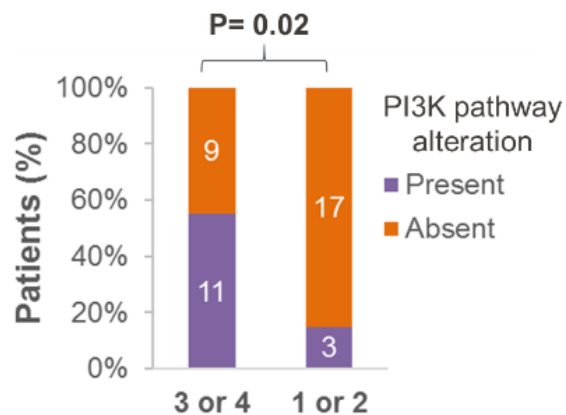


Figure 21: PI3K alterations are more frequent among microsatellite stable colorectal cancer with high immune density score of 3 or 4.

Increased immune checkpoint expression by IHC in PI3K-altered CRC:

As seen with immune infiltrates, expression of all immune co-stimulatory and inhibitory checkpoint markers was higher at the invasive margin of tumors as compared to the center ($P < 0.05$ for all). The center of PI3K-altered MSS CRC had increased median percentage of cell staining positive for PD-1, PD-L1 on epithelial cells, VISTA and LAG-3 expression by IHC as compared to MSS CRC without PI3K alterations ($P < 0.05$ for all). In addition, HLA expression was increased on epithelial cells at the center of tumor among PI3K-altered CRC ($P = 0.03$). There was no difference in the expression of co-stimulatory molecules (ICOS and OX40) in presence or absence of PI3K pathway alterations in early stage CRC, irrespective of microsatellite status. These data are shown in Figure 22.

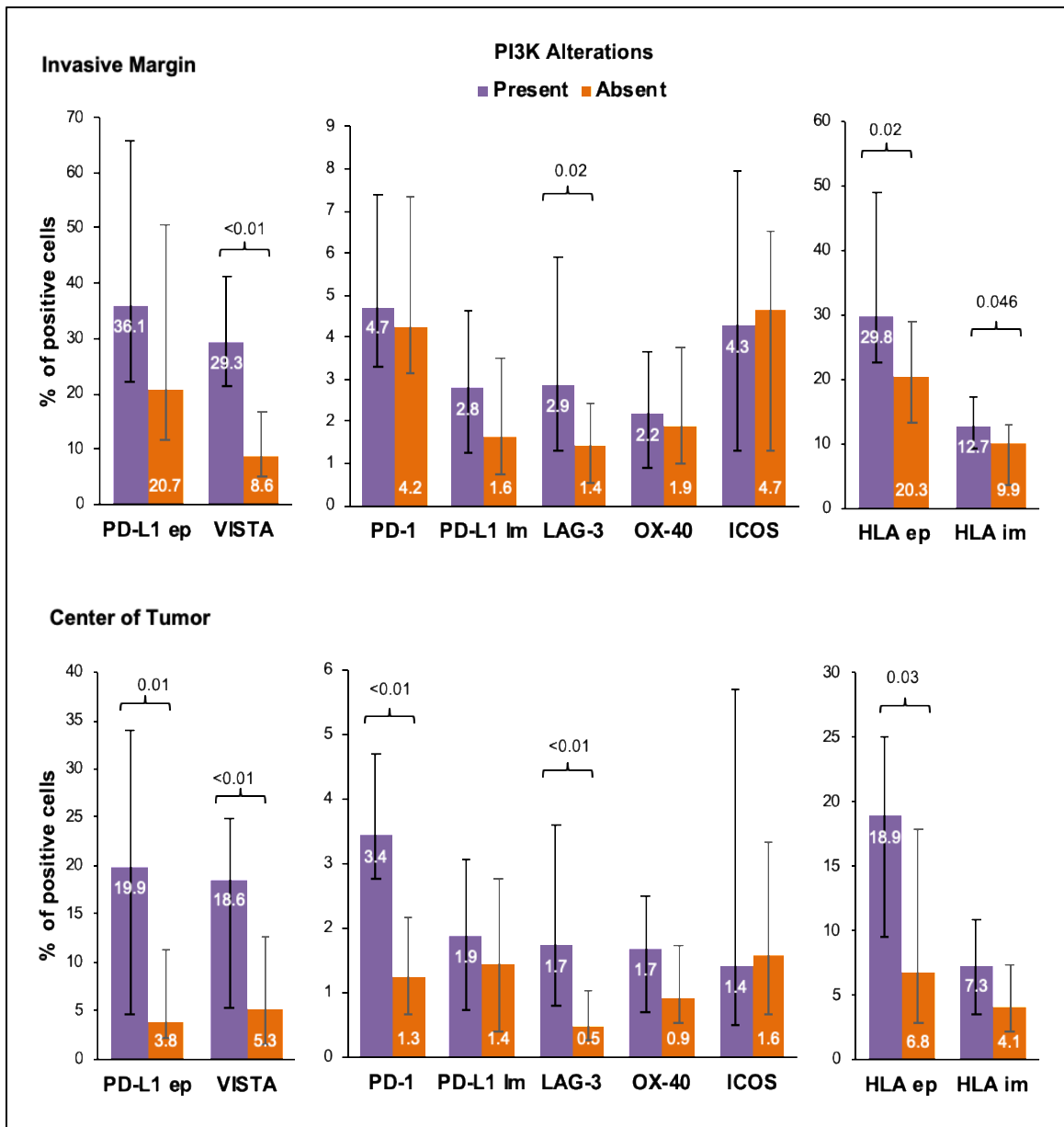


Figure 22: Quantitative IHC for immunomodulatory proteins shown increased checkpoint expression among MSS CRC with PI3K pathway alterations. Abbreviations: ep, epithelial cell; im, immune cell.

Subgroup analysis of *PIK3CA* mutant CRC: I further analyzed quantitative IHC data for MSS CRC with *PIK3CA*^{mut} (n=7) and PTEN^{loss} (n=7) separately, excluding 1 case in which both alterations were present (Figure 23). There was an increase in median densities of CD3+ cells [1112 (IQ range 865-1421) vs 435 (IQ range 300-744) cells/mm³; P=0.037] and CD8+ cells [554 (IQ range 331-1200) vs 185 (IQ range 60-473) cells/mm³; P=0.037], and a trend towards increase in CD45RO+ cells at the center of *PIK3CA*^{mut} MSS CRC as compared to *PIK3CA*^{wild}. There was also a significant increase in median percentage of cells staining positive for granzyme B at the center of *PIK3CA*^{mut} MSS CRC as compared to *PIK3CA*^{wild} (2.4% vs 0.8%, P=0.04). There was no difference in densities of immune infiltrates or percentage of cells staining positive for granzyme B among PTEN^{loss} as compared to PTEN^{intact} MSS CRC. These data were presented at 2019 ASCO Annual Meeting.⁷⁶

IHC analysis of immunomodulatory proteins showed that *PIK3CA*^{mut} MSS CRC had significantly higher median percentage of cells expressing PD-L1 (on epithelial cells as well as on immune cells) and LAG3 (P<0.05 for all), and a trend towards higher VISTA and PD-1 positive cells at the invasive margin as compared to *PIK3CA*^{wild}. Similarly, at the center of the tumor, *PIK3CA*^{mut} MSS CRC had higher percentage of PD-1 positive cells (P=0.02), and a trend towards higher PD-L1, VISTA and LAG3. PTEN^{loss} MSS CRC had significantly higher HLA expression at the invasive margin as well as center of the tumor as compared to PTEN^{intact}, while a trend towards increase in several checkpoints was seen at the center of the tumor. These data are shown in Figure 24. Again, these changes in immune infiltrates and checkpoints were not seen among MSI CRC.

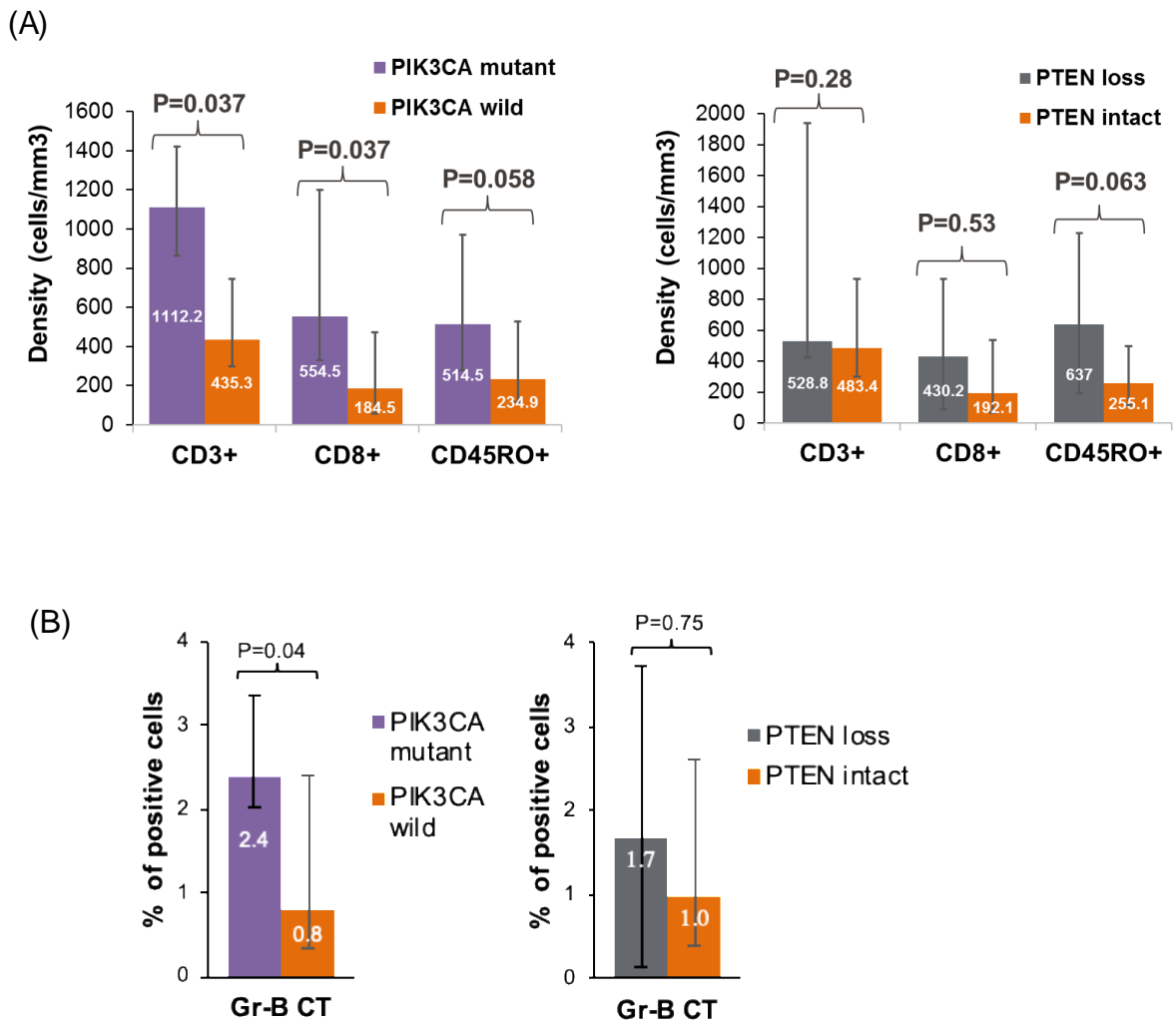


Figure 23: Increased T cell engagement is seen in *PIK3CA*^{mut}, but not in *PTEN*^{loss} MSS primary CRC. (A) Median density of T cell infiltrates at the center of the tumor. (B) Median percentage of cells staining positive for granzyme B (Gr-B) at the center of the tumor (CT).

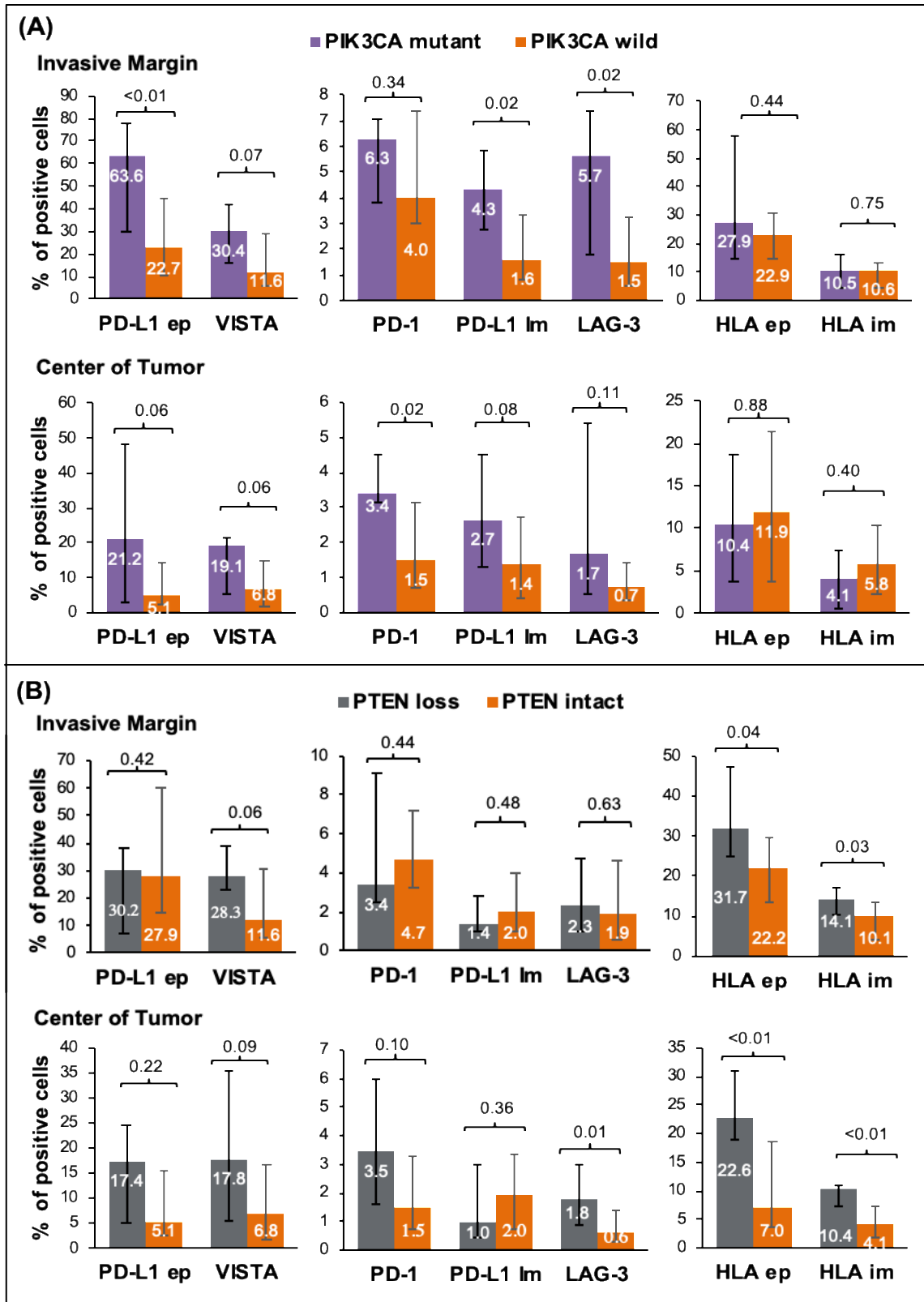


Figure 24: IHC expression of immunomodulatory proteins among *PIK3CA*^{mut} (A) and *PTEN*^{loss} (B) MSS primary CRC.

Immune signature of PI3K-altered CRC using Agilent Microarray

The mRNA cohort of 73 patients included 16 (22%) with PI3K pathway alterations. Among all cases, PI3K-altered CRC had higher mRNA expression of PD-L1 ($P=0.031$). Alternate checkpoints were also increased in patients with PI3K pathway alterations, including CTLA4, TIM3, and TIGIT ($P<0.05$ for all). Among MSS CRC patients, PI3K pathway alterations were associated with higher mRNA expression of PD-L1 ($P=0.046$) and TIGIT ($P<0.001$) as shown in Figure 25. Similarly, mRNA expression of several HLA genes (HLA-B, HLA-DMA, HLA-DMB, HLA-DRA, HLA-DRB1) was higher in MSS CRC with PI3K pathway alterations ($P<0.05$ for all).

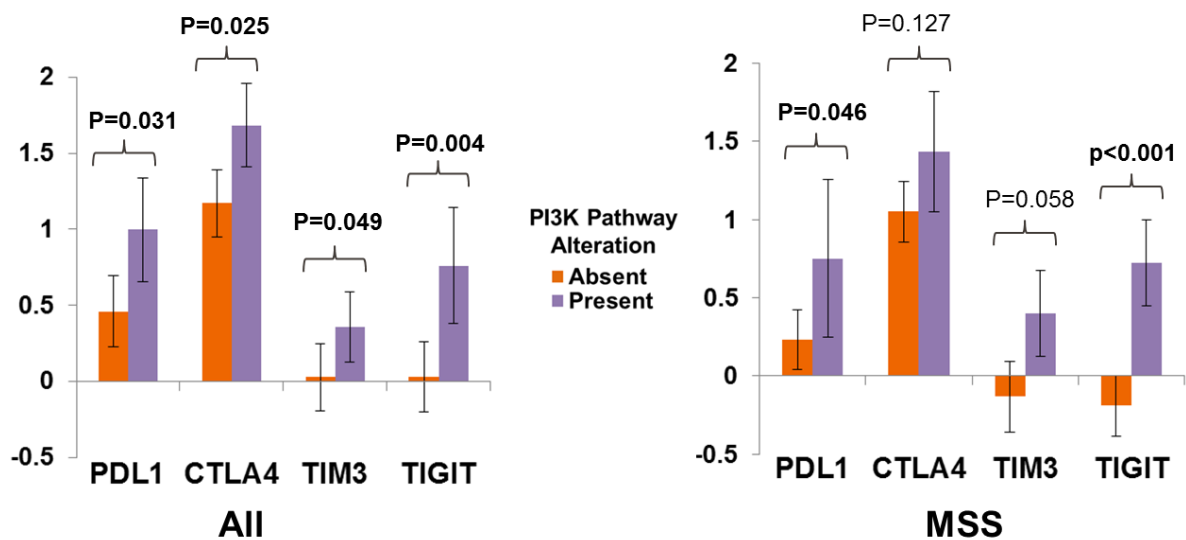


Figure 25: Analysis of mRNA data showed higher expression of immune checkpoints among PI3K altered primary CRC. MSS = Microsatellite stable.

Hierarchal clustering analysis of mRNA data showed that the immune signature of PI3K-altered MSS CRC clustered with that of CMS1 and CMS4 tumors (Figure 26). These data were presented at 2018 ASCO Gastrointestinal Cancers Symposium.⁷⁷

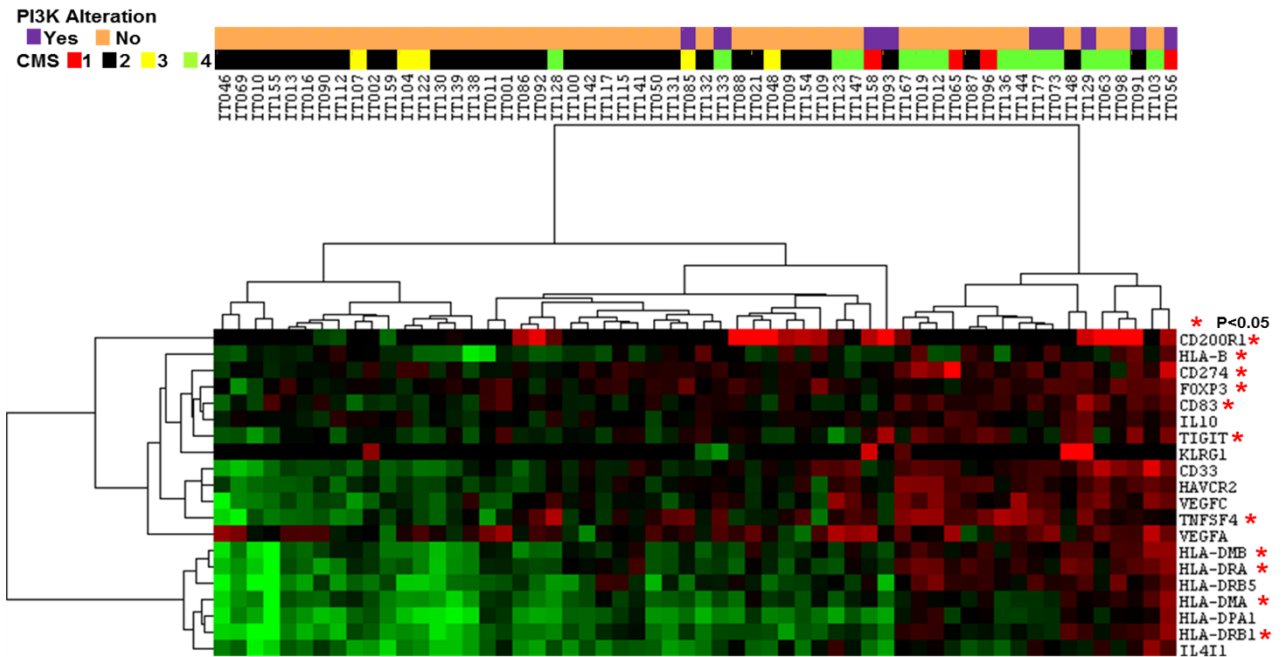


Figure 26: Hierarchal clustering analysis of top 20 differentially expressed genes in MSS CRC with and without PI3K alterations.

Outcomes on immunotherapy among *PIK3CA* mutant CRC patients:

Increased cytotoxic T cell infiltration and PD-L1 expression have been reported to be independent predictors of response to immunotherapy.⁵³ As my results showed higher cytotoxic T cell infiltration and PD-L1 expression among *PIK3CA*^{mut} MSS CRC patients as compared to *PIK3CA*^{wild}, I evaluated outcomes with immunotherapy among MSS CRC patients by *PIK3CA* mutation status (Figure 27). Out of 43 MSS CRC patients enrolled in 7 immunotherapy trials, *PIK3CA*^{mut} were present in 8/43 (18.6%) patients (E545K, 3; G118D, 2; E545A, 1; E542K + H1047R, 1; and Q546K, 1). Clinical benefit (CB) was defined as CR, PR, or SD of 24 weeks. Half (4/8) of *PIK3CA*^{mut} patients derived CB from immunotherapy as compared to 3/35 (8.6%) *PIK3CA*^{wild} patients (P=0.015). *PIK3CA*^{mut} patients had trend towards longer time to progression (TTP, 3.8 vs 2.1 months, P=0.08). CB or TTP did not differ by colon sidedness, monotherapy / combination therapy, number of mutations, or mutations in other key genes (*APC*, *SMAD4*, *TP53*, *KRAS*, *NRAS* or *BRAF*). These data were presented at 2019 ASCO Annual Meeting.⁷⁶

For validation, I also evaluated outcomes on phase I immunotherapy trials among 27 MSS adenocarcinoma patients (Figure 28). Breast, colon and esophageal cancers were the most common cancers with 7, 5 and 3 patients, respectively. Activating *PIK3CA*^{mut} were present in 7/27 (26%) patients (H1047R, 3; E545K, 2; E542K, 1; R88Q + K111N, 1). Patients with activating *PIK3CA*^{mut} had trend towards longer median time to treatment failure as compared to *PIK3CA*^{wild} patients (6.6 vs. 3.1 months, P=0.1). Similarly, 3/7 (42.9%) patients with *PIK3CA*^{mut} had stable disease > 6 months as compared to 2/20 (10%) patients with *PIK3CA*^{wild} (P=0.09).

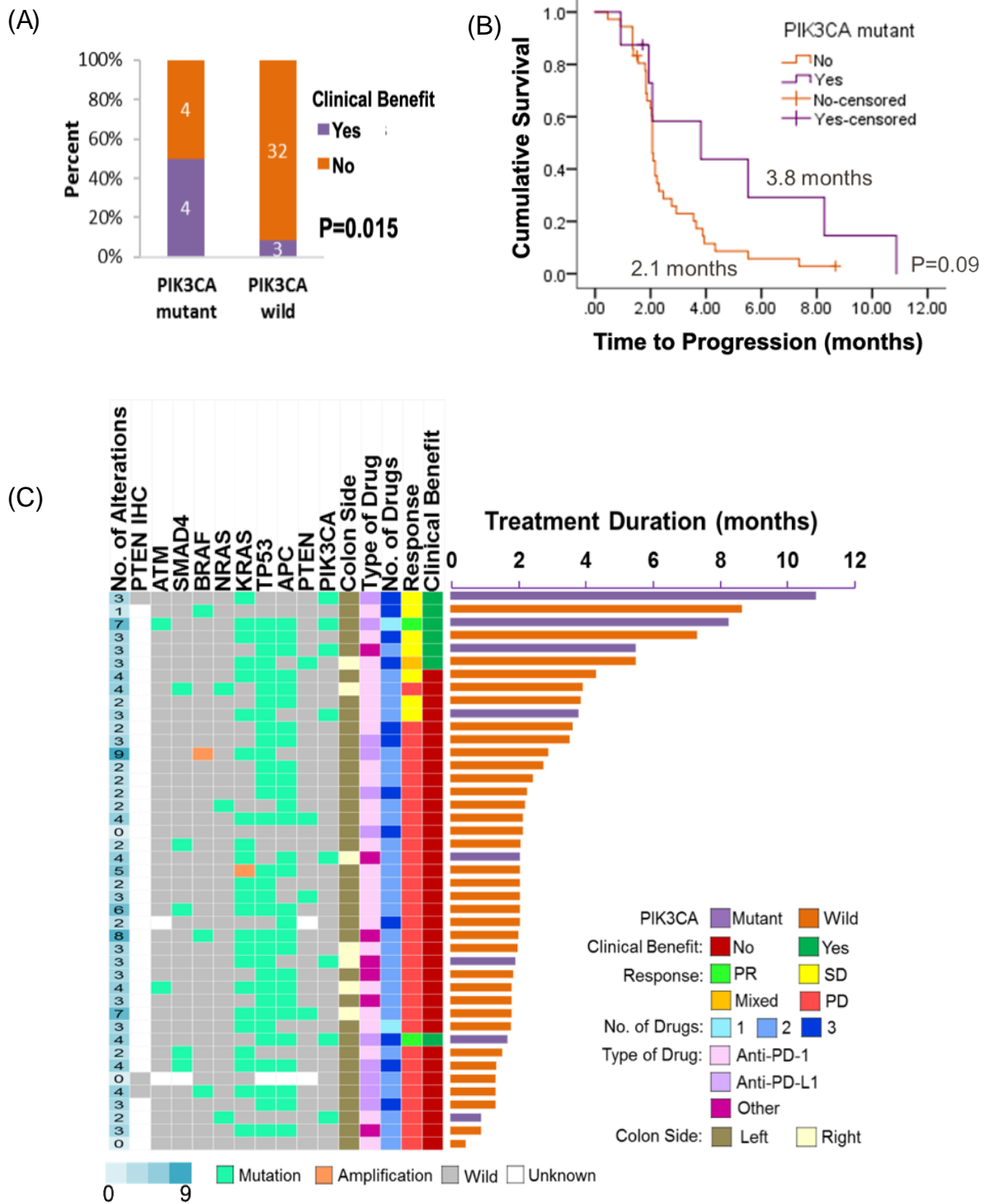


Figure 27: Outcomes on immunotherapy clinical trials among MSS CRC patients

(A) Clinical benefit. (B) Time to progression. (C) Swimmer's plot and molecular profile.

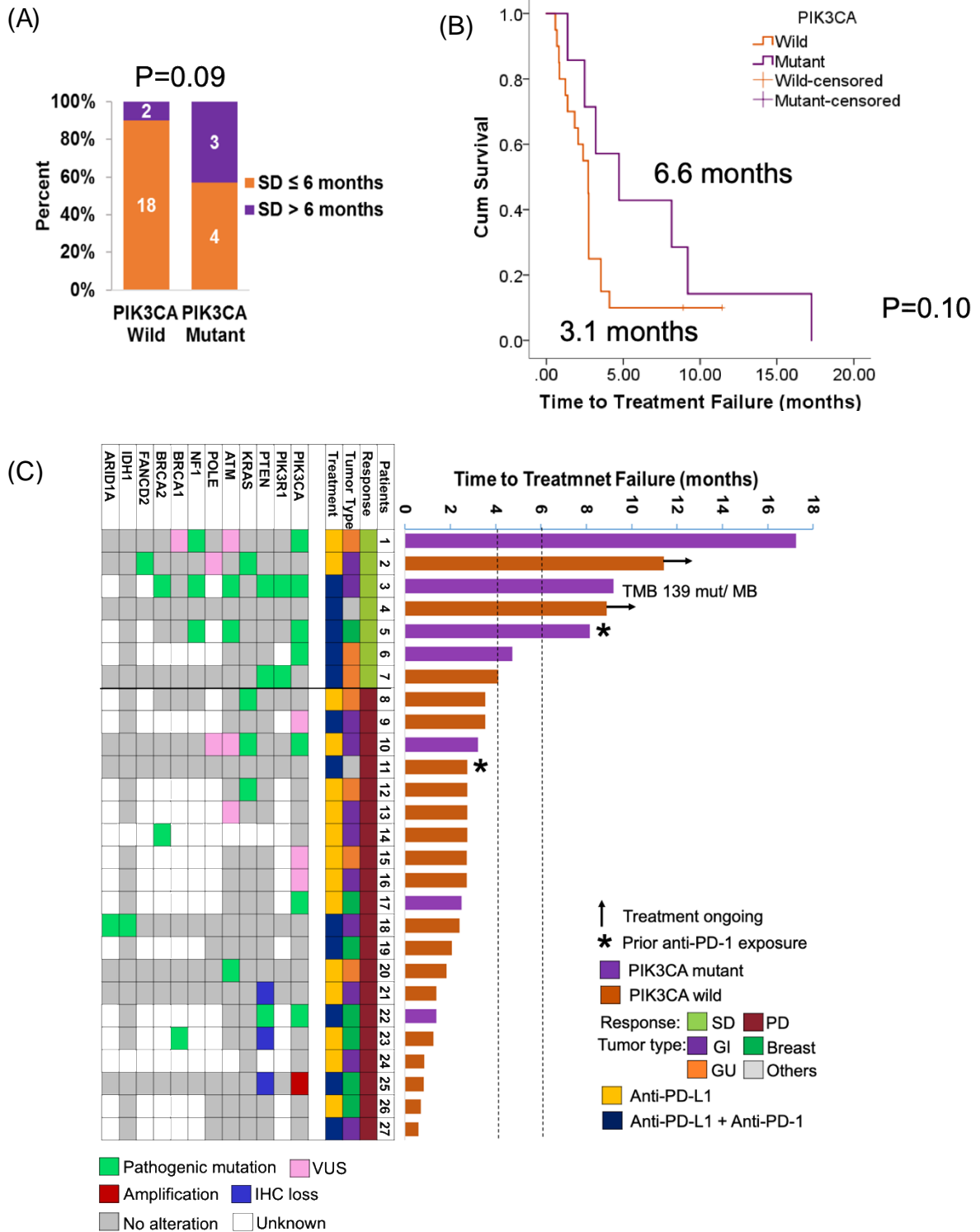


Figure 28: Outcomes with immunotherapy among MSS adenocarcinoma patients (A)

Clinical benefit. (B) Time to progression. (C) Swimmer's plot and molecular profile.

Synergism between PI3K inhibition and immunotherapy:

Next, I investigated synergism between PI3K inhibition and immunotherapy using a pan-PI3K inhibitor, copanlisib, in a CT26 mouse model (Figure 29). With 10 mice in each treatment arm, I showed that combination therapy resulted in greatest reduction of tumor volume as compared to either drug alone.

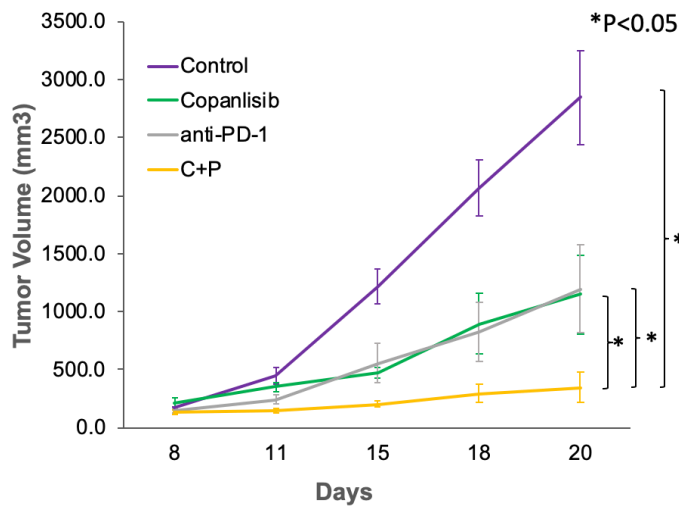


Figure 29: Synergism between anti-PD1 and PI3K inhibitor in CT26 mouse model of CRC (N=40). Error bars represent standard error of mean.

Given similar in vivo evidence of synergism in other tumors^{62,67}, I wrote the protocol of an NCI CTEP-sponsored phase Ib/II biomarker-based study of PI3K inhibitor (Copanlisib) in combination with immunotherapy (Nivolumab ± Ipilimumab) in patients with advanced solid cancers, under mentorship of Dr Timothy Yap (NCT04317105). Several translational correlatives are built into this protocol for further investigation of immunomodulatory changes associated with combined PI3K and checkpoint inhibition.

Conclusion:

PI3K pathway alterations are associated with an immunologically distinct subset of early stage MSS CRC with a prevalence of 25%. These tumors are characterized by increased immune engagement, but also up-regulation of key immune checkpoints resulting in an overall ineffective immune microenvironment. More specifically, *PIK3CA*^{mut} MSS CRC have increased cytotoxic T cell infiltration, higher checkpoint expression, and greater clinical benefit from immunotherapy. The immune signature of PI3K-altered MSS CRC tumors clusters with that from CMS1 and CMS4 tumors, which are the most inflamed subgroups. Finally, there's evidence of in vivo synergism between PI3K inhibition and immunotherapy.

Chapter IV: Discussion

PI3K signaling pathway alterations, *PIK3CA*^{mut} and PTEN^{loss}, are common and present in upto 40% of CRC patients. Targeted therapy with PI3K-AKT pathway inhibitors has been ineffective in CRC, including a phase II clinical trial of AKT inhibitor, MK2206, in biomarker-selected CRC patients conducted at MD Anderson. An in-depth understanding of target inhibition with the drug, as well as molecular perturbations in cell signaling that occur in response to AKT inhibition in CRC is important for the development of more effective treatment combinations. A huge recent success in CRC therapeutics is the development of immunotherapy for MSI CRC patients, and there's growing interest in immuno-oncology efforts to increase immune responsiveness in other CRC subsets. The immunomodulatory effects of PI3K pathway alterations have been reported in other cancers and have yet to be investigated in CRC. My thesis aims to investigate the molecular basis for clinical inactivity of AKT inhibition in metastatic CRC and to determine the tumor immune microenvironment of primary CRC with PI3K pathway alterations. The results lead to further hypothesis generation for new clinical trials using synergistic targeted therapy combinations as well as immunotherapy-based approaches for CRC patients with PI3K pathway alterations.

Aim 1: Demonstrate pharmacodynamics inhibition of AKT pathway in tumor and surrogate tissue from a clinical trial of MK2206 in CRC

Despite encouraging results with new drugs in preclinical experiments and phase I trials, few drugs show promise in subsequent stages of drug development.

With a targeted therapy such as AKT inhibitor, that is aimed at blocking transmission of signaling down the PI3K pathway, it is important to determine whether the signal was adequately inhibited with the drug at the dosing regimen used. We used reverse phase protein array to determine changes in protein expression of PD markers of AKT inhibition on cycle 1 day 15 as compared to baseline in paired patient samples from a clinical trial of MK2206 in metastatic CRC patients with *PIK3CA*^{mut} or *PTEN*^{loss}. We also studied PD inhibition with MK2206 in preclinical models, including cancer cell lines and PDXs.

In our study, among 15 patients with paired tumor biopsies, phosphorylation of AKT was decreased by a median of -37.9% at S473 (IQ range -26% to -46%) and by -4.8% at T308 (IQ range -40% to +6%) relative to total AKT levels. None of the patients in our study had 70% inhibition at either site. In previously published preclinical studies, 56.8 nmol/L drug concentration in whole blood was required for 70% inhibition of AKT S473 and was associated with antitumor activity. In the first-in-man phase I trial in advanced solid cancers, MK2206 at maximum tolerated dose of 60 mg oral dosing on alternate days inhibited AKT pS473 by a median of 88.8% in tumor tissue, and decreased PRAS40 pT246 by 48% in normal tissue (hair follicles). The average steady-state trough levels of MK-2206 in blood were higher than 56.8 nmol/L that were required to achieve 70% PD inhibition of AKT pS473.⁷⁸ Due its long half-life of 60-80 hours, a subsequent phase I study established 200 mg oral weekly as the maximum tolerated dose of MK2206, which is the dose used in our phase II clinical trial in CRC patients.⁷⁹ At this dose, mean 48 hour trough plasma concentration was 187 nmol/L; and in 5 patients with paired tumor biopsies, AKT

pS473 decreased from 37.5%–60.3% of baseline (mean 50% decrease).⁷⁹

Consistent with the results of our study, other phase II clinical trials of MK2206 in different tumor types have also reported less and insignificant decrease in phosphorylation of PD markers than that seen in phase I trials.⁸⁰⁻⁸²

Our analysis showed that changes in protein levels of AKT pS473 in patients' tumors showed the expected correlation with downstream PD markers, whereas changes in AKT pT308 did not. Hence, AKT pS473 seems to be a more reliable PD marker for MK2006. Inhibition of phosphorylation at both S473 and T308 is needed for complete inhibition of AKT signaling. In our study, inhibition of downstream PD markers in patients was less than that of AKT pS473. This is likely due to incomplete AKT inhibition as minimal change in AKT pT308 levels was observed in our study. Higher MK2206 concentrations maybe needed to inhibit AKT pT308 and downstream PD markers as suggested by other studies.⁸³

In our study, blood and tumor samples were collected 20 to 28 hours after MK-2206 dosing on cycle 1 day 15, to allow for sampling after maximum plasma concentration had been achieved and sustained for a few hours. In phase 1 clinical trial, the median time to plasma concentration was reported to be 4-6 hours with weekly dosing, and the inhibition of phosphorylation was sustained for at least 96 hours.⁷⁹ Hence our sample collection was adequately timed for assessment of PD effects of the drug.

We noted increase in phosphorylation of several PD markers in some patients on our clinical trial of MK2206. One patient had 529% increase from baseline in phosphorylation of S6 at both S235/236 and S240/244 sites. This patient also had

the greatest decrease in FoxO3a pS318/321 levels by 53.6% and the greatest rise in IR-b of 275.7%, which is suggestive of pathway reactivation through disruption of feedback loop. The pattern was not as clear in other patients. Paradoxical hyperphosphorylation of AKT regulatory sites (S473 and T308) was reported with ATP-competitive AKT inhibitor in cells.⁸⁴ This was found to be directly mediated by inhibitor binding to the ATP site of AKT which promoted its membrane localization, in absence of feedback loop dysregulation.⁸⁴ MK-2206 is an allosteric AKT inhibitor, and has been shown to inhibit autophosphorylation of AKT S473 and T308 in cell lines by inducing a conformational change in AKT.⁸⁵

Our analysis of PD markers in peripheral blood mononuclear cells used as surrogate tissue did not show any changes after treatment with MK2206. One possible reason for this is degradation of phosphoproteins during storage.

In line with prior preclinical models, our PDX model derived from a patient included in our clinical trial showed significant decrease in AKT pS473, AKT pT308, FoxO3a pS318/S321 and p70-S6K pT389 as compared to controls ($p < 0.02$ for all). The differences between our results of PD inhibition in mice and in humans maybe due to host or tumor characteristics that limit drug delivery to the tumor in patients.

Future Directions: Further studies are needed to understand host and tumor factors that limit intratumoral drug delivery in patients and account for discrepancy in preclinical and clinical pharmacodynamics. The search continues for drugs with greater therapeutic window to allow higher doses needed for inhibition of target and downstream signaling in the tumor. There are inherent limitations of RPPA that also apply to our study. The RPPA is performed on frozen biopsy samples and the ratio

of tumor to normal tissue may differ between samples. Other MK2206 clinical trials have utilized the same RPPA core lab for PD assessment and obtained results similar to that of RPPA by other means such as immunohistochemistry and immunoblotting.^{80, 82} The limited amount of tumor tissue obtained from paired patient biopsies in our clinical trial is currently being used to investigate immunomodulatory effects of AKT inhibition in CRC; and if there is tissue left after immune analysis, we can confirm our RPPA results with focused IHC staining for AKT pS473.

Aim 2: Determine the mechanisms of adaptive resistance to AKT inhibition in PI3K activated colorectal cancer patients, patient derived xenografts and cell lines.

Cells contain an intricate network of signaling pathways that are interconnected at different levels. Targeted inhibition of one protein triggers changes in expression or functioning of a number of other proteins, often producing unanticipated results. We have performed an in-depth analysis of adaptive resistance to AKT inhibition using reverse phase protein array on treated and untreated tumor samples from patients, PDXs and cell lines. Our results showed that allosteric AKT inhibition increased nuclear localization of FOXO, which resulted in induction of several receptor tyrosine kinases, and rephosphorylation of AKT pS473. Levels of IGF1R were significantly upregulated in all three models, whereas IR and HER3 levels were significantly increased in our preclinical models. Only IR levels correlated with phosphorylation of PI3K signaling proteins. We further showed that

disruption of one feedback loop after AKT inhibition activated the other feedback loop in most patients.

Using immunohistochemistry on PDX tumors, we showed that AKT inhibition results in nuclear localization of FOXO. FOXO is family of transcription factors for a variety of genes. When phosphorylated by AKT, FOXO proteins are sequestered in cytoplasm and prevented from translocating to the nucleus to carry on their function.^{27, 74} Chandarlapaty et al showed in BT-474 cells, that FOXO knockdown markedly decreases AKT inhibitor induced induction of IGF1R, IR and HER3 mRNAs. This effect is most potent with the knockdown of FoxO3 isoform. Using chromatin immunoprecipitation (ChIP) assays, they further showed binding of FOXO proteins to the promoters of these three receptors in BT-474 cells.²⁶ Similarly, other studies have also shown that inhibiting FoxO3a diminishes induction of IGF1R, IR, and HER3 mRNAs after AKT inhibition in breast cancer cell lines.^{42, 43} Our results also show an increase in total AKT levels after MK2206 treatment which correlate inversely with FoxO3a phosphorylation, suggesting that FoxO3a may also be a transcriptional promoter for AKT induction which warrants confirmatory studies. Upregulation of AKT3 expression has also been reported in breast cancer cell lines resistant to MK2206 treatment, mediated epigenetically by bromodomain and external terminal domain (BET) proteins.⁸⁶

We showed significant upregulation of IGF1R after AKT inhibition in patients, PDXs as well as cell lines, which is consistent with other published studies in breast and ovarian cancer cell lines.^{26, 43, 87} Our analysis of preclinical models showed significant induction of IR and HER3 in addition to IGF-1R after AKT inhibition, which

corroborates with results of other preclinical models of cancer from other labs.^{26, 42, 43} Our RPPA analysis from paired patient tumor biopsies showed higher expression of PDGFR after MK2206 treatment as compared to baseline that was approaching statistical significance. Induction of PDGFR α , alongwith induction of IGF-1R and IR, has been shown in a non-transformed breast epithelial cell line after AKT inhibition.²⁶ Induction of PDGFR in our post-treatment patient samples but not in our CRC PDX and tumor cell lines samples maybe reflective of normal tissue presence in frozen patient biopsy specimens submitted for RPPA. It is also possible that PDGFR maybe another transcriptional target of FOXO.

An interested finding in our patient analysis is that only one feedback loop appeared to be active at a time. It has been shown previously by other labs that mTOR inhibition with rapamycin increases phosphorylation of FOXO isomers.²⁶ Here I have shown that FOXO mediated RTK induction and pathway reactivation correlates directly with increased S6K phosphorylation and indirectly with decreased IRS1 levels as well as decreased phosphorylated RTK levels. How RTK phosphorylation is suppressed by mTORC1/S6K feedback loop is not entirely clear. Hence, our RPPA results from patients show an inverse correlation between IGF1R levels and phosphorylated IGF1R levels. While Chandarlapaty et al have shown that RTK induction after AKT inhibition was mostly accompanied by receptor phosphorylation, they also showed that FOXO silencing significantly decreased RTK phosphorylation after AKT inhibition, suggesting that increase in RTK phosphorylation maybe the result of mTORC1 inhibition.²⁶ In our study, we did see a direct correlation between IR levels and AKT pS473, which maybe mediating

pathway reactivation. It is also possible that AKT re-phosphorylation is a composite effect of signaling through several RTKs, and not one individual RTK. Another study has shown in renal cancer cells using ChIP analysis that RICTOR (a component of mTORC2, which phosphorylates AKT pS473) is also under transcriptional control of FoxO1 and FoxO3, and contribute to AKT re-phosphorylation.⁸⁸

Our results suggest further investigation of IGF1R inhibition along with PI3K-AKT inhibition in the treatment of PI3K-altered CRC patients, as has shown promise in preclinical studies in other tumor types.⁴³ However, such combinations have been poorly tolerated in prior early phase clinical trials with limited clinical activity (NCT01708161, NCT01243762).^{89, 90} While search for better tolerated IGF1R inhibitors or dual IGF1R / IR inhibitors continues, inhibition of HER kinase with PI3K-AKT inhibition has also shown promise in preclinical studies.⁴²

We did not notice a significant change in proteins of other signaling pathways after AKT inhibition. As our knowledge of functional significance of different molecular alterations expanded and multigene next generation sequencing became more readily available, MAP kinase pathway alterations (e.g, BRAF non-V600E mutations and NRAS mutations) were noted in some patients enrolled in our MK2206 trial, which may have contributed to inhibitor inactivity in these patients.

Finally, our results show a fair concordance of adaptive resistance analysis between patient samples, PDX tumors and cell lines.

Future Directions: Our results improve our understanding of signaling perturbations in response to AKT inhibition in CRC and generate hypothesis for

combination therapies that may block the induction of adaptive resistance and improve treatment efficacy. A dual IGF1R/IR signaling inhibitor maybe more effective at curbing down the adaptive response than IGF1R inhibitor alone. Vertical pathway inhibition using PI3K alpha inhibitor has also shown preclinical synergism with AKT inhibition in some studies, possibly by blocking pathway reactivation.⁹¹ For HER dependent tumors, combinations of PI3K-AKT inhibitors with HER kinase inhibitors also appear promising and may have implications for HER2 amplified CRC patients.⁹² Along the same lines, I recently co-authored an NCI-CTEP sponsored phase Ib/II clinical trial protocol of copanlisib (pan-PI3K inhibitor) in combination with trastuzumab and pertuzumab (dual HER2-targeted therapy) after induction treatment of HER2 positive metastatic breast cancer patients with PI3K pathway alterations (NCT04108858). There is also a role for strategies to decrease insulin surge and signaling to improve efficacy of PI3K-AKT inhibition such as through ketogenic diet or with SGLT2 inhibitors.⁹³ Finally, biomarker selection for future clinical trial enrollment will improve as our knowledge and testing capabilities improve.

Aim 3: Evaluate the impact of PI3K activating alterations on immune landscape of colorectal cancer, and design a therapeutic intervention to improve the immune microenvironment.

MSS CRC patients respond infrequently to immunotherapy, suggesting the presence of a rare MSS immunogenic subset. PI3K pathway alterations are known to modulate anti-tumor immune microenvironment and response to immunotherapy in different tumor types. In this Aim, we have shown PI3K pathway alterations

(comprising $PTEN^{loss}$ and $PIK3CA^{mut}$) to be a genomic modulator of immune repertoire in early stage MSS CRC patients. Using quantitative immunohistochemistry and Agilent microarrays on primary CRC, I showed that PI3K pathway alterations (particularly $PIK3CA^{mut}$) are associated with an immunologically distinct subset of MSS CRC, which exhibits increased immune engagement, but also up-regulation of several key immune checkpoints (including PD-L1) resulting in an overall ineffective immune microenvironment. Given increased immune infiltration and checkpoint upregulation in PI3K-altered cases, this maybe a potential subset of MSS CRC that can be targeted with immunotherapy combinations.

We found increased cytotoxic T cell infiltration at the center of PI3K-altered MSS but not MSI primary CRC. This maybe because of masking of PI3K effect by the robust immune repertoire of MSI tumors. Further subgroup analysis revealed increased T cell infiltration at the center of $PIK3CA^{mut}$ MSS CRC, but not $PTEN^{loss}$ MSS CRC. Similar increase in CD8+ cells among $PIK3CA^{mut}$ cases (specifically $PIK3CA^{E545K}$ and $PIK3CA^{H1047R}$) as compared to $PIK3CA^{wild}$ cases was seen an exploratory analysis of a breast cancer clinical trial.⁹⁴ Also, a recent analysis of The Cancer Genome Atlas data reported higher CD8+ T cells and NK cells, alongwith decreased regulatory T cell / CD8+ cell ratio across other cancer types with PIK3CA mutations.⁹⁵ Other studies in melanoma have shown decrease in cytotoxic T cell infiltration among $PTEN^{loss}$ as compared to $PTEN^{intact}$ tumors.⁶² We did not see any significant change in immune infiltration by PTEN status in CRC patients. This suggests that $PIK3CA^{mut}$ and $PTEN^{loss}$ have different modulatory effects on the immune repertoire of MSS CRC. In melanoma, $PTEN^{loss}$ effects were found to be

mediated by increase in immunoinhibitory cytokines such as VEGF.⁶² We postulate that increased effector T cell infiltration in *PIK3CA*^{mut} MSS CRC is partly mediated by generation of neo-peptides by mutant *PIK3CA*. Hotspot *PIK3CA*^{mut} (E545K, H1047R) have been reported to produce clonal neoantigens in MSS cancers other than CRC.⁹⁶

We also found increase in checkpoint expression by immunohistochemistry as well as Agilent microarrays in MSS CRC patients with PI3K pathway alterations. It appears that a highly robust immune engagement in the presence of PI3K pathway alterations results in compensatory upregulation of immune checkpoints by tumor cells as a means to immune evasion. Such compensatory increase in checkpoints has been reported in MSI CRC patients in the setting of high intra-tumoral T cells.⁹⁷ Consequently, in MSI CRC patients, immune checkpoint blockade has resulted in impressive durable responses by removing the negative regulation of pre-existing intra-tumoral cytotoxic T cells.^{19, 20} While several studies have identified *PTEN*^{loss} as a genomic predictor of resistance to immunotherapy in different tumor types, a recent meta-analysis has reported that *PI3KCA*^{mut} are enriched in MSS tumors with complete or partial response to immune checkpoint inhibitors.^{57, 58, 62, 98}

Recognizing cytotoxic T cell infiltration and PD-L1 upregulation as independent predictors of response to immunotherapy, I investigated the outcomes of MSS CRC patients who participated in seven immunotherapy clinical trials at MD Anderson, and found enrichment of *PIK3CA*^{mut} in patients who had tumor shrinkage or prolonged stable disease with immunotherapy. I validated this finding in another independent cohort of MSS adenocarcinoma patients enrolled in phase I

immunotherapy trials. About half of *PIK3CA*^{mut} MSS patients were seen to derive clinical benefit from immunotherapy in both cohorts. While the mechanism underlying this observation is yet to be investigated, it may be partly explained by high binding affinity mutant *PIK3CA* neopeptide generation in the context of the right HLA. HLA typing of *PIK3CA*^{mut} patients in the above MSS CRC cohort and phase I cohort is ongoing. Further investigation of immunotherapy outcomes in the context of neoepitope-HLA allele interaction may help identify a subset of *PIK3CA*^{mut} MSS CRC pts who are likely to benefit from immunotherapy.

In our study, hierarchical clustering analysis of mRNA data showed that the immune-related gene signature of early stage MSS CRC tumors clusters with that from CMS1 and CMS4 tumors. CMS1 tumors are associated with increased expression of cytotoxic lymphocyte related genes, whereas CMS4 tumors exhibit an immunosuppressive gene signature.⁹⁹ When the two signatures co-exist in highly immunogenic MSI CRC patients, increased immune checkpoint expression has shown to overpower the favorable impact of higher cytotoxic T cell infiltration, thereby decreasing overall survival as compared to MSI CRC with low expression of immune-checkpoints.¹⁰⁰ Hence, similar to our quantitative IHC data, the mRNA data is suggestive of an overall immune-inhibitory signature in MSS CRC with PI3K pathway alterations.

The impact of MAP kinase pathway mutations (*BRAF* and *KRAS* mutations) on immune microenvironment of CRC has been described.¹⁰¹ In our study, the distribution of these mutations was not different in the two groups of interest, CRC

with and without PI3K pathway alterations, and we assume that the impact of these mutations on immune analysis would also not differ in the two groups.

Our CT26 CRC model showed synergism between PI3K inhibition and anti-PD-1, consistent with prior preclinical studies in other tumor types.^{62, 67} This model does not contain PI3K pathway alterations and is suggestive of favorable immunomodulation by PI3K inhibition, the exact specifics of which are unclear and are under investigation. The tumor tissue from our mouse experiments has been submitted for multiplex immunohistochemistry for immune markers for further insight into these mechanisms.

Future Directions: Our work sets the stage for larger studies focusing on immunomodulatory effects of PTEN^{loss} separately from *PIK3CA*^{mut} in MSS CRC patients. The total tumor mutation burden in the presence and absence of PI3K pathway alterations remains to be determined. My ongoing research includes investigation of the immune microenvironment of PI3K-altered metastatic CRC, and the impact of PI3K-AKT pathway inhibition on the immune repertoire of these patients with support from a Conquer Cancer Foundation of ASCO Young Investigator Award. I am further investigating immunomodulation associated with different PI3K-AKT pathway inhibitors in *PIK3CA*^{mut} genetically engineered mice. Assessment of response to combined checkpoint blockade, such as anti-PD1 with anti-LAG-3, merits investigation in PI3K-altered MSS CRC patients. HLA typing of *PIK3CA*^{mut} patients in the above MSS CRC cohort and phase I cohort is ongoing. Evaluation of the predicted HLA affinities of peptides generated by *PIK3CA*^{mut} and other common CRC mutations is also planned for the future. This analysis has the

potential to identify HLA-neopeptide biomarkers that would be predictive of response to immunotherapy among *PIK3CA*^{mut} MSS CRC patients. Large scale studies are needed to determine prognosis with and without adjuvant chemotherapy in MSS CRC patients with PI3K pathway alterations.

Conclusions

Allosteric AKT inhibitor, MK2206, causes significant inhibition of PD markers in preclinical models but not in patient's tumors. The inverse correlation between AKT pS473 and downstream FoxO3a pS318/321 maybe reflective of partial AKT re-phosphorylation due to FoxO3a-mediated adaptive changes. AKT inhibition with MK2206 induces FOXO-mediated adaptive upregulation of receptor tyrosine kinases, namely IGF1R but also HER3 and IR. Combined analysis of cell lines, PDXs and patient samples allows in-depth interrogation of adaptive resistance and identifies rational combination therapies worthy of further investigation. PI3K-altered early stage MSS CRC is an immunologically distinct subset with higher immune engagement, but also upregulation of immune checkpoints, such as PD-L1, resulting in an overall ineffective immune microenvironment. In particular, *PIK3CA*^{mut} MSS CRC are associated with higher cytotoxic T cell infiltration, PD-L1 expression and clinical benefit from immunotherapy. Larger studies to validate our observations are warranted, including assessment of neopeptide load and HLA types, which may help identify an immunotherapy sensitive subset of *PIK3CA*^{mut} MSS adenocarcinoma.

Bibliography

1. Siegel RL, Miller KD, Jemal A. Cancer statistics, 2020. *CA: A Cancer Journal for Clinicians*. 2020;70(1):7-30.
2. Siegel RL, Fedewa SA, Anderson WF, Miller KD, Ma J, Rosenberg PS, Jemal A. Colorectal Cancer Incidence Patterns in the United States, 1974-2013. *J Natl Cancer Inst*. 2017;109(8):djw322.
3. Lui RN, Tsoi KKF, Ho JMW, Lo CM, Chan FCH, Kyaw MH, Sung JJY. Global Increasing Incidence of Young-Onset Colorectal Cancer Across 5 Continents: A Joinpoint Regression Analysis of 1,922,167 Cases. *Cancer Epidemiol Biomarkers Prev*. 2019;28(8):1275-82.
4. Pearlman R, Frankel WL, Swanson B, Zhao W, Yilmaz A, Miller K, Bacher J, Bigley C, Nelsen L, Goodfellow PJ, Goldberg RM, Paskett E, Shields PG, Freudenheim JL, Stanich PP, Lattimer I, Arnold M, Liyanarachchi S, Kalady M, Heald B, Greenwood C, Paquette I, Prues M, Draper DJ, Lindeman C, Kuebler JP, Reynolds K, Brell JM, Shaper AA, Mahesh S, Buie N, Weeman K, Shine K, Haut M, Edwards J, Bastola S, Wickham K, Khanduja KS, Zacks R, Pritchard CC, Shirts BH, Jacobson A, Allen B, de la Chapelle A, Hampel H, Ohio Colorectal Cancer Prevention Initiative Study G. Prevalence and Spectrum of Germline Cancer Susceptibility Gene Mutations Among Patients With Early-Onset Colorectal Cancer. *JAMA Oncol*. 2017;3(4):464-71.
5. Willauer AN, Liu Y, Pereira AAL, Lam M, Morris JS, Raghav KPS, Morris VK, Menter D, Broaddus R, Meric-Bernstam F, Hayes-Jordan A, Huh W, Overman

- MJ, Kopetz S, Loree JM. Clinical and molecular characterization of early-onset colorectal cancer. *Cancer*. 2019;125(12):2002-10.
6. Wolf AMD, Fontham ETH, Church TR, Flowers CR, Guerra CE, LaMonte SJ, Etzioni R, McKenna MT, Oeffinger KC, Shih YT, Walter LC, Andrews KS, Brawley OW, Brooks D, Fedewa SA, Manassaram-Baptiste D, Siegel RL, Wender RC, Smith RA. Colorectal cancer screening for average-risk adults: 2018 guideline update from the American Cancer Society. *CA Cancer J Clin*. 2018;68(4):250-81.
 7. American Cancer Society. *Colorectal Cancer Facts & Figures 2017-2019*. Atlanta: American Cancer Society; 2017.
 8. Hochster HS, Hart LL, Ramanathan RK, Childs BH, Hainsworth JD, Cohn AL, Wong L, Fehrenbacher L, Abubakr Y, Saif MW, Schwartzberg L, Hedrick E. Safety and efficacy of oxaliplatin and fluoropyrimidine regimens with or without bevacizumab as first-line treatment of metastatic colorectal cancer: results of the TREE Study. *J Clin Oncol*. 2008;26(21):3523-9.
 9. Saltz LB, Clarke S, Diaz-Rubio E, Scheithauer W, Figer A, Wong R, Koski S, Lichinitser M, Yang TS, Rivera F, Couture F, Sirzen F, Cassidy J. Bevacizumab in combination with oxaliplatin-based chemotherapy as first-line therapy in metastatic colorectal cancer: a randomized phase III study. *J Clin Oncol*. 2008;26(12):2013-9.
 10. Grothey A, Van Cutsem E, Sobrero A, Siena S, Falcone A, Ychou M, Humblet Y, Bouche O, Mineur L, Barone C, Adenis A, Tabernero J, Yoshino T, Lenz HJ, Goldberg RM, Sargent DJ, Cihon F, Cupit L, Wagner A, Laurent D, Group

- CS. Regorafenib monotherapy for previously treated metastatic colorectal cancer (CORRECT): an international, multicentre, randomised, placebo-controlled, phase 3 trial. *Lancet*. 2013;381(9863):303-12.
11. Mayer RJ, Van Cutsem E, Falcone A, Yoshino T, Garcia-Carbonero R, Mizunuma N, Yamazaki K, Shimada Y, Tabernero J, Komatsu Y, Sobrero A, Boucher E, Peeters M, Tran B, Lenz HJ, Zaniboni A, Hochster H, Cleary JM, Prenen H, Benedetti F, Mizuguchi H, Makris L, Ito M, Ohtsu A, Group RS. Randomized trial of TAS-102 for refractory metastatic colorectal cancer. *N Engl J Med*. 2015;372(20):1909-19.
 12. Yaeger R, Chatila WK, Lipsyc MD, Hechtman JF, Cercek A, Sanchez-Vega F, Jayakumaran G, Middha S, Zehir A, Donoghue MTA, You D, Viale A, Kemeny N, Segal NH, Stadler ZK, Varghese AM, Kundra R, Gao J, Syed A, Hyman DM, Vakiani E, Rosen N, Taylor BS, Ladanyi M, Berger MF, Solit DB, Shia J, Saltz L, Schultz N. Clinical Sequencing Defines the Genomic Landscape of Metastatic Colorectal Cancer. *Cancer Cell*. 2018;33(1):125-36 e3.
 13. Cancer Genome Atlas N. Comprehensive molecular characterization of human colon and rectal cancer. *Nature*. 2012;487(7407):330-7.
 14. Guinney J, Dienstmann R, Wang X, de Reynies A, Schlicker A, Sonesson C, Marisa L, Roepman P, Nyamundanda G, Angelino P, Bot BM, Morris JS, Simon IM, Gerster S, Fessler E, De Sousa EMF, Missiaglia E, Ramay H, Barras D, Homiczko K, Maru D, Manyam GC, Broom B, Boige V, Perez-Villamil B, Laderas T, Salazar R, Gray JW, Hanahan D, Tabernero J, Bernards R, Friend SH, Laurent-Puig P, Medema JP, Sadanandam A,

- Wessels L, Delorenzi M, Kopetz S, Vermeulen L, Tejpar S. The consensus molecular subtypes of colorectal cancer. *Nat Med*. 2015;21(11):1350-6.
15. Allegra CJ, Rumble RB, Hamilton SR, Mangu PB, Roach N, Hantel A, Schilsky RL. Extended RAS Gene Mutation Testing in Metastatic Colorectal Carcinoma to Predict Response to Anti-Epidermal Growth Factor Receptor Monoclonal Antibody Therapy: American Society of Clinical Oncology Provisional Clinical Opinion Update 2015. *J Clin Oncol*. 2016;34(2):179-85.
 16. Kopetz S, Grothey A, Yaeger R, Van Cutsem E, Desai J, Yoshino T, Wasan H, Ciardiello F, Loupakis F, Hong YS, Steeghs N, Guren TK, Arkenau HT, Garcia-Alfonso P, Pfeiffer P, Orlov S, Lonardi S, Elez E, Kim TW, Schellens JHM, Guo C, Krishnan A, Dekervel J, Morris V, Calvo Ferrandiz A, Tarpgaard LS, Braun M, Gollerkeri A, Keir C, Maharry K, Pickard M, Christy-Bittel J, Anderson L, Sandor V, Tabernero J. Encorafenib, Binimetinib, and Cetuximab in BRAF V600E-Mutated Colorectal Cancer. *N Engl J Med*. 2019;381(17):1632-43.
 17. Lee HM, Morris V, Napolitano S, Kopetz S. Evolving Strategies for the Management of BRAF-Mutant Metastatic Colorectal Cancer. *Oncology (Williston Park)*. 2019;33(6):206-11.
 18. Meric-Bernstam F, Hurwitz H, Raghav KPS, McWilliams RR, Fakih M, VanderWalde A, Swanton C, Kurzrock R, Burris H, Sweeney C, Bose R, Spigel DR, Beattie MS, Blotner S, Stone A, Schulze K, Cuchelkar V, Hainsworth J. Pertuzumab plus trastuzumab for HER2-amplified metastatic

- colorectal cancer (MyPathway): an updated report from a multicentre, open-label, phase 2a, multiple basket study. *Lancet Oncol.* 2019;20(4):518-30.
19. Overman MJ, McDermott R, Leach JL, Lonardi S, Lenz HJ, Morse MA, Desai J, Hill A, Axelson M, Moss RA, Goldberg MV, Cao ZA, Ledezine JM, Maglente GA, Kopetz S, Andre T. Nivolumab in patients with metastatic DNA mismatch repair-deficient or microsatellite instability-high colorectal cancer (CheckMate 142): an open-label, multicentre, phase 2 study. *Lancet Oncol.* 2017.
 20. Overman MJ, Lonardi S, Wong KYM, Lenz HJ, Gelsomino F, Aglietta M, Morse MA, Van Cutsem E, McDermott R, Hill A, Sawyer MB, Hendlisz A, Neyns B, Svrcek M, Moss RA, Ledezine JM, Cao ZA, Kamble S, Kopetz S, Andre T. Durable Clinical Benefit With Nivolumab Plus Ipilimumab in DNA Mismatch Repair-Deficient/Microsatellite Instability-High Metastatic Colorectal Cancer. *J Clin Oncol.* 2018;36(8):773-9.
 21. Drilon A, Laetsch TW, Kummar S, DuBois SG, Lassen UN, Demetri GD, Nathenson M, Doebele RC, Farago AF, Pappo AS, Turpin B, Dowlati A, Brose MS, Mascarenhas L, Federman N, Berlin J, El-Deiry WS, Baik C, Deeken J, Boni V, Nagasubramanian R, Taylor M, Rudzinski ER, Meric-Bernstam F, Sohal DPS, Ma PC, Raez LE, Hechtman JF, Benayed R, Ladanyi M, Tuch BB, Ebata K, Cruickshank S, Ku NC, Cox MC, Hawkins DS, Hong DS, Hyman DM. Efficacy of Larotrectinib in TRK Fusion-Positive Cancers in Adults and Children. *N Engl J Med.* 2018;378(8):731-9.
 22. Clifton K, Rich TA, Parseghian C, Raymond VM, Dasari A, Pereira AAL, Willis J, Loree JM, Bauer TM, Chae YK, Sherrill G, Fanta P, Grothey A, Hendifar A,

- Henry D, Mahadevan D, Nezami MA, Tan B, Wainberg ZA, Lanman R, Kopetz S, Morris V. Identification of Actionable Fusions as an Anti-EGFR Resistance Mechanism Using a Circulating Tumor DNA Assay. *JCO Precision Oncology*. 2019(3):1-15.
23. Vanhaesebroeck B, Guillermet-Guibert J, Graupera M, Bilanges B. The emerging mechanisms of isoform-specific PI3K signalling. *Nat Rev Mol Cell Biol*. 2010;11(5):329-41.
24. Cantley LC. The Phosphoinositide 3-Kinase Pathway. *Science*. 2002;296(5573):1655-7.
25. Manning BD, Toker A. AKT/PKB Signaling: Navigating the Network. *Cell*. 2017;169(3):381-405.
26. Chandarlapaty S, Sawai A, Scaltriti M, Rodrik-Outmezguine V, Grbovic-Huezo O, Serra V, Majumder PK, Baselga J, Rosen N. AKT inhibition relieves feedback suppression of receptor tyrosine kinase expression and activity. *Cancer Cell*. 2011;19(1):58-71.
27. Brunet A, Bonni A, Zigmond MJ, Lin MZ, Juo P, Hu LS, Anderson MJ, Arden KC, Blenis J, Greenberg ME. Akt promotes cell survival by phosphorylating and inhibiting a Forkhead transcription factor. *Cell*. 1999;96(6):857-68.
28. Danielsen SA, Eide PW, Nesbakken A, Guren T, Leithe E, Lothe RA. Portrait of the PI3K/AKT pathway in colorectal cancer. *Biochim Biophys Acta*. 2015;1855(1):104-21.
29. Kim HJ, Lee SY, Oh SC. The Inositide Signaling Pathway As a Target for Treating Gastric Cancer and Colorectal Cancer. *Front Physiol*. 2016;7:168.

30. Zhang J, Roberts TM, Shivdasani RA. Targeting PI3K signaling as a therapeutic approach for colorectal cancer. *Gastroenterology*. 2011;141(1):50-61.
31. Thorpe LM, Yuzugullu H, Zhao JJ. PI3K in cancer: divergent roles of isoforms, modes of activation and therapeutic targeting. *Nat Rev Cancer*. 2015;15(1):7-24.
32. Iida S, Kato S, Ishiguro M, Matsuyama T, Ishikawa T, Kobayashi H, Higuchi T, Uetake H, Enomoto M, Sugihara K. PIK3CA mutation and methylation influences the outcome of colorectal cancer. *Oncol Lett*. 2012;3(3):565-70.
33. Zhu YF, Yu BH, Li DL, Ke HL, Guo XZ, Xiao XY. PI3K expression and PIK3CA mutations are related to colorectal cancer metastases. *World J Gastroenterol*. 2012;18(28):3745-51.
34. Wang Q, Shi YL, Zhou K, Wang LL, Yan ZX, Liu YL, Xu LL, Zhao SW, Chu HL, Shi TT, Ma QH, Bi J. PIK3CA mutations confer resistance to first-line chemotherapy in colorectal cancer. *Cell Death Dis*. 2018;9(7):739.
35. Sartore-Bianchi A, Martini M, Molinari F, Veronese S, Nichelatti M, Artale S, Di Nicolantonio F, Saletti P, De Dosso S, Mazzucchelli L, Frattini M, Siena S, Bardelli A. PIK3CA mutations in colorectal cancer are associated with clinical resistance to EGFR-targeted monoclonal antibodies. *Cancer Res*. 2009;69(5):1851-7.
36. Xu JM, Wang Y, Wang YL, Wang Y, Liu T, Ni M, Li MS, Lin L, Ge FJ, Gong C, Gu JY, Jia R, Wang HF, Chen YL, Liu RR, Zhao CH, Tan ZL, Jin Y, Zhu YP, Ogino S, Qian ZR. PIK3CA Mutations Contribute to Acquired Cetuximab

- Resistance in Patients with Metastatic Colorectal Cancer. *Clin Cancer Res.* 2017;23(16):4602-16.
37. Liao X, Lochhead P, Nishihara R, Morikawa T, Kuchiba A, Yamauchi M, Imamura Y, Qian ZR, Baba Y, Shima K, Sun R, Nosho K, Meyerhardt JA, Giovannucci E, Fuchs CS, Chan AT, Ogino S. Aspirin use, tumor PIK3CA mutation, and colorectal-cancer survival. *N Engl J Med.* 2012;367(17):1596-606.
 38. Papadatos-Pastos D, Rabbie R, Ross P, Sarker D. The role of the PI3K pathway in colorectal cancer. *Crit Rev Oncol Hematol.* 2015;94(1):18-30.
 39. Bahrami A, Khazaei M, Hasanzadeh M, ShahidSales S, Joudi Mashhad M, Farazestanian M, Sadeghnia HR, Rezayi M, Maftouh M, Hassanian SM, Avan A. Therapeutic Potential of Targeting PI3K/AKT Pathway in Treatment of Colorectal Cancer: Rational and Progress. *J Cell Biochem.* 2017.
 40. Janku F. Phosphoinositide 3-kinase (PI3K) pathway inhibitors in solid tumors: From laboratory to patients. *Cancer Treat Rev.* 2017;59:93-101.
 41. Hanker AB, Kaklamani V, Arteaga CL. Challenges for the Clinical Development of PI3K Inhibitors: Strategies to Improve Their Impact in Solid Tumors. *Cancer Discov.* 2019;9(4):482-91.
 42. Chakrabarty A, Sanchez V, Kuba MG, Rinehart C, Arteaga CL. Feedback upregulation of HER3 (ErbB3) expression and activity attenuates antitumor effect of PI3K inhibitors. *Proc Natl Acad Sci U S A.* 2012;109(8):2718-23.
 43. Fox EM, Kuba MG, Miller TW, Davies BR, Arteaga CL. Autocrine IGF-I/insulin receptor axis compensates for inhibition of AKT in ER-positive breast cancer

- cells with resistance to estrogen deprivation. *Breast Cancer Res.* 2013;15(4):R55.
44. Bindea G, Mlecnik B, Tosolini M, Kirilovsky A, Waldner M, Obenauf AC, Angell H, Fredriksen T, Lafontaine L, Berger A, Bruneval P, Fridman WH, Becker C, Pages F, Speicher MR, Trajanoski Z, Galon J. Spatiotemporal dynamics of intratumoral immune cells reveal the immune landscape in human cancer. *Immunity.* 2013;39(4):782-95.
 45. Garziera M, Toffoli G. Inhibition of host immune response in colorectal cancer: human leukocyte antigen-G and beyond. *World J Gastroenterol.* 2014;20(14):3778-94.
 46. Galon J, Costes A, Sanchez-Cabo F, Kirilovsky A, Mlecnik B, Lagorce-Pages C, Tosolini M, Camus M, Berger A, Wind P, Zinzindohoue F, Bruneval P, Cugnenc PH, Trajanoski Z, Fridman WH, Pages F. Type, density, and location of immune cells within human colorectal tumors predict clinical outcome. *Science.* 2006;313(5795):1960-4.
 47. Mlecnik B, Tosolini M, Kirilovsky A, Berger A, Bindea G, Meatchi T, Bruneval P, Trajanoski Z, Fridman WH, Pages F, Galon J. Histopathologic-based prognostic factors of colorectal cancers are associated with the state of the local immune reaction. *J Clin Oncol.* 2011;29(6):610-8.
 48. Pages F, Galon J, Dieu-Nosjean MC, Tartour E, Sautes-Fridman C, Fridman WH. Immune infiltration in human tumors: a prognostic factor that should not be ignored. *Oncogene.* 2010;29(8):1093-102.

49. Naito Y, Saito K, Shiiba K, Ohuchi A, Saigenji K, Nagura H, Ohtani H. CD8+ T cells infiltrated within cancer cell nests as a prognostic factor in human colorectal cancer. *Cancer Res.* 1998;58(16):3491-4.
50. Pages F, Berger A, Camus M, Sanchez-Cabo F, Costes A, Molitor R, Mlecnik B, Kirilovsky A, Nilsson M, Damotte D, Meatchi T, Bruneval P, Cugnenc PH, Trajanoski Z, Fridman WH, Galon J. Effector memory T cells, early metastasis, and survival in colorectal cancer. *N Engl J Med.* 2005;353(25):2654-66.
51. Pages F, Mlecnik B, Marliot F, Bindea G, Ou FS, Bifulco C, Lugli A, Zlobec I, Rau TT, Berger MD, Nagtegaal ID, Vink-Borger E, Hartmann A, Geppert C, Kolwelter J, Merkel S, Grutzmann R, Van den Eynde M, Jouret-Mourin A, Kartheuser A, Leonard D, Remue C, Wang JY, Bavi P, Roehrl MHA, Ohashi PS, Nguyen LT, Han S, MacGregor HL, Hafezi-Bakhtiari S, Wouters BG, Masucci GV, Andersson EK, Zavadova E, Vocka M, Spacek J, Petruzelka L, Konopasek B, Dundr P, Skalova H, Nemejcova K, Botti G, Tatangelo F, Delrio P, Ciliberto G, Maio M, Laghi L, Grizzi F, Fredriksen T, Buttard B, Angelova M, Vasaturo A, Maby P, Church SE, Angell HK, Lafontaine L, Bruni D, El Sissy C, Haicheur N, Kirilovsky A, Berger A, Lagorce C, Meyers JP, Paustian C, Feng Z, Ballesteros-Merino C, Dijkstra J, van de Water C, van Lent-van Vliet S, Knijn N, Musina AM, Scripcariu DV, Popivanova B, Xu M, Fujita T, Hazama S, Suzuki N, Nagano H, Okuno K, Torigoe T, Sato N, Furuhashi T, Takemasa I, Itoh K, Patel PS, Vora HH, Shah B, Patel JB, Rajvik KN, Pandya SJ, Shukla SN, Wang Y, Zhang G, Kawakami Y, Marincola FM, Ascierto PA,

- Sargent DJ, Fox BA, Galon J. International validation of the consensus Immunoscore for the classification of colon cancer: a prognostic and accuracy study. *Lancet*. 2018;391(10135):2128-39.
52. Mlecnik B, Bindea G, Angell HK, Maby P, Angelova M, Tougeron D, Church SE, Lafontaine L, Fischer M, Fredriksen T, Sasso M, Bilocq AM, Kirilovsky A, Obenauf AC, Hamieh M, Berger A, Bruneval P, Tuech JJ, Sabourin JC, Le Pessot F, Mauillon J, Raffi A, Laurent-Puig P, Speicher MR, Trajanoski Z, Michel P, Sesboue R, Frebourg T, Pages F, Valge-Archer V, Latouche JB, Galon J. Integrative Analyses of Colorectal Cancer Show Immunoscore Is a Stronger Predictor of Patient Survival Than Microsatellite Instability. *Immunity*. 2016;44(3):698-711.
53. Chen PL, Roh W, Reuben A, Cooper ZA, Spencer CN, Prieto PA, Miller JP, Bassett RL, Gopalakrishnan V, Wani K, De Macedo MP, Austin-Breneman JL, Jiang H, Chang Q, Reddy SM, Chen WS, Tetzlaff MT, Broaddus RJ, Davies MA, Gershenwald JE, Haydu L, Lazar AJ, Patel SP, Hwu P, Hwu WJ, Diab A, Glitza IC, Woodman SE, Vence LM, Wistuba II, Amaria RN, Kwong LN, Prieto V, Davis RE, Ma W, Overwijk WW, Sharpe AH, Hu J, Futreal PA, Blando J, Sharma P, Allison JP, Chin L, Wargo JA. Analysis of Immune Signatures in Longitudinal Tumor Samples Yields Insight into Biomarkers of Response and Mechanisms of Resistance to Immune Checkpoint Blockade. *Cancer Discov*. 2016;6(8):827-37.

54. Hughes PE, Caenepeel S, Wu LC. Targeted Therapy and Checkpoint Immunotherapy Combinations for the Treatment of Cancer. *Trends Immunol.* 2016;37(7):462-76.
55. Boland PM, Ma WW. Immunotherapy for Colorectal Cancer. *Cancers (Basel).* 2017;9(5).
56. Bendell J, Tae Won K, Cheng Ean C, Yung-Jue B, Lee C, Desai J, Lewin J, Wallin J, Das Thakur M, Mwawasi G, Cha E, Infante J. LBA-01 Safety and efficacy of cobimetinib (cobi) and atezolizumab (atezo) in a Phase 1b study of metastatic colorectal cancer (mCRC). *Annals of Oncology.* 2016;27(suppl_2):ii140-ii.
57. George S, Miao D, Demetri GD, Adeegbe D, Rodig SJ, Shukla S, Lipschitz M, Amin-Mansour A, Raut CP, Carter SL, Hammerman P, Freeman GJ, Wu CJ, Ott PA, Wong KK, Van Allen EM. Loss of PTEN Is Associated with Resistance to Anti-PD-1 Checkpoint Blockade Therapy in Metastatic Uterine Leiomyosarcoma. *Immunity.* 2017;46(2):197-204.
58. Roh W, Chen PL, Reuben A, Spencer CN, Prieto PA, Miller JP, Gopalakrishnan V, Wang F, Cooper ZA, Reddy SM, Gumbs C, Little L, Chang Q, Chen WS, Wani K, De Macedo MP, Chen E, Austin-Breneman JL, Jiang H, Roszik J, Tetzlaff MT, Davies MA, Gershenwald JE, Tawbi H, Lazar AJ, Hwu P, Hwu WJ, Diab A, Glitza IC, Patel SP, Woodman SE, Amaria RN, Prieto VG, Hu J, Sharma P, Allison JP, Chin L, Zhang J, Wargo JA, Futreal PA. Integrated molecular analysis of tumor biopsies on sequential CTLA-4

- and PD-1 blockade reveals markers of response and resistance. *Sci Transl Med.* 2017;9(379).
59. Macintyre AN, Finlay D, Preston G, Sinclair LV, Waugh CM, Tamas P, Feijoo C, Okkenhaug K, Cantrell DA. Protein kinase B controls transcriptional programs that direct cytotoxic T cell fate but is dispensable for T cell metabolism. *Immunity.* 2011;34(2):224-36.
 60. Crompton JG, Sukumar M, Roychoudhuri R, Clever D, Gros A, Eil RL, Tran E, Hanada K, Yu Z, Palmer DC, Kerkar SP, Michalek RD, Upham T, Leonardi A, Acquavella N, Wang E, Marincola FM, Gattinoni L, Muranski P, Sundrud MS, Klebanoff CA, Rosenberg SA, Fearon DT, Restifo NP. Akt inhibition enhances expansion of potent tumor-specific lymphocytes with memory cell characteristics. *Cancer Res.* 2015;75(2):296-305.
 61. Dituri F, Mazzocca A, Giannelli G, Antonaci S. PI3K functions in cancer progression, anticancer immunity and immune evasion by tumors. *Clin Dev Immunol.* 2011;2011:947858.
 62. Peng W, Chen JQ, Liu C, Malu S, Creasy C, Tetzlaff MT, Xu C, McKenzie JA, Zhang C, Liang X, Williams LJ, Deng W, Chen G, Mbofung R, Lazar AJ, Torres-Cabala CA, Cooper ZA, Chen PL, Tieu TN, Spranger S, Yu X, Bernatchez C, Forget MA, Haymaker C, Amaria R, McQuade JL, Glitza IC, Cascone T, Li HS, Kwong LN, Heffernan TP, Hu J, Bassett RL, Jr., Bosenberg MW, Woodman SE, Overwijk WW, Lizee G, Roszik J, Gajewski TF, Wargo JA, Gershenwald JE, Radvanyi L, Davies MA, Hwu P. Loss of

- PTEN Promotes Resistance to T Cell-Mediated Immunotherapy. *Cancer Discov.* 2016;6(2):202-16.
63. Song M, Chen D, Lu B, Wang C, Zhang J, Huang L, Wang X, Timmons CL, Hu J, Liu B, Wu X, Wang L, Wang J, Liu H. PTEN loss increases PD-L1 protein expression and affects the correlation between PD-L1 expression and clinical parameters in colorectal cancer. *PLoS One.* 2013;8(6):e65821.
64. Tumeo PC, Harview CL, Yearley JH, Shintaku IP, Taylor EJ, Robert L, Chmielowski B, Spasic M, Henry G, Ciobanu V, West AN, Carmona M, Kivork C, Seja E, Cherry G, Gutierrez AJ, Grogan TR, Mateus C, Tomasic G, Glaspy JA, Emerson RO, Robins H, Pierce RH, Elashoff DA, Robert C, Ribas A. PD-1 blockade induces responses by inhibiting adaptive immune resistance. *Nature.* 2014;515(7528):568-71.
65. So L, Yea SS, Oak JS, Lu M, Manmadhan A, Ke QH, Janes MR, Kessler LV, Kucharski JM, Li LS, Martin MB, Ren P, Jessen KA, Liu Y, Rommel C, Fruman DA. Selective inhibition of phosphoinositide 3-kinase p110alpha preserves lymphocyte function. *J Biol Chem.* 2013;288(8):5718-31.
66. Liu N, Haike K, Glaeske S, Paul J, Mumberg D, Kreft B, Ziegelbauer K. Copanlisib in combination with anti-PD-1 induces regression in animal tumor models insensitive or resistant to the monotherapies of PI3K and checkpoint inhibitors. *Hematological Oncology.* 2017;35:257-8.
67. Sai J, Owens P, Novitskiy SV, Hawkins OE, Vilgelm AE, Yang J, Sobolik T, Lavender N, Johnson AC, McClain C, Ayers GD, Kelley MC, Sanders M, Mayer IA, Moses HL, Boothby M, Richmond A. PI3K Inhibition Reduces

- Mammary Tumor Growth and Facilitates Antitumor Immunity and Anti-PD1 Responses. *Clin Cancer Res.* 2017;23(13):3371-84.
68. Dasari A, Overman MJ, Fogelman DR, Kee BK, Menter D, Raghav KPS, Morris VK, Oh J, Wu J, Jiang Z, Tian F, Adam L, Brimer M, Morris J, Meric-Bernstam F, Kopetz S. A phase II and co-clinical study of an AKT inhibitor in patients (pts) with biomarker-enriched, previously treated metastatic colorectal cancer (mCRC). *Journal of Clinical Oncology.* 2016;34(15_suppl):3563-.
69. Medico E, Russo M, Picco G, Cancelliere C, Valtorta E, Corti G, Buscarino M, Isella C, Lamba S, Martinoglio B, Veronese S, Siena S, Sartore-Bianchi A, Beccuti M, Mottolese M, Linnebacher M, Cordero F, Di Nicolantonio F, Bardelli A. The molecular landscape of colorectal cancer cell lines unveils clinically actionable kinase targets. *Nat Commun.* 2015;6:7002.
70. Tang YC, Ho SC, Tan E, Ng AWT, McPherson JR, Goh GYL, Teh BT, Bard F, Rozen SG. Functional genomics identifies specific vulnerabilities in PTEN-deficient breast cancer. *Breast Cancer Res.* 2018;20(1):22.
71. Hennessy BT, Lu Y, Gonzalez-Angulo AM, Carey MS, Myhre S, Ju Z, Davies MA, Liu W, Coombes K, Meric-Bernstam F, Bedrosian I, McGahren M, Agarwal R, Zhang F, Overgaard J, Alsner J, Neve RM, Kuo WL, Gray JW, Borresen-Dale AL, Mills GB. A Technical Assessment of the Utility of Reverse Phase Protein Arrays for the Study of the Functional Proteome in Non-microdissected Human Breast Cancers. *Clin Proteomics.* 2010;6(4):129-51.

72. Khoury JD, Wang W-L, Prieto VG, Medeiros LJ, Kalhor N, Hameed M, Broaddus R, Hamilton SR. Validation of Immunohistochemical Assays for Integral Biomarkers in the NCI-MATCH EAY131 Clinical Trial. *Clinical Cancer Research*. 2017.
73. Nusrat M, Oh J, Jiang Z-Q, Dasari A, Fogelman DR, Kee BK, Menter D, Raghav KPS, Morris VK, Wu J, Meric-Bernstam F, Morris J, Overman MJ, Kopetz S. Proteomic profiling of phosphatidylinositol 3-kinase (PI3K) altered metastatic colorectal cancer (mCRC) after protein kinase B (Akt) inhibition: Insulin like growth factor 1 receptor (IGF1R) mediates adaptive resistance. *Journal of Clinical Oncology*. 2018;36(15_suppl):3549-.
74. Myatt SS, Lam EW. The emerging roles of forkhead box (Fox) proteins in cancer. *Nat Rev Cancer*. 2007;7(11):847-59.
75. Galon J, Mlecnik B, Bindea G, Angell HK, Berger A, Lagorce C, Lugli A, Zlobec I, Hartmann A, Bifulco C, Nagtegaal ID, Palmqvist R, Masucci GV, Botti G, Tatangelo F, Delrio P, Maio M, Laghi L, Grizzi F, Asslaber M, D'Arrigo C, Vidal-Vanaclocha F, Zavadova E, Chouchane L, Ohashi PS, Hafezi-Bakhtiari S, Wouters BG, Roehrl M, Nguyen L, Kawakami Y, Hazama S, Okuno K, Ogino S, Gibbs P, Waring P, Sato N, Torigoe T, Itoh K, Patel PS, Shukla SN, Wang Y, Kopetz S, Sinicrope FA, Scripcariu V, Ascierto PA, Marincola FM, Fox BA, Pages F. Towards the introduction of the 'Immunoscore' in the classification of malignant tumours. *J Pathol*. 2014;232(2):199-209.

76. Nusrat M, Roszik J, Katkhuda R, Menter D, Raghav KPS, Morris VK, Sharma P, Allison JP, Blando JM, Maru DM, Lizee G, Janku F, Overman MJ, Kopetz S. Association of PIK3CA mutations (mut) with immune engagement and clinical benefit from immunotherapy in microsatellite stable (MSS) colorectal cancer (CRC) patients (pts). *Journal of Clinical Oncology*. 2019;37(15_suppl):3604-.
77. Nusrat M, Roszik J, Katkhuda R, Menter D, Raghav KPS, Morris VK, Sharma P, Allison JP, Blando JM, Maru DM, Overman MJ, Kopetz S. Association of phosphatidylinositol 3-kinase (PI3K) pathway activation with increased immune checkpoint expression in colorectal cancer (CRC) patients. *Journal of Clinical Oncology*. 2018;36(4_suppl):653-.
78. Yap TA, Yan L, Patnaik A, Fearen I, Olmos D, Papadopoulos K, Baird RD, Delgado L, Taylor A, Lupinacci L, Riisnaes R, Pope LL, Heaton SP, Thomas G, Garrett MD, Sullivan DM, de Bono JS, Tolcher AW. First-in-man clinical trial of the oral pan-AKT inhibitor MK-2206 in patients with advanced solid tumors. *J Clin Oncol*. 2011;29(35):4688-95.
79. Yap TA, Yan L, Patnaik A, Tunariu N, Biondo A, Fearen I, Papadopoulos KP, Olmos D, Baird R, Delgado L, Tetteh E, Beckman RA, Lupinacci L, Riisnaes R, Decordova S, Heaton SP, Swales K, deSouza NM, Leach MO, Garrett MD, Sullivan DM, de Bono JS, Tolcher AW. Interrogating two schedules of the AKT inhibitor MK-2206 in patients with advanced solid tumors incorporating novel pharmacodynamic and functional imaging biomarkers. *Clin Cancer Res*. 2014;20(22):5672-85.

80. Xing Y, Lin NU, Maurer MA, Chen H, Mahvash A, Sahin A, Akcakanat A, Li Y, Abramson V, Litton J, Chavez-MacGregor M, Valero V, Piha-Paul SA, Hong D, Do KA, Tarco E, Riall D, Eterovic AK, Wulf GM, Cantley LC, Mills GB, Doyle LA, Winer E, Hortobagyi GN, Gonzalez-Angulo AM, Meric-Bernstam F. Phase II trial of AKT inhibitor MK-2206 in patients with advanced breast cancer who have tumors with PIK3CA or AKT mutations, and/or PTEN loss/PTEN mutation. *Breast Cancer Res.* 2019;21(1):78.
81. Kalinsky K, Sparano JA, Zhong X, Andreopoulou E, Taback B, Wiechmann L, Feldman SM, Ananthakrishnan P, Ahmad A, Cremers S, Sireci AN, Cross JR, Marks DK, Mundi P, Connolly E, Crew KD, Maurer MA, Hibshoosh H, Lee S, Hershman DL. Pre-surgical trial of the AKT inhibitor MK-2206 in patients with operable invasive breast cancer: a New York Cancer Consortium trial. *Clin Transl Oncol.* 2018;20(11):1474-83.
82. Konopleva MY, Walter RB, Faderl SH, Jabbour EJ, Zeng Z, Borthakur G, Huang X, Kadia TM, Ruvolo PP, Feliu JB, Lu H, Debose L, Burger JA, Andreeff M, Liu W, Baggerly KA, Kornblau SM, Doyle LA, Estey EH, Kantarjian HM. Preclinical and early clinical evaluation of the oral AKT inhibitor, MK-2206, for the treatment of acute myelogenous leukemia. *Clin Cancer Res.* 2014;20(8):2226-35.
83. Iida M, Brand TM, Campbell DA, Starr MM, Luthar N, Traynor AM, Wheeler DL. Targeting AKT with the allosteric AKT inhibitor MK-2206 in non-small cell lung cancer cells with acquired resistance to cetuximab. *Cancer Biol Ther.* 2013;14(6):481-91.

84. Okuzumi T, Fiedler D, Zhang C, Gray DC, Aizenstein B, Hoffman R, Shokat KM. Inhibitor hijacking of Akt activation. *Nat Chem Biol.* 2009;5(7):484-93.
85. Yan L. Abstract #DDT01-1: MK-2206: A potent oral allosteric AKT inhibitor. *Cancer Research.* 2009;69(9 Supplement):DDT01-1-DDT-1.
86. Stottrup C, Tsang T, Chin YR. Upregulation of AKT3 Confers Resistance to the AKT Inhibitor MK2206 in Breast Cancer. *Mol Cancer Ther.* 2016;15(8):1964-74.
87. Singh RK, Dhadve A, Sakpal A, De A, Ray P. An active IGF-1R-AKT signaling imparts functional heterogeneity in ovarian CSC population. *Sci Rep.* 2016;6:36612.
88. Lin A, Piao HL, Zhuang L, Sarbassov dos D, Ma L, Gan B. FoxO transcription factors promote AKT Ser473 phosphorylation and renal tumor growth in response to pharmacologic inhibition of the PI3K-AKT pathway. *Cancer Res.* 2014;74(6):1682-93.
89. Juric D, Rodón J, Bauer TM, Wainberg Z, Tolaney S, Modi S, Martín AG, Hengelage T, Melendez M, Choudhury S, Nauwelaerts H, Bedard PL. 342 A Phase Ib/II study of alpelisib (BYL719) and ganitumab (AMG 479) in adult patients with selected advanced solid tumors. *European Journal of Cancer.* 2015;51:S68.
90. Brana I, Berger R, Golan T, Haluska P, Edenfield J, Fiorica J, Stephenson J, Martin LP, Westin S, Hanjani P, Jones MB, Almhanna K, Wenham RM, Sullivan DM, Dalton WS, Gunchenko A, Cheng JD, Siu LL, Gray JE. A parallel-arm phase I trial of the humanised anti-IGF-1R antibody dalotuzumab

in combination with the AKT inhibitor MK-2206, the mTOR inhibitor ridaforolimus, or the NOTCH inhibitor MK-0752, in patients with advanced solid tumours. *Br J Cancer*. 2014;111(10):1932-44.

91. O'Reilly KE, Rojo F, She QB, Solit D, Mills GB, Smith D, Lane H, Hofmann F, Hicklin DJ, Ludwig DL, Baselga J, Rosen N. mTOR inhibition induces upstream receptor tyrosine kinase signaling and activates Akt. *Cancer Res*. 2006;66(3):1500-8.
92. Elster N, Cremona M, Morgan C, Toomey S, Carr A, O'Grady A, Hennessy BT, Eustace AJ. A preclinical evaluation of the PI3K alpha/delta dominant inhibitor BAY 80-6946 in HER2-positive breast cancer models with acquired resistance to the HER2-targeted therapies trastuzumab and lapatinib. *Breast Cancer Res Treat*. 2015;149(2):373-83.
93. Hopkins BD, Pauli C, Du X, Wang DG, Li X, Wu D, Amadiume SC, Goncalves MD, Hodakoski C, Lundquist MR, Bareja R, Ma Y, Harris EM, Sboner A, Beltran H, Rubin MA, Mukherjee S, Cantley LC. Suppression of insulin feedback enhances the efficacy of PI3K inhibitors. *Nature*. 2018;560(7719):499-503.
94. Sobral-Leite M, Salomon I, Opdam M, Kruger DT, Beelen KJ, van der Noort V, van Vlierberghe RLP, Blok EJ, Giardiello D, Sanders J, Van de Vijver K, Horlings HM, Kuppen PJK, Linn SC, Schmidt MK, Kok M. Cancer-immune interactions in ER-positive breast cancers: PI3K pathway alterations and tumor-infiltrating lymphocytes. *Breast Cancer Res*. 2019;21(1):90.

95. Siemers NO, Holloway JL, Chang H, Chasalow SD, Ross-MacDonald PB, Voliva CF, Szustakowski JD. Genome-wide association analysis identifies genetic correlates of immune infiltrates in solid tumors. *PLoS One*. 2017;12(7):e0179726.
96. Miao D, Margolis CA, Gao W, Voss MH, Li W, Martini DJ, Norton C, Bosse D, Wankowicz SM, Cullen D, Horak C, Wind-Rotolo M, Tracy A, Giannakis M, Hodi FS, Drake CG, Ball MW, Allaf ME, Snyder A, Hellmann MD, Ho T, Motzer RJ, Signoretti S, Kaelin WG, Jr., Choueiri TK, Van Allen EM. Genomic correlates of response to immune checkpoint therapies in clear cell renal cell carcinoma. *Science*. 2018;359(6377):801-6.
97. Llosa NJ, Cruise M, Tam A, Wicks EC, Hechenbleikner EM, Taube JM, Blosser RL, Fan H, Wang H, Lubner BS, Zhang M, Papadopoulos N, Kinzler KW, Vogelstein B, Sears CL, Anders RA, Pardoll DM, Housseau F. The Vigorous Immune Microenvironment of Microsatellite Instable Colon Cancer Is Balanced by Multiple Counter-Inhibitory Checkpoints. *Cancer Discovery*. 2015;5(1):43-51.
98. Miao D, Margolis CA, Vokes NI, Liu D, Taylor-Weiner A, Wankowicz SM, Adeegbe D, Keliher D, Schilling B, Tracy A, Manos M, Chau NG, Hanna GJ, Polak P, Rodig SJ, Signoretti S, Sholl LM, Engelman JA, Getz G, Janne PA, Haddad RI, Choueiri TK, Barbie DA, Haq R, Awad MM, Schadendorf D, Hodi FS, Bellmunt J, Wong KK, Hammerman P, Van Allen EM. Genomic correlates of response to immune checkpoint blockade in microsatellite-stable solid tumors. *Nat Genet*. 2018;50(9):1271-81.

99. Becht E, de Reynies A, Giraldo NA, Pilati C, Buttard B, Lacroix L, Selves J, Sautes-Fridman C, Laurent-Puig P, Fridman WH. Immune and Stromal Classification of Colorectal Cancer Is Associated with Molecular Subtypes and Relevant for Precision Immunotherapy. *Clin Cancer Res.* 2016;22(16):4057-66.
100. Marisa L, Svrcek M, Collura A, Becht E, Cervera P, Wanherdrick K, Buhard O, Goloudina A, Jonchère V, Selves J, Milano G, Guenot D, Cohen R, Colas C, Laurent-Puig P, Olschwang S, Lefèvre JH, Parc Y, Boige V, Lepage C, André T, Fléjou J-F, Dérangère V, Ghiringhelli F, de Reynies A, Duval A. The Balance Between Cytotoxic T-cell Lymphocytes and Immune Checkpoint Expression in the Prognosis of Colon Tumors. *JNCI: Journal of the National Cancer Institute.* 2018;110(1):68-77.
101. Lal N, White BS, Goussous G, Pickles O, Mason MJ, Beggs AD, Taniere P, Willcox BE, Guinney J, Middleton GW. KRAS Mutation and Consensus Molecular Subtypes 2 and 3 Are Independently Associated with Reduced Immune Infiltration and Reactivity in Colorectal Cancer. *Clin Cancer Res.* 2018;24(1):224-33.

Vita

Maliha Nusrat was born in Lahore, Pakistan, the daughter of Dr. Naseem Nusrat and Nusrat Shaikh. She completed Secondary School Certificate at Divisional Public School, Lahore, Pakistan in 2002. Subsequently, she completed Higher Secondary School Certificate in pre-medical group at Kinnaird College for Women, Lahore, Pakistan in 2004. In October of 2004, she enrolled in the Aga Khan University Medical College in Karachi, Pakistan, and earned a degree in Bachelor of Medicine, Bachelor of Surgery (M.B., B.S.) with honors in December 2009. After completing United States Medical Licensing Exams, she entered residency training in Internal Medicine at The University of Texas Health Science Center, Houston, Texas from June 2012 to June 2015. She then completed fellowships in Hematology and Medical Oncology (July 2015 – June 2018) and Investigational Cancer Therapeutics (July 2018 – June 2019) at the University of Texas MD Anderson Cancer Center, Houston, Texas. She entered MD Anderson Cancer Center UTHealth Graduate School of Biomedical Sciences in 2016 during fellowship. She is currently a faculty member on the Gastrointestinal Oncology service in the department of Medicine at Memorial Sloan Kettering Cancer Center in New York.

Permanent address:

SD 357, Lane 11-A, Askari V,
Walton, Gulberg III,
Lahore, Pakistan 54600